1. Report No. FHWA/TX-90+465-2F	2. Government Accession No.	3. Recipient's Catalog No.
4. Title and Subtitle FRETTING FATIGUE IN POST-TENSIONED CONCRETE		5. Report Date November 1988
		6. Performing Organization Code
7. Author's) G. P. Wollmann, D. L. Yates, J. E. Breen, and M. E. Kreger		8. Performing Organization Report No. Research Report 465-2F
9. Performing Organization Name and Address Center for Transportation Research The University of Texas at Austin Austin, Texas 78712-1075		10. Work Unit No.
		11. Contract or Grant No. Research Study 3-5-86/8-465
12. Sponsoring Agency Name and Address Texas State Department of Highways and Public Transportation; Transportation Planning Division P. O. Box 5051 Austin, Texas 78763-5051		13. Type of Report and Period Covered Final
		14. Sponsoring Agency Code

15. Supplementary Notes
Study conducted in cooperation with the U. S. Department of Transportation, Federal Highway Administration
Research Study Title: "Fatigue Strength of Post-Tensioned Concrete"

16. Abstract
    This report summarizes an experimental investigation of fatigue strength of post-tensioned concrete girders. The test series included strand-in-air tests to characterize the prestressing strands utilized, reduced beam specimens with single strands in a tendon, reduced beam specimens with multiple strands in a tendon, and complete beams with multiple strands in a tendon. The variables explored included the effect of stress range, type of duct material, lateral contact force per unit length, and type of strand. Duct materials included both metallic and plastic sheaths. Both epoxy coated and uncoated strands were used. All specimens were tested in a cracked condition and fatigue failures occurred in the regions of high curvature (and hence high lateral force) in the vicinity of cracks.

    The results indicate that the expected fatigue life of prestressing strand as determined from strand-in-air tests can be substantially reduced in post-tensioned concrete applications due to fretting fatigue of the prestressing tendon. Such fretting fatigue can occur in cracked concrete sections at locations of tendon curvature. With metal ducts the rubbing between sheath and strand greatly aggravated fretting. With plastic ducts, the ducts showed marked evidence of rubbing and wearing, but with single strand tendons, fretting was not a serious problem. However, with plastic ducts and multiple strand tendons in more than one layer, fretting occurred between layers of strands and was a serious problem.

    The report gives design recommendations in a form compatible with the overall AASHTO fatigue approach for steel bridge members.

17. Key Words fatigue strength, post-tensioned concrete, girders, strands, prestressing, tendon, beam specimens, fatigue life, fretting, sheath, duct material	18. Distribution Statement No restrictions. This document is available to the public through the National Technical Information Service, Springfield, Virginia 22161.

19. Security Classif. (of this report) Unclassified	20. Security Classif. (of this page) Unclassified	21. No. of Pages 168	22. Price

Form DOT F 1700.7 (8-69)

FRETTING FATIGUE IN POST-TENSIONED CONCRETE

by

G.P. Wollmann, D.L. Yates, J.E. Breen, and
M.E. Kreger

PREFACE

This report is the second in a series which summarizes an investigation of the behavior of prestressed concrete beams with post-tensioning. The earlier report summarized an exploratory investigation of fatigue strength in shear of prestressed concrete beams. In that report the prestressed concrete beams were pretensioned since that has little effect on stirrup stresses.

This report details the results of a comprehensive fatigue investigation of post-tensioned concrete specimens. The various tests included strand-in-air tests to characterize the prestressing strand utilized, a series of reduced beam specimens with single strands in a tendon, a series of reduced beam specimens with multiple strands in a tendon, and a series of complete beam specimens with multiple strands in a tendon. The report summarizes all results from the post- tensioned specimens along with the results of several other test programs and concludes with design recommendations.

SUMMARY

This report summarizes an experimental investigation of fatigue strength of post-tensioned concrete girders. The test series included strand-in-air tests to characterize the prestressing strands utilized, reduced beam specimens with single strands in a tendon, reduced beam specimens with multiple strands in a tendon, and complete beams with multiple strands in a tendon. The variables explored included the effect of stress range, type of duct material, lateral contact force per unit length, and type of strand. Duct materials included both metallic and plastic sheaths. Both epoxy coated and uncoated strands were used. All specimens were tested in a cracked condition and fatigue failures occurred in the regions of high curvature (and hence high lateral force) in the vicinity of cracks.

The results indicate that the expected fatigue life of prestressing strand as determined from strand-in-air tests can be substantially reduced in post-tensioned concrete applications due to fretting fatigue of the prestressing tendon. Such fretting fatigue can occur in cracked concrete sections at locations of tendon curvature. With metal ducts the rubbing between sheath and strand greatly aggravated fretting. With plastic ducts, the ducts showed marked evidence of rubbing and wearing, but with single strand tendons, fretting was not a serious problem. However, with plastic ducts and multiple strand tendons in more than one layer, fretting occurred between layers of strands and was a serious problem.

The report gives design recommendations in a form compatible with the overall AASHTO fatigue approach for steel bridge members.

IMPLEMENTATION

This report summarizes the results of a comprehensive investigation of the fatigue strength of post-tensioned concrete specimens. The results indicate that fretting fatigue could be a serious problem in cracked post-tensioned concrete girders with curved tendon layouts. The results indicate the effects of major variables and the report suggests several strategies for minimizing fretting fatigue damage. It can be used in development of project specifications or in setting design specification criteria.

The results indicate that one of the most effective protections against fatigue of post-tensioning tendons is to use fully prestressed (or uncracked) concrete. Fretting concentrates at cracks. Stress ranges are very low in uncracked post- tensioned girders. Since girders may be cracked from environmental, construction, or overload conditions, it is also desirable to limit stress range in cracked concrete sections. The report indicates measures which can be taken to reduce lateral contact forces through tendon curvature limits. In addition in particularly demanding applications, the use of epoxy coated strand provides substantial improvement.

The report presents results in a form compatible with AASHTO design specifications for fatigue of steel bridges so that they can be considered by AASHTO as a possible design guideline for post-tensioned concrete fatigue.

TABLE OF CONTENTS

LIST OF TABLES

LIST OF FIGURES

C H A P T E R 1

INTRODUCTION

1.1 General

The use of prestressed concrete in the United States has rapidly increased since its first introduction by the Belgian Engineer Gustave Magnel in 1949 [16]. Today there are wide applications of prestressed concrete in all type of structures, including bridge and offshore structures. The effects of repeated loading on prestressed concrete have been studied by several investigators in the past [2,13,14,17,21,25]. However, with few exceptions U.S. fatigue research has been focused on pretensioned girders.

It was found that in most cases failure of such girders under cyclic loading is initiated by a fatigue failure of the tendon and can be related to the fatigue life of the prestressing steel [21]. Generally, prestressing steel fatigue in uncracked girders is not a problem. However, if the girder becomes cracked, fatigue is a possibility. A very accurate determination of the tendon stress range in a cracked girder is essential and should be based on a cracked section analysis. The actual effective prestress level in the tendons must be known if the calculations are to be meaningful. An "exact" determination of stress range under varying applied loads is only possible if the magnitude of prestress losses is known very closely. In practical design applications, generous estimates of such losses must be assumed. In addition, tendon stresses increase dramatically at the location of cracks as shown in Figure 1.1. Previous studies indicate that indirect design for fatigue in prestressed concrete by assuming an uncracked section and then by limiting the "fictitious" stresses computed in the concrete tensile zone, may be unconservative [21].

Recent test results at the Swiss Federal Institute of Technology [26] and the Technical University of Munich [18] indicate that the fatigue life for post-tensioned girders can be substantially lower than for pretensioned concrete. In both studies tendon wires fractured prematurely at locations where flexural cracks in the girder and large tendon curvature coincided. Closer investigation showed signs of severe rubbing of the prestressing steel on the duct. The majority of fractures initiated at contact points between duct and steel. It was concluded that the lateral pressure due to tendon curvature, slip of steel along the duct at flexural cracks, and surface microcracks in the prestressing steel caused the premature failure.

This problem is well known in mechanical engineering as fretting fatigue. Numerous parameters have been studied, such as materials involved, coatings, slip amplitude, contact pressure, stress range, frequency, and environment [31]. However, the effects of fretting fatigue are not well known when applied to prestressed concrete. Design recommendations developed for pretensioned concrete may not directly or correctly apply to

1
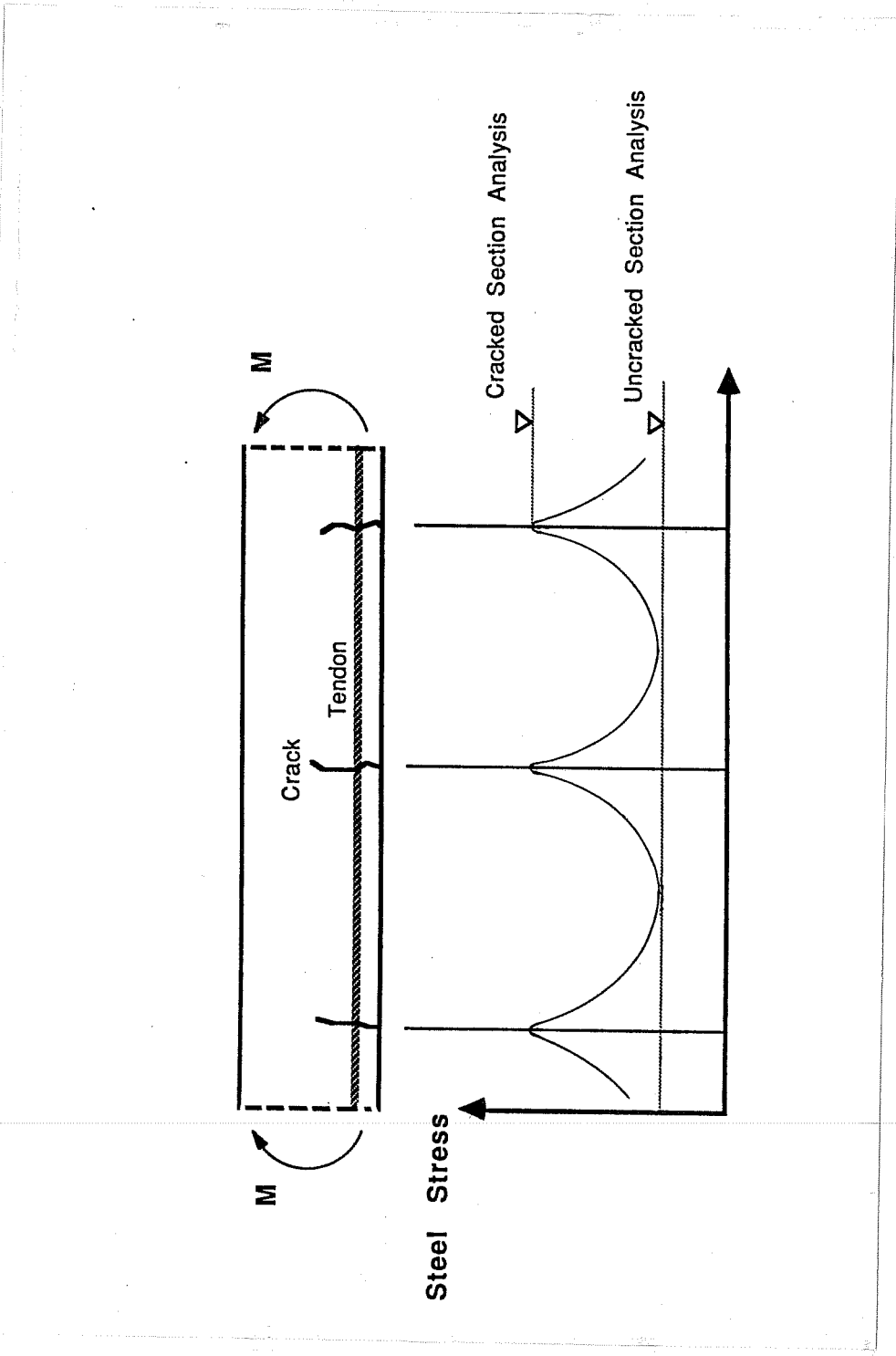
Figure 1.1   Tendon Stress Concentrations at Cracks

post-tensioned concrete girders [31]. Parameters such as lateral pressure, duct material, type of prestressing steel, and stress range may have an important influence and must be considered.

A comprehensive research project at the Ferguson Structural Engineering Laboratory of the University of Texas at Austin was initiated in 1985 to learn more about the adverse effects of fretting fatigue and to develop design recommendations for post-tensioned concrete girders.

The study includes an extensive literature search and review and three major test series:

1) fatigue tests of single strand tendons in post-tensioned concrete reduced beam specimens [31],

2) fatigue tests of multiple strand tendons in post-tensioned reduced beam specimens [34],

3) fatigue tests of full size post-tensioned girders [11,15].

1.2 Objectives

The objectives of the overall project are

1) to investigate the fatigue life of typical post-tensioned girders,

2) to study the influence of important variables such as duct type, tendon coating, lateral pressure, prestress level, and stress range on the fatigue strength of post-tensioned concrete,

3) to develop fatigue design recommendations to ensure satisfactory fatigue performance of post-tensioned concrete girders during their entire service life.

1.3 Scope

In the following chapters the test series of the research program will be documented and evaluated in detail.

Chapter 2 includes basic information on fatigue of prestressed concrete girders and fretting fatigue. A very comprehensive literature review on these topics can be found in Reference 31. Therefore only the most essential information will be repeated herein. Finally present code provisions in the United States and Europe are summarized.

In Chapter 3 the various beam specimens, the test setups, and the general test procedures are described.

4

A presentation of the test results is given in Chapter 4, while evaluation and discussion of these and related tests is included in Chapter 5. Finally, in Chapter 6 the findings are summarized, conclusions are drawn, and recommendations for design and further research are given.

CHAPTER 2
FATIGUE OF PRESTRESSED CONCRETE GIRDERS

2.1 General

An extensive literature review on fatigue of prestressed concrete, fretting fatigue, and on related previous research has been presented by Yates [31]. The interested reader is referred to his excellent study for more details. This chapter includes a condensed presentation of the essential background information and of results of previous studies pertinent to fatigue of post-tensioned concrete.

2.2 Fatigue of Prestressed Concrete

2.2.1 General. Cyclic loading generally is not a problem for uncracked prestressed concrete girders. However, if flexural cracks occur the bonded prestressing steel is subjected to a sharply increased stress range at the location of these cracks, and repeated loading may result in fatigue failure of the tendon.

Cracks may be caused by overloads or even regular service loads, by shrinkage or temperature stresses, or excessive prestress losses. The significant decrease of concrete tensile strength under cyclic loading favors the formation of cracks for structures subjected to such load conditions [21].

The fatigue life of prestressed concrete girders is affected by many variables, which can be classified in two groups according to their principal impact:

1) Variables which influence the potential formation of cracks:

- degree of prestress and prestress losses

- concrete tensile strength

- presence of occasional overloads

- environmental factors such as temperature gradients and shrinkage

2) Variables which influence the conditions in the tendon after cracking:

- load range

- tendon curvature

- type of prestressing system (pretensioned, post-tensioned, bonded, unbonded)

- fatigue characteristics of prestressing steel

5

    -   amount and distribution of passive reinforcement

    -   duct material and strand coating

The stiffness history of a typical bonded prestressed concrete girder subjected to cycling loading shows three distinct sections as indicated in Figure 2.1. The initial loss of stiffness within the first few cycles is caused by the formation and propagation of cracks and by bond deterioriation between steel and concrete. Debonding continues during cyclic loading, resulting in further slight losses of stiffness. Finally the first wire breaks, and subsequent fractures of the increasingly higher stressed remaining wires take place at an increasing rate, leading to large and rapid stiffness losses.

Fatigue of isolated tendons and the differences between pretensioned and post-tensioned concrete girders are discussed in the following sections.

2.2.2 Isolated Tendon Fatigue. Fatigue is the tendency of a material to fail after a large number of repeated loadings at a stress level that would not cause failure for static loading. The mechanism of fatigue is the gradual growth of a crack under the influence of fluctuating stresses until a critical depth is reached and brittle fracture occurs. Any condition leading to a stress concentration can act as a crack initiation, such as material flaws, welds, or surface damage. The smaller the range of the fluctuating stress the slower is the crack growth rate, and the maximum stress range for which no crack propagation takes place is known as the endurance limit. Generally, the influence of upper and lower stress level on the endurance limit is small. Typical plots of fatigue strength versus number of cycles are shown in Figure 2.2. If both ordinates are drawn to a logarithmic scale the plot usually can be approximated as two straight lines.

The results of fatigue tests of isolated tendons in air reveal a deleterious influence of increased specimen length on the fatigue life. This length effect has been explained by the higher probability of material flaws for longer samples [8,21,22].

Paulson conducted a very comprehensive study at the University of Texas at Austin including both limited testing and synthesis of previously reported data yielding the fatigue characteristics of over 700 prestressing strand samples from different manufacturers [22]. He was able to recommend a lower five percent fractile design model for the fatigue life of prestressing strand which is shown in Figure 2.3, together with the data points evaluated. A very recently published paper by Tilly confirms this design model [28]. Very few data points were available at lower stress ranges since long life specimens often fail outside of the test region and an endurance limit could not be verified sufficiently.

2.2.3 Fatigue of Pretensioned Concrete. Several previous studies indicate that fatigue models for strand tested in air also apply to both cracked and uncracked preten-sioned girders [14,21,22]. Overman emphasizes the importance of a very accurate determi-nation of the actual tendon stress range and suggests the use of a cracked section analysis
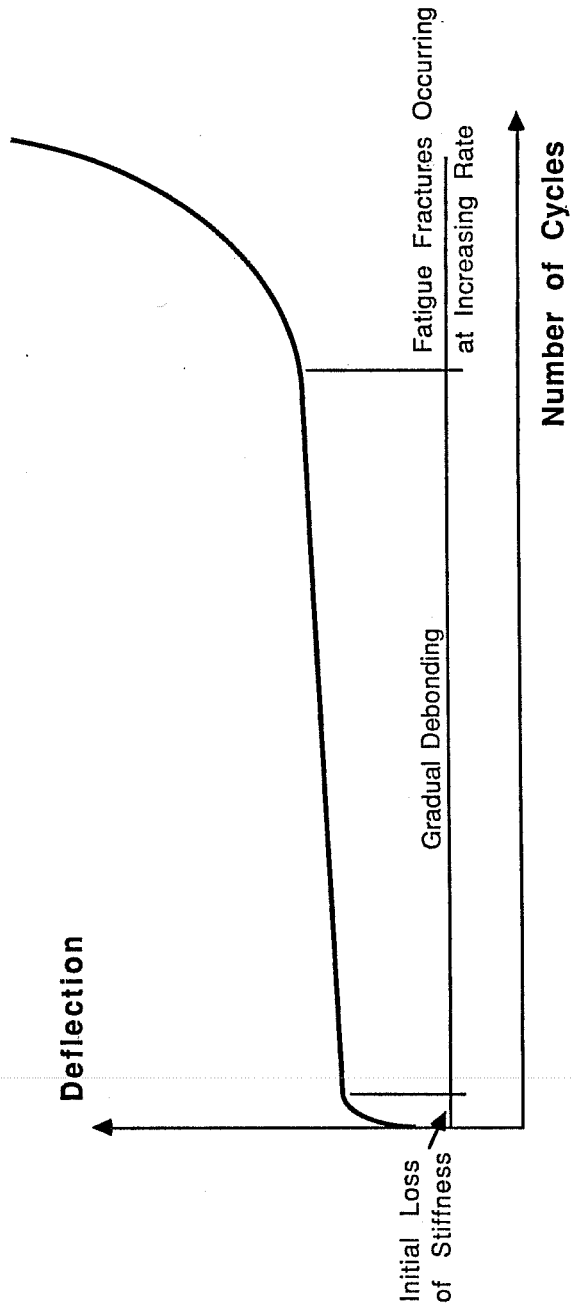
Figure 2.1 Change in Girder Stiffness

Stress Range

Endurance Limit ▽

Number of Cycles (Log Scale)

Stress Range (Log Scale)

Endurance Limit ▽

Number of Cycles (Log Scale)
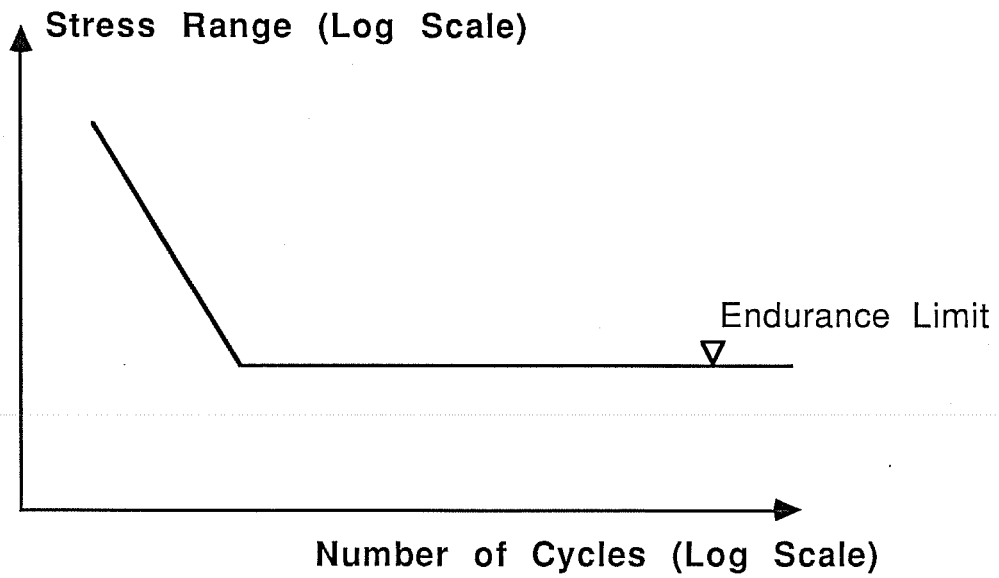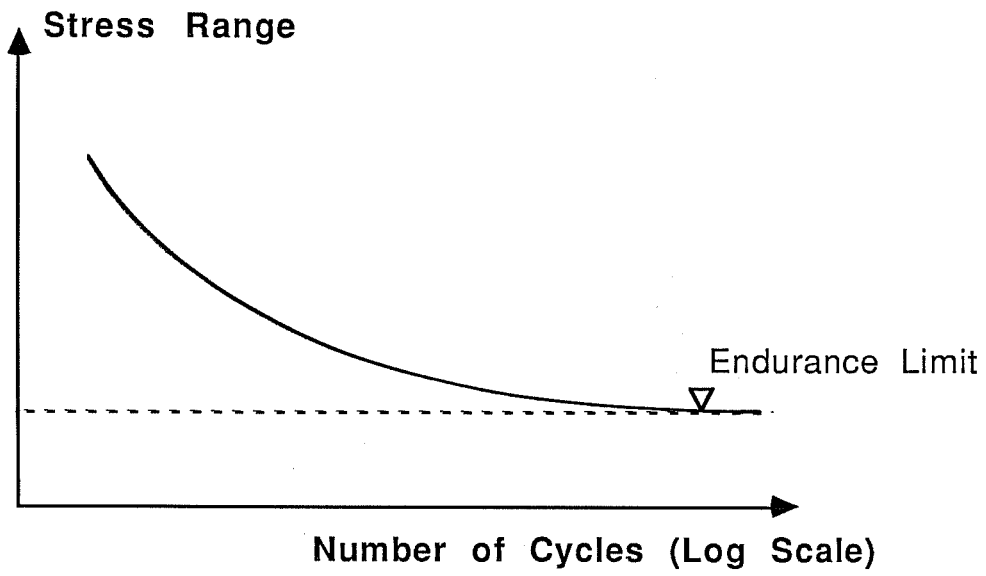
Figure 2.2   Typical Fatigue Strength Plots
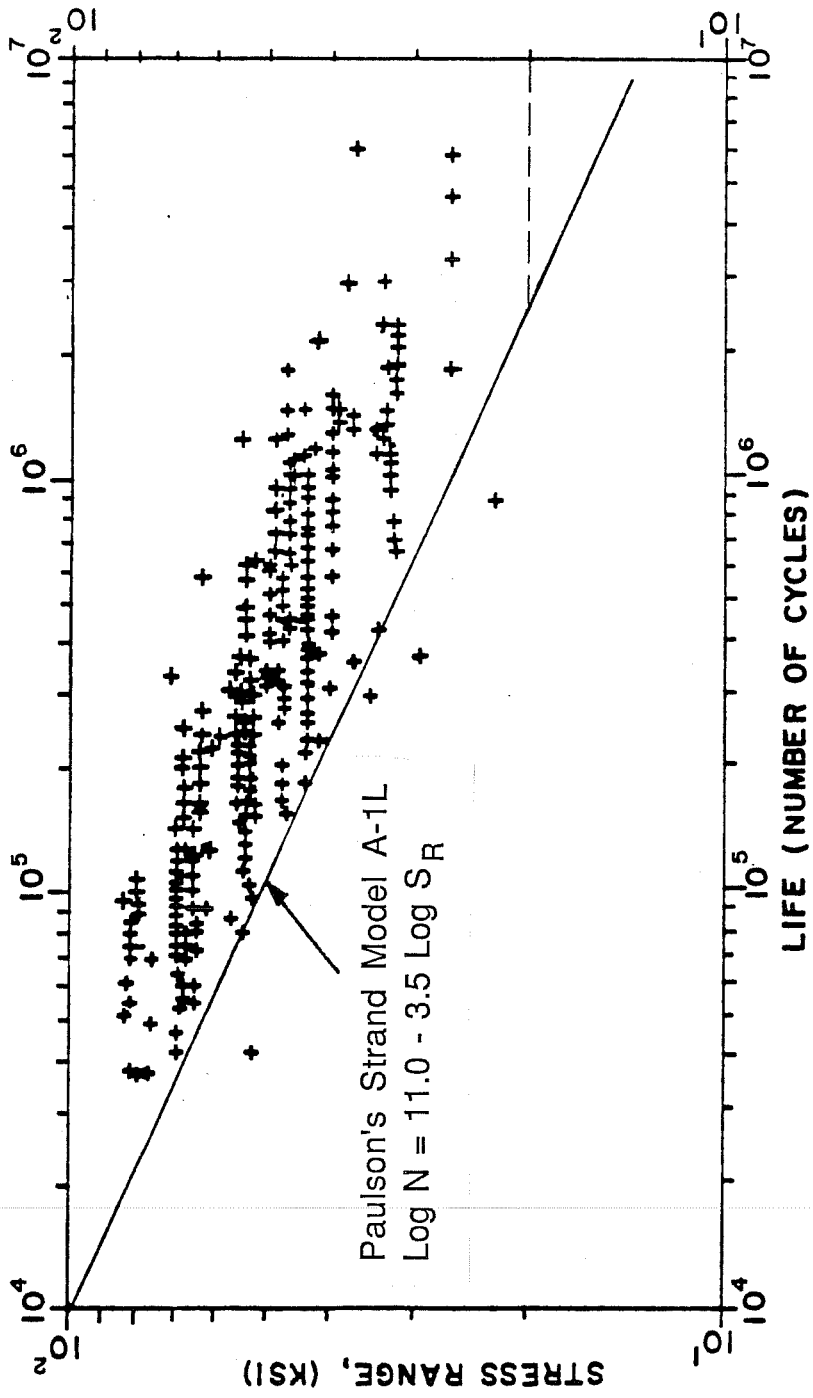
Figure 2.3   Paulson's Strand in Air
Fatigue Model (from Paulson [22])

together with a "conservative assessment of prestress losses" [21]. He states that a tendon stress range of 16 ksi or less ensures a fatigue life of at least six million cycles, but no actual endurance limit was found.

2.2.4 Fatigue of Post-Tensioned Concrete. In the past, little differentiation has been made between pretensioned and post-tensioned concrete, and most prestressed concrete fatigue research has been focused on pretensioned concrete. However, test results in the United States, Switzerland, and Germany indicate that the fatigue life for post-tensioned girders may be substantially lower [17,18,26].

A closer look at the tendon conditions in a post-tensioned concrete beam reveals significant differences as compared to pretensioned concrete. Most notable is the presence of a sheath in post-tensioned concrete beams, to form a void in which prestressing steel is inserted after curing of the concrete. Very often the tendon is curved to generate lateral deviation forces for load balancing. Stressing of the prestressing steel brings it into contact with the duct along the inner side of the curvature, and individual strands or wires (which are usually isolated in pretensioning applications) touch each other as well (Fig. 2.4).

It is this contact between prestressing steel and adjacent metal that aggravates the conditions in the tendon and leads to a greatly reduced fatigue life. At the location of cracks debonding will take place, allowing individual strands or wires to slip relative to each other and the duct. This minute slip causes severe abrasions, and increases stresses between the contacting elements which can initiate surface cracks that will propagate under cyclic loading. Fretting action tends to greatly accelerate crack initiation, but has much less of an effect on crack propagation. Thus, the result of fretting in an element whose fatigue life is dominated by crack propagation (such as a thick plate with good fracture toughness) is almost negligible in the finite life region of the S-N curve. Fretting of such an element could, however, result in a reduction of its endurance limit since cracks would be initiated at stress ranges below the endurance limit for the unfretted material.

On the other hand, if the fatigue life of an element depends largely on crack initiation, then fretting would result in a reduction of the finite life portion of the curve as well as the endurance limit. Such an element might be relatively small, have low fracture toughness, or both. In practice, many components (such as the wires within prestressing strands) fall into this category.

In addition to the fluctuating axial stresses, lateral pressure and friction stresses act on the prestressing steel and create a very complex state of stress in post-tensioned concrete girders. Fig 2.5a shows a comparison of an ordinary fatigue fracture and a fretting fatigue fracture in wires of two different prestressing strand samples. The ordinary fatigue crack propagated perpendicular to the axial stress, and no surface damage of the wire is visible. Overman et al. [21] found that strands in cracked pretensioned concrete girders subjected to cyclic loading show the same fatigue crack characteristics as strands fractured
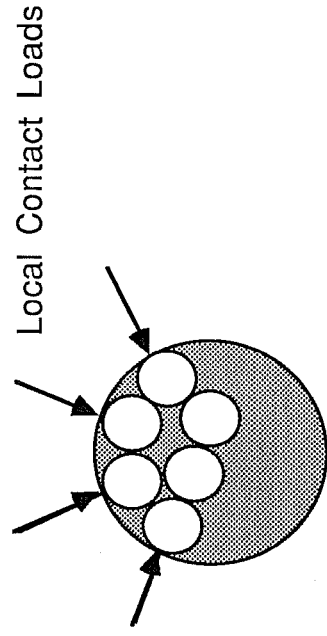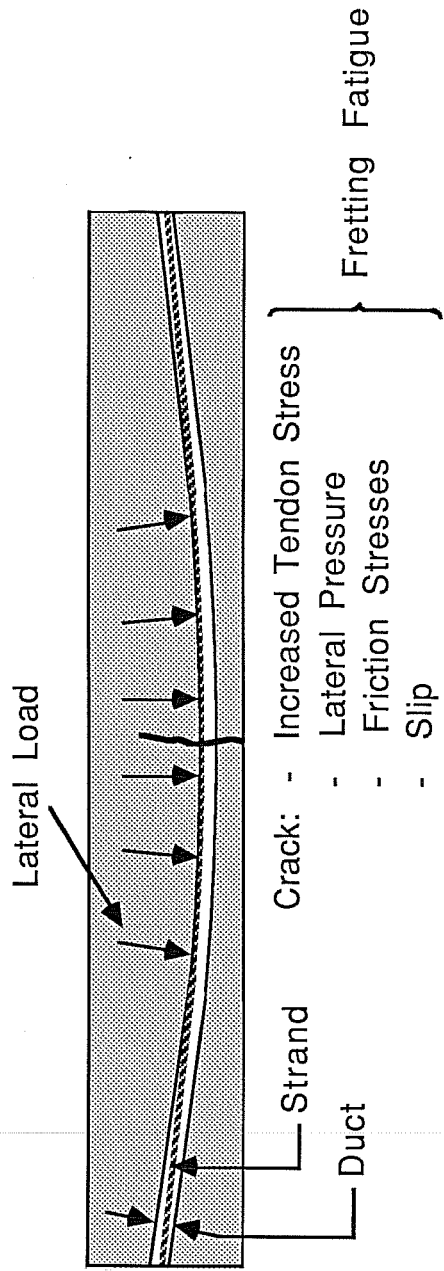
Figure 2.4   Post-Tensioned Beam

12
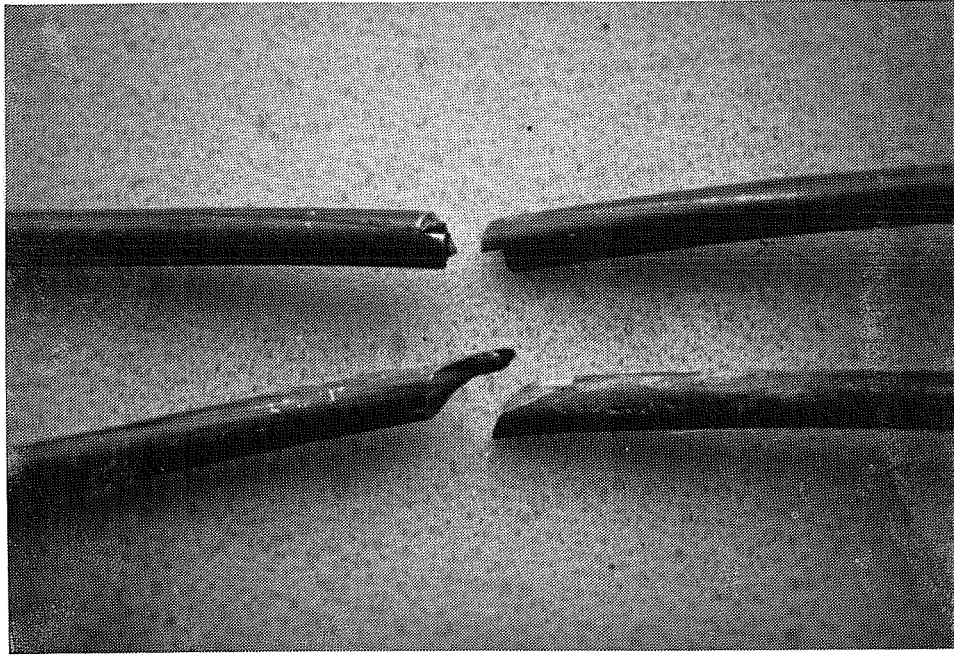
a) Crack Surfaces (from Yates [31])
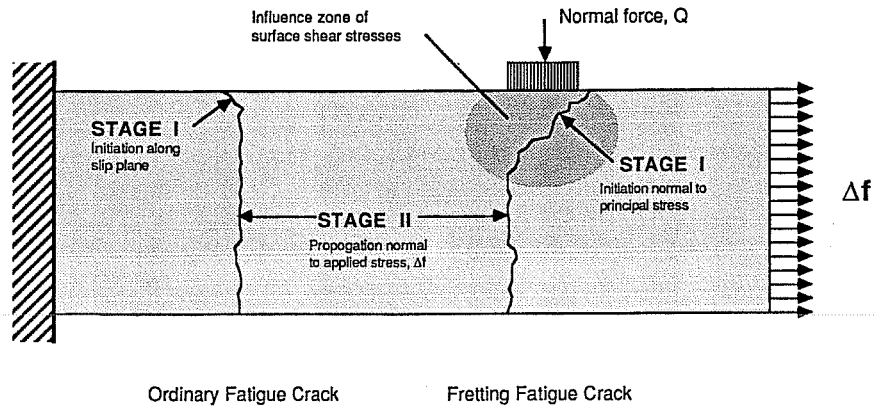
b) Crack Characteristics (after Waterhouse [29])

Figure 2.5   Comparison of Fatigue Cracks

due to ordinary fatigue. In contrast, in post-tensioned girders with curved tendons the initial part of the crack is inclined due to the influence of the lateral and friction stresses (Fig. 2.5a). Furthermore, the strand is severely damaged due to fretting wear. Once the crack reaches a critical depth, brittle fracture with a jagged crack surface occurs, as shown in the picture.

Figure 2.5b schematically illustrates the difference between ordinary fatigue cracks and fretting fatigue cracks. For elements of sufficient thickness the fretting fatigue crack propagates perpendicular to the axis as in ordinary fatigue tests, once it has grown beyond the influence of the local surface zone subject to lateral pressure and friction stresses. However, the thin wires of prestressing strand often suffer brittle fracture before this transition can occur.

The problem of metal on metal rubbing under the influence of lateral and fluctuating axial stresses is known as "fretting". Several mechanisms of fatigue crack initiation have been attributed to the fretting process [35, 36, 37]. While there seems to be disagreement about some aspects of fretting, there is a general consensus about the mechanism which is predominant in post-tensioning tendons. This mechanism is labeled asperity contact initiation and is depicted in Fig. 2.5.

The two materials are initially in contact under the influence of an applied lateral force, Q. Even though this force may be small, extremely high local contact pressures can be developed between the asperities at the material interface since the real area of contact is very small. These local pressures can greatly exceed the elastic limit of the materials causing localized plastic deformation. When cyclic displacements are imposed between the two materials, the oxide film that is normally present on steel surfaces is rapidly abraded. Without this protective film, the material asperities readily fuse together as a result of the intense clamping pressure (a process commonly called cold welding). Each time slip of sufficient magnitude is imposed at the interface, these points of adhesion (cold welds) are destroyed and new ones are created. This process generates cyclic surface shear stresses that combine with existing stresses in the materials to create a very complex stress condition. This complex stress state, when it is of sufficient magnitude, is the driving force for crack initiation. The propagation of these cracks depends mostly on the fluctuating stress applied, as in ordinary fatigue [18,29,31].

A large number of studies on fretting fatigue have been conducted, but few of them apply directly to post-tensioned concrete tendons. However, some important tendencies can be recognized, and the most important variables will be discussed briefly:

- Stress Range: The rate of crack growth depends greatly on the magnitude of the fluctuating stress in the element. A larger stress range reduces the fatigue life, and arresting of the crack is possible for sufficiently low stress ranges [29]. However,

the applicability of these results to such thin elements as wires of prestressing strand has not been shown.

In ordinary fatigue tests only the stress range (not upper and lower stress level) has a significant influence on the fatigue life. In post-tensioned concrete, lateral forces are generated due to the tendon curvature and are an important variable affecting the fatigue performance. This lateral contact load is proportional to the tendon force. Therefore upper and lower stress levels affect the fatigue life indirectly.

- Slip Amplitude: It has been shown in previous studies that extremely small slip amplitudes such as those that occur between individual wires of a strand or parallel bundled wires can have a significant impact on the fatigue behavior [18]. If the slip amplitude becomes large enough to wear away any surface cracks previously formed, no cracks are initiated from fretting. This was confirmed by Oertle's tests of ungrouted tendons in post-tensioned concrete reduced beam specimens [19]. Although fretting caused substantial wear where metal duct and prestressing steel were in contact, fracture was initiated on the opposite side of the contact point. This is the location where maximum stresses occur due to the curvature of the tendon. The unbonded tendons showed a considerably longer fatigue life than comparable bonded tendons for both single strand and single wire specimens (Fig. 2.6).

- Lateral Pressure: Waterhouse observed a general tendency for reduced fatigue life with increased lateral pressure [29]. In post-tensioned concrete the lateral pressure depends on the tendon force and will fluctuate with the fluctuating tendon stresses.

An accurate determination of the local lateral pressure on prestressing steel in post-tensioned concrete is extremely difficult, since it depends on many variables, such as local curvature of the duct, duct size and material, arrangement of strands or wires in the duct, type of prestressing steel, and prestress level (Fig. 2.7). Yates described a procedure to compute a nominal lateral pressure [31] based on a method developed by Oertle [20], but actual stresses may substantially exceed that value. Bending of the duct with constant curvature is difficult to achieve, and in practice curvature concentrations are inevitable. The contact area of strand is smaller than that of parallel wires, which causes higher local stresses. For uncoupled threaded prestressing bars fretting fatigue is not a problem, since only the crests of the ribs are in contact with the duct [18].

- Material Properties: Fracture toughness, corrosion resistance, and fatigue characteristics of the prestressing steel have an influence on the behavior in fretting,
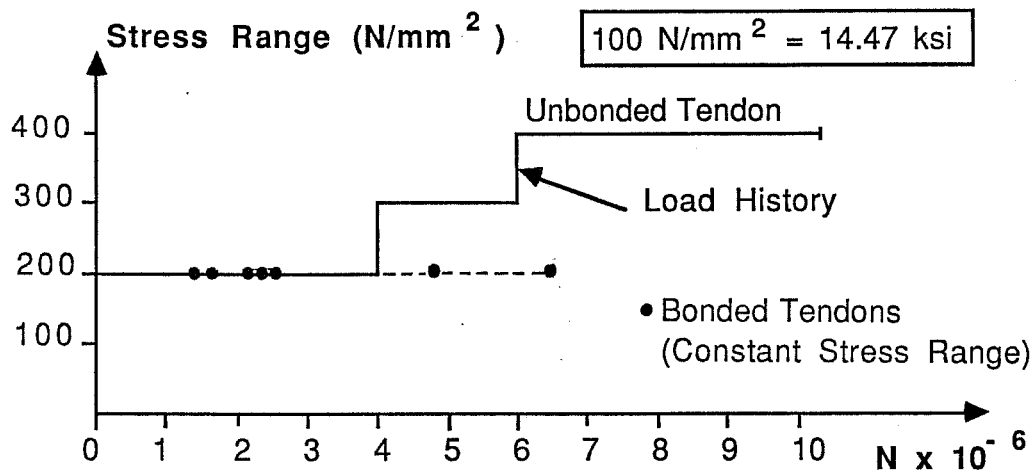
a) Single Wire Tendons
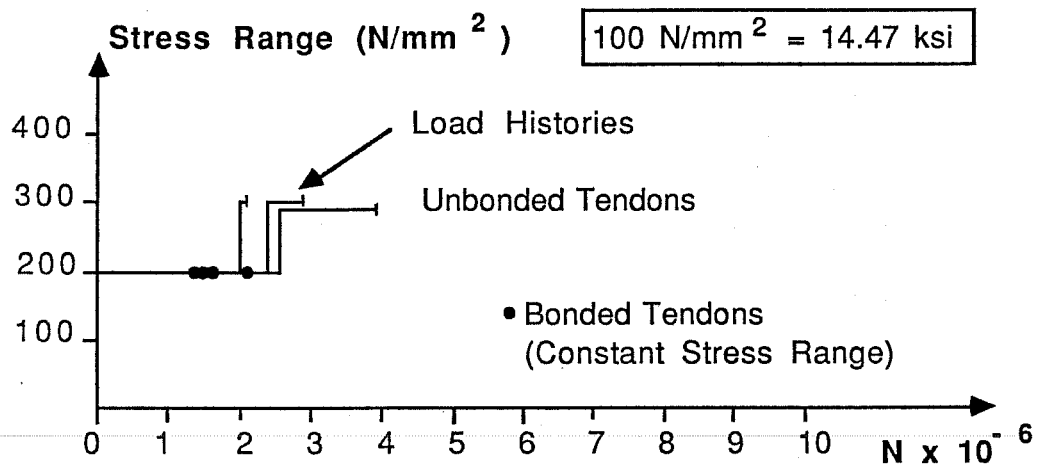
b) Single Strand Tendons

Figure 2.6   Comparison of Bonded and Unbonded Tendons
with Metal Duct (from Oertle, et al. [19])

16

4-0.6" dia strands
2.0" I.D. duct

K=0.69

0.29   0.27
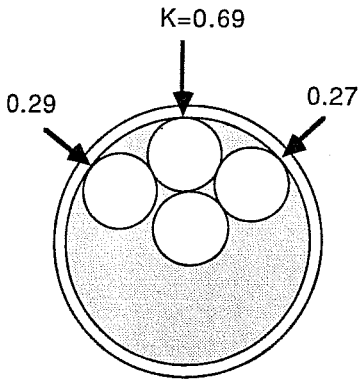
4-0.6" dia strands
39mm (1.54") I.D. duct

K=0.83

0.50   0.50
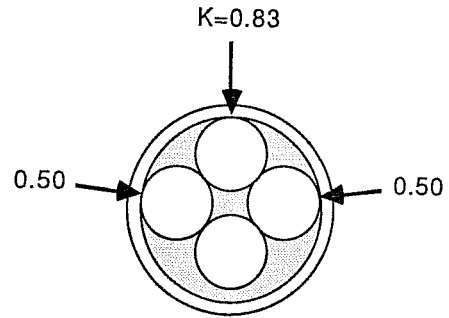
q = K x Q   Local Contact Load q   Tendon Force F
Q = F/R   Lateral Load Q   Radius of Curvature R

a) Influence of Duct Size on Lateral
    Pressure (from Yates [31])

Prestressing Steel
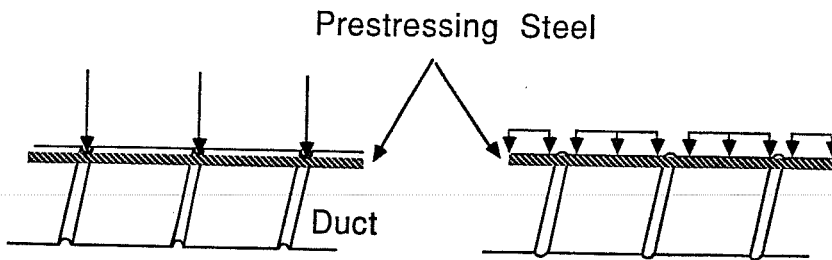
Duct

b) Influence of Duct Corrugation on Lateral Pressure

Figure 2.7   Sensitivity of Lateral Pressure to Tendon Geometry

but no data concerning fretting fatigue of prestressing steel in post-tensioned concrete is available.

- Contact Surfaces: Rubbing of metal on metal, such as slip of strand or wires on adjacent wires or a metal sheath has the most detrimental effect. Rubbing on concrete or grout causes wear but has little impact on fretting fatigue [19,21].

  Coating of one or both of the fretting partners can increase the fatigue life by two distinct effects:

  - The coating can accomodate the slip by elastic deformation.

  - The coating must be worn through before metal on metal fretting can occur.

- Environment: Fretting involves very complex mechanical and chemical reactions, and environmental effects can be significant. The presence of oxygen has been found to reduce the fretting fatigue life, while the influence of corrosive agents in the environment on fretting fatigue is small [31].

A direct application of these results to the fretting fatigue behavior of post-tensioning tendons is not likely. It should be noted that the influence of each of these effects was obtained from isolated variable studies. In actuality, all parameters have a complex interaction, and the most detrimental combination of these variables will cause fracture.

2.3 Previous Studies

2.3.1 Introduction. Several approaches have been used in the past to study fretting fatigue of prestressing tendons in post-tensioned concrete. The most direct way is to test full size or smaller- scale girders in the laboratory. However, this method is involved and expensive. Furthermore prestress losses and effective tendon stresses are difficult to assess, which renders an accurate determination of the tendon stress range very difficult.

To overcome these problems a "reduced beam specimen" was developed by Oertle, Thurlimann, and Esslinger, and tested in such a manner that the tendon forces could be determined from a simple equilibrium equation and were known exactly [19] (Fig. 2.8). Also, the reduced beams were smaller and therefore could be fabricated and tested faster and more economically than girders.

Fretting simulation tests carry this simplification one step further. A regular strand in air test is modified to allow application of a lateral force which acts via a piece of duct on the tendon [9] (Fig. 2.9).

The latter two methods do not represent exactly the conditions in a girder. Thus, they should be compared to companion girder tests to verify their validity.
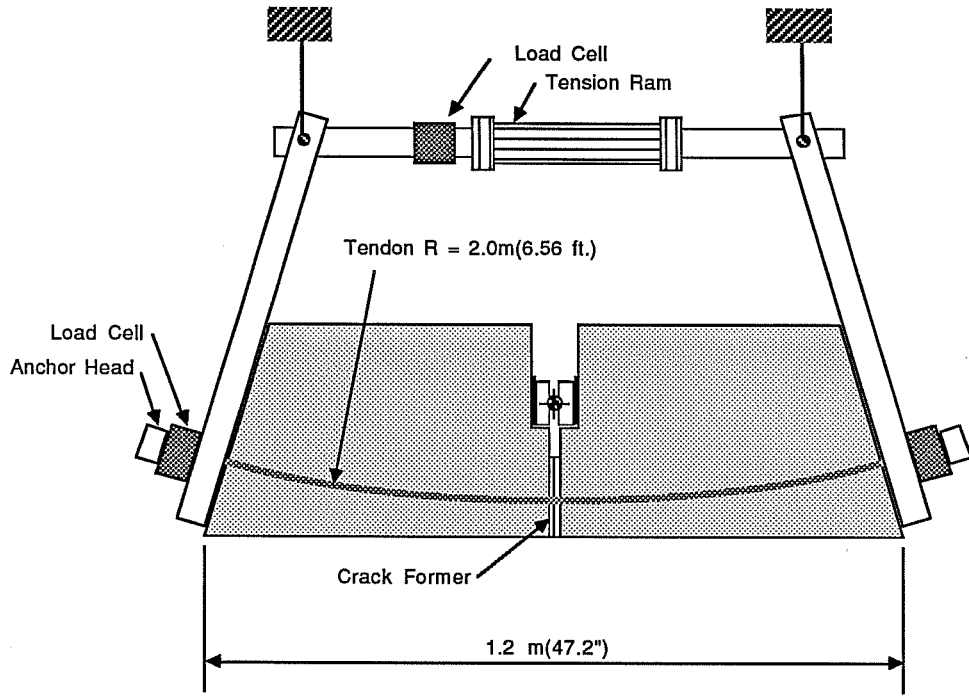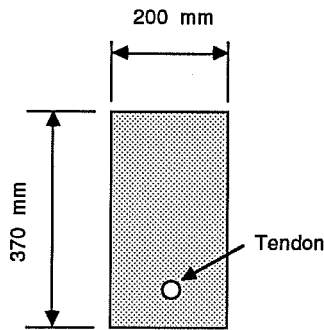
a) Elevation

Tendon	Duct	Grouted	Ungrouted
1-7 mm dia Wire	Metal	●	●
	Plastic	●	
5-7 mm dia Parallel wires	Metal	●	
	Plastic	●	
1-0.6 in dia 7 wire strand	Metal	●	●
	Plastic	●	●

b) Section   c) Test Program

Fig. 2.8   Reduced beams tested by Oertle, Thurlimann and Esslinger [19].

$\Delta \, \mathbf{F}$

$\Delta L = e \times L$

$(e = \text{strain})$

Grout

Lateral Force, F_L

Metal Duct

Rigid Frame

Test Specimen

Clamping Force, F_c

L

$\Delta \, \mathbf{F}$
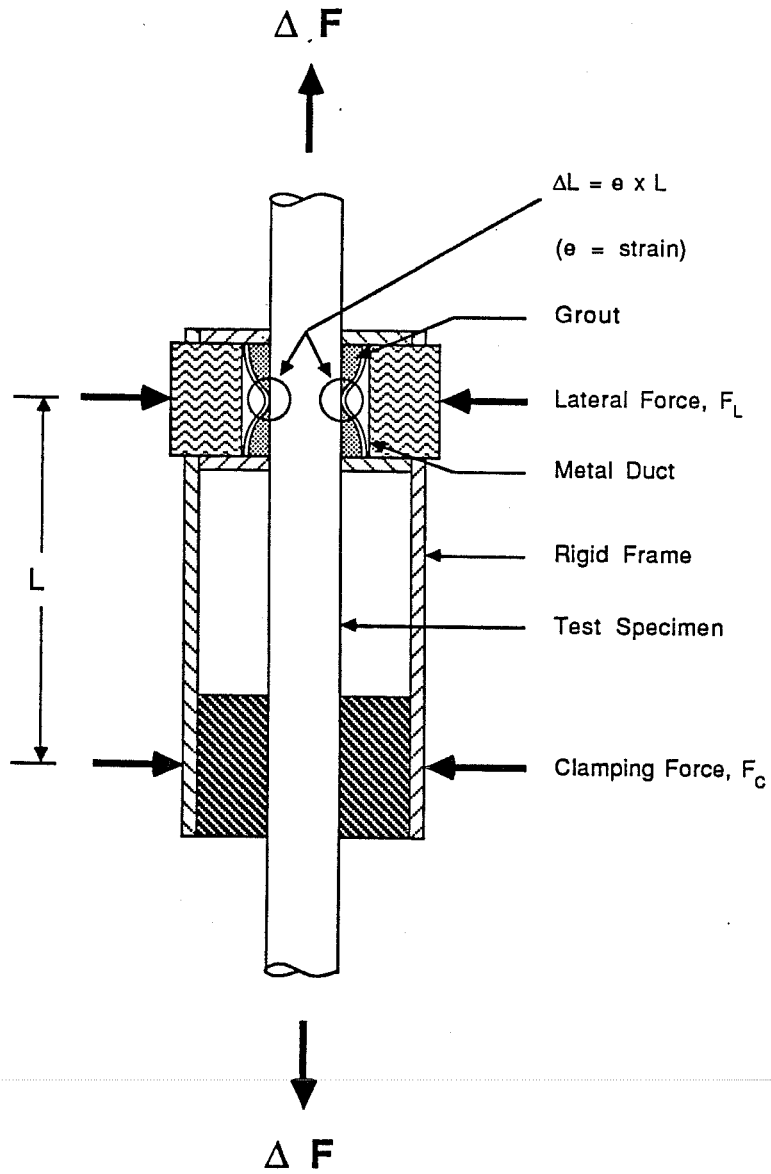
Figure 2.9   Fretting Simulation Apparatus
(after Cordes, et al. [9])

2.3.2 Girder Tests. The earliest indication of the reduced fatigue life for post-tensioned girders with draped tendons was found in a study by **Magura and Hognestad** in 1966 [17]. They compared two post-tensioned and two pretensioned girders. Two were fully prestressed while the other two were partially prestressed (Fig. 2.10a). While the pretensioned girders behaved satisfactory, even after cracking, the post-tensioned girders experienced "serviceability distress and reduced flexural capacity from load repetitions" [17].

Rigon and Thurlimann tested 15 post-tensioned and grouted concrete girders [26]. Eight beams were prestressed with 16-7.0 mm diameter parallel wires, the remaining seven beams had tendons composed of four 0.6 in. diameter seven wire strands. For one girder of each group, plastic duct was used instead of the usual metal duct (Fig. 2.10b).

The tendon stress range was indirectly determined from the elongations of a passive reinforcement bar over a length of 200 mm. Hence, the corresponding stresses represent an average value over this distance, and local stress concentrations, as occur at cracks, could not be determined. Furthermore prestress losses were not monitored, and calculation of the tendon force had to be based on assumptions of 10% and 20% losses, respectively. These circumstances render the reported tendon stress ranges inaccurate, and the data has to be interpreted with care [19]. However, some important observations were made upon examination of the tendon after failure:

- The duct was fractured at the location of cracks.

- At the contact points between prestressing steel and metal duct in the vicinity of cracks, the wires were abraded and the duct indented. Duct and prestressing steel showed traces of corrosion at these contact points. Corrosion was most severe where the tendon curvature was largest, and was more intense for parallel wires than for strand.

- The majority of fractures were initiated by fretting between metal duct and tendon. When plastic duct was used with parallel wires, fractures also occurred within the bundle.

- Fretting between adjacent wires becomes significant once a wire is broken, or if fretting between wire and duct is prevented, for example by use of a plastic duct.

- The use of plastic duct improved the fatigue life of parallel wire tendons significantly. The test with a multiple strand tendon in plastic duct failed prematurely due to fretting of the strand on a tie after the plastic had been worn through, but still showed an increased fatigue life.

In a follow - up study **Oertle, Thurlimann, and Esslinger** [19] tested four more girder specimens with the same geometry and tendon types as Rigon and Thurlimann [26]. Metal and plastic duct were used. Determination of tendon stress range was based

Main Tendon Profile

P P

R = 3.5 m (11.5 ft.)

6.22 m (20.3 ft.)

Elevation

Secondary Tendons (2-0.6" dia,strands)

Instrumented Bars

Main Tendon
16-7mm dia, Parallel Wires
4-0.6 in, dia, Seven Wire Strands
Metal Duct
Plastic Duct

1.2 m (47.2")

0.7m (27.5")

0.8 m (31.4")

Midspan Section

b) Beams tested by Rigon, Thurlimann, Oertle, and Esslinger [19, 26]

C L

P

parabolically draped or straight tendons

25 ft

Elevation

Tendons
16 or 20 - 3/8 in, dia 7 Wire Strands
10 - 0.916 in dia Parallel Wires per Tendon (4 to 6 Tendons)
Draped or Straight Tendons
Metal Duct

56"

22.5"

25"

Midspan Section

a) Beams tests by Magura and Hognestad [17]

Figure 2.10 Girder tests

P

Tendon Profile
$R = R_{min}$

3.0 m (9.84 ft.)

a) Elevation

0.16 m (6.3 in.)

H

D_{ps}

H = 0.5 m (19.7 in.)
D_{ps} = 0.87 x H
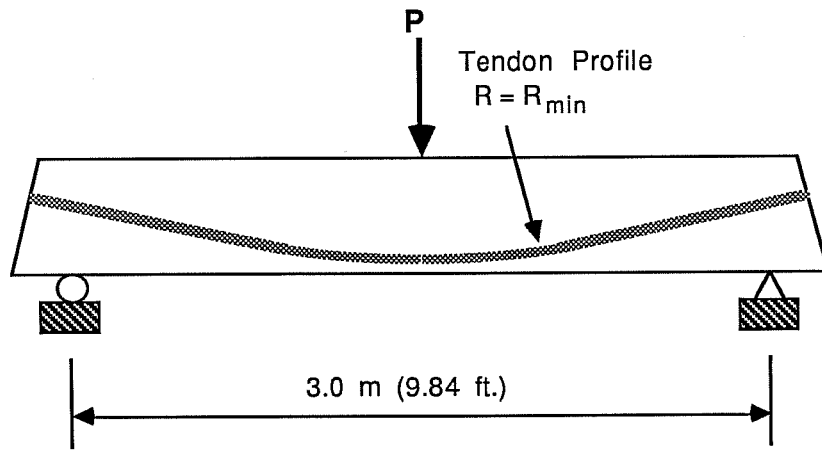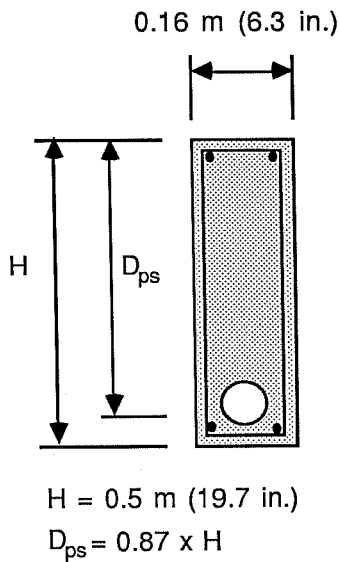
Tendon Type	Minium Radius, R_{min} m (ft.)
Dywidag 26.5 mm dia 1-Threaded bar	8.90 (29.2)
Sawoe 12.2mm dia 3-Parallel wires	3.50 (11.5)
Dywidag 0.6 in. dia 3-7 wire strands	4.80 (15.8)

b) Midspan Section   c) Tendons

c)   Beams tested by Muller [18]

Figure 2.10   Girder tests (cont).

on an analytical method, and cyclic loading was held above the decompression moment in order to minimize uncertainities due to the difficult assessment of prestress losses.

Parallel wire tendons again showed a significantly better fatigue performance with plastic duct than with metal duct. For strand type tendons, the test results are not clear: The tendon with plastic duct was tested at a higher stress range and failed earlier than the corresponding girder with metal duct.

Müller tested a series of grouted specimens with parallel wires, strand, and threaded bar tendons, all with metal duct [18] (Fig. 2.10c). Fretting fatigue was found not to be a problem for threaded bars, since only the crests of the ribs are in contact with the duct. Fatigue was initiated at the outside of the tendon curvature, away from the contact surface where superimposed bending stresses result in larger extreme fiber stresses.

For parallel wire tendons and strand tendons, fractures initiated from contact points between prestressing steel and duct in most cases. Fretting between individual wires of a bundle or a strand also caused fractures.

Figure 2.11 shows logarithmic plots of stress range versus number of cycles before first wire fracture for the girder tests described above.

2.3.3 Reduced Beam Tests. Concurrently to their girder tests **Oertle, Thurlimann, and Esslinger** also tested a large number of reduced beam specimens [19]. Tendons were composed of one or five 7.0 mm diameter parallel wires or of one 0.6-in. diameter seven wire strand, respectively. Plastic and metal duct was used, and behavior of both grouted and ungrouted tendons was examined. Geometry and dimensions of the specimen are shown in Figure 2.8a.

The data reported by Oertle, et al. lead to the following observations:

- Unbonded tendons showed a better fatigue performance than bonded tendons.

- Multiple wire tendons had a lower fatigue life than single wire tendons (Fig. 2.12).

- The use of plastic duct resulted in a substantial improvement of the fatigue performance of parallel wire tendons (no multiple strand reduced beams were tested).

In his recently published dissertation [33] Oertle concluded from his girder and reduced-beam tests that the use of plastic duct greatly increases the fatigue life of both wire- and strand- type tendons. He suggests the following allowable stress ranges for strand and wire tendons:

- metal duct ..... 100 N/mm^2 (14.5 ksi)

- plastic duct ... 200 N/mm^2 (29.0 ksi)

24
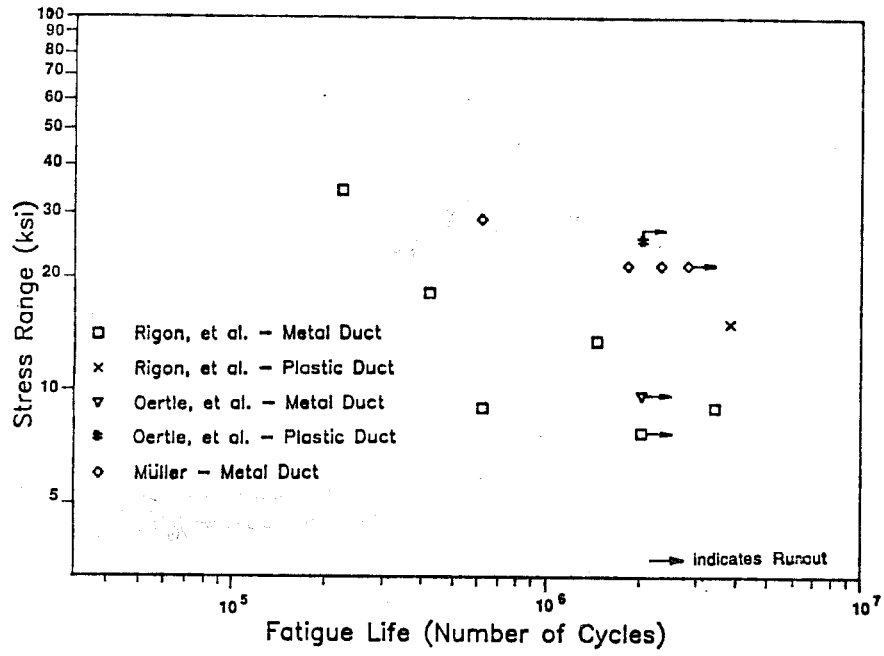
a) Strand Type Tendon
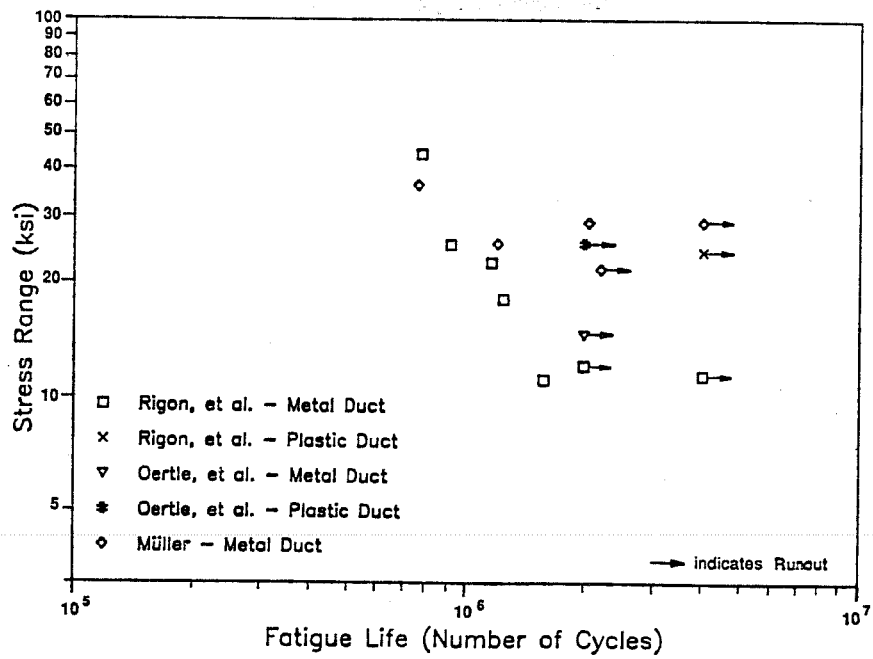
b) Parallel Wire Tendon

Figure 2.11   Results of Girder Tests
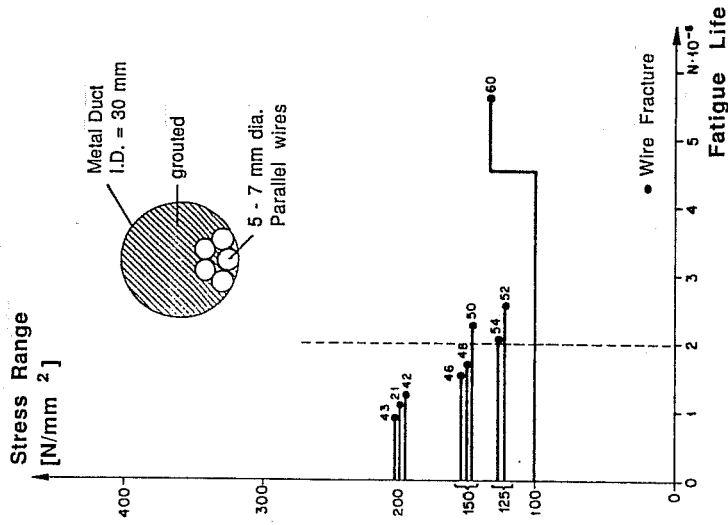
a) Single Wire Tendons
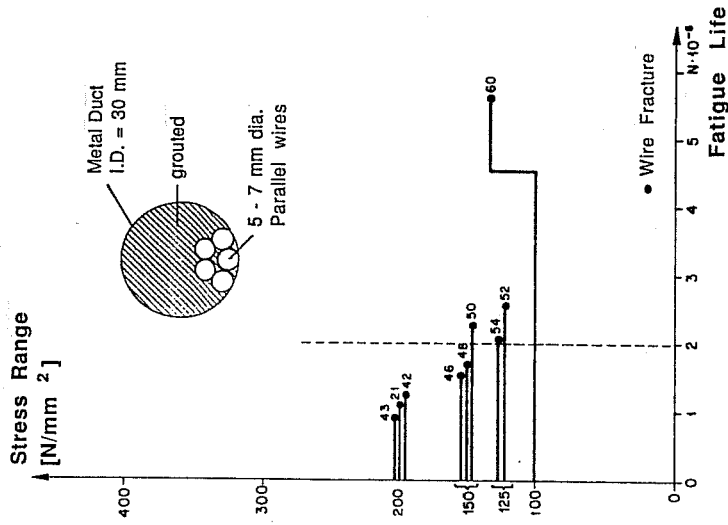
b) Multiple Wire Tendons

Figure 2.12   Comparison of Single Wire and Multiple Wire Tendons (from Oertle, et al. [19])

These stress ranges ensured a fatigue life of at least four million cycles for Oertle's specimens. The recommendations are valid for a contact load between corrugations of the duct and the prestressing steel of not more than 2 kN (0.45 kips). A method to determine these contact loads from the tendon geometry, tendon curvature, prestress force, and distance between duct corrugations is included in Oertle's dissertation.

It should be noted that Oertle's proposed value of allowable stress range, using plastic duct, of 200 N/mm^2 (29 ksi) for a life of four million cycles would be extremely high even when compared to the tests of strand in air reported earlier in this chapter. Further discussion of these recommendations will be made later.

Oertle also points out that tendons with plastic duct should always be grouted to minimize the slip between prestressing steel and duct, and thus to reduce the risk of rubbing through the plastic duct. In order to reduce the contact loads between duct and prestressing steel and to prevent rubbing through the plastic, Oertle developed a new configuration of plastic duct. This duct is characterized by a smaller number of corrugations and a larger wall thickness. Figure 2.13 shows the test result for the reduced beams described.

2.3.4 Fretting Simulation Tests. **Cordes, Lapp-Emden, and Trost** developed an apparatus to simulate fretting on a prestressing strand, which allows isolated parameter studies [9] (Fig. 2.9). Tests included 0.6 in. diameter seven wire strand, 7.0 mm diameter drawn wire, and 12.2 mm diameter, quenched and tempered wire. The slip amplitude was held constant at 0.15 mm. Lateral load was 0.75 and 1.0 kN/cm, respectively (5.1 and 6.8 kips/ft). Only the influence of metal duct was studied. All tests showed the typical characteristics of fretting fatigue:

- Cracks were initiated at contact points between duct and steel and were initially inclined.

- Traces of corrosion were found at these contact points.

Cordes, et al. also observed that fretting fatigue does not govern for large stress ranges. Fractures occurred outside the contact points at fatigue lifes similar to those found for strand in air tests (Fig. 2.14).

They also report tendon stress ranges which ensure a fatigue life of two million cycles, alhough a true endurance limit could not be found. These stress ranges are for

- 12.2 mm dia. quenched and tempered wire   :   170 N/mm^2 (25 ksi)

- 7.0 mm dia. drawn wire   :   160 N/mm^2 (23 ksi)

- 0.6 in dia. seven wire strand   :   170 N/mm^2 (25 ksi)
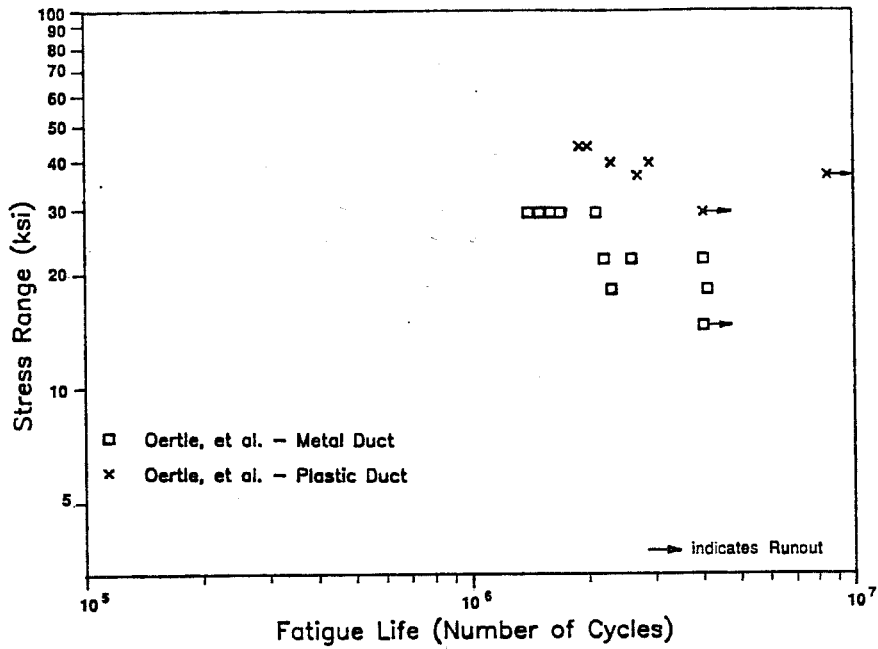
a) Strand Type Tendon
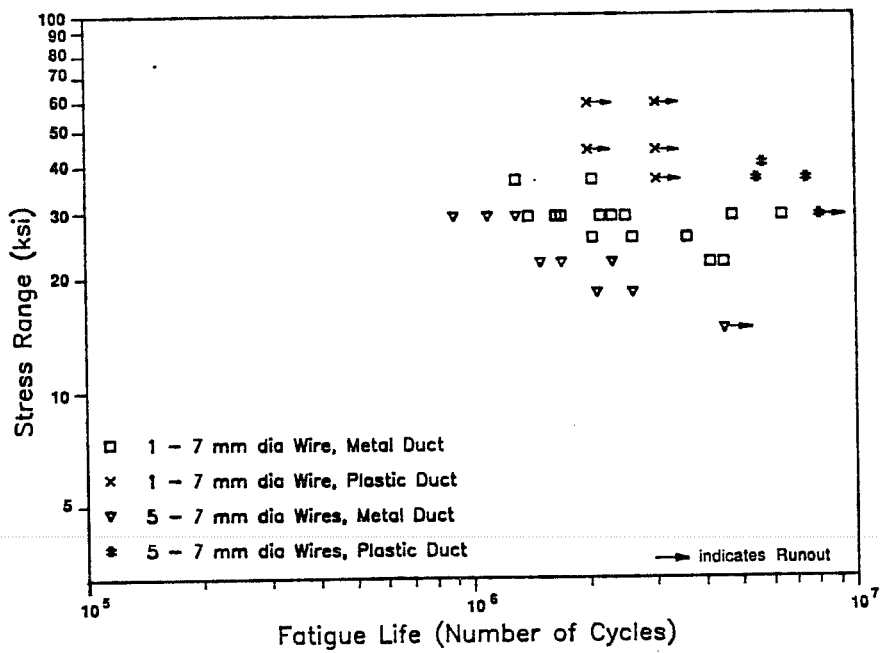
b) Parallel Wire Tendons (all Tests by Oertle [19])

Figure 2.13   Results of reduced beam tests

28
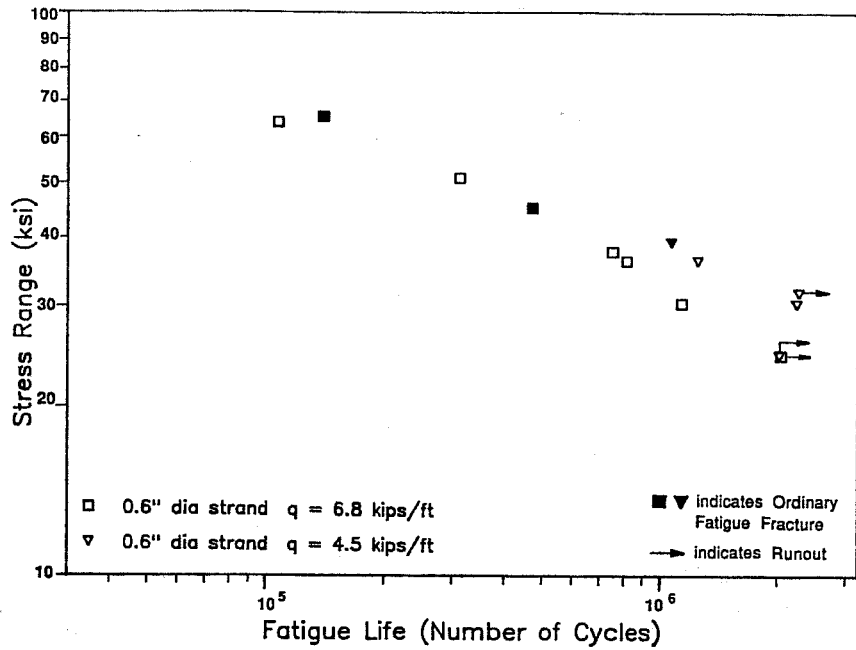
a) Strand Specimens
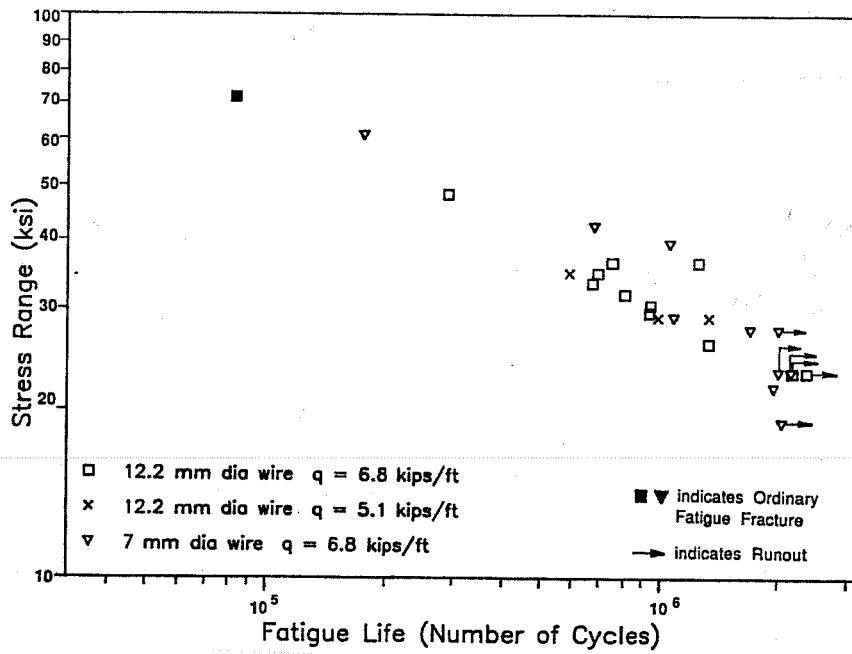
b) Wire Specimens

Figure 2.14 Results of fretting simulation tests

2.4 Code Provisions

2.4.1 United States. The *AASHTO Standard Specifications for Highway Structures* require dynamic tests of anchorages for unbonded tendons in prestressed concrete [1]. Generally, no dynamic tests are required for bonded tendons. No provisions are included concerning allowable tendon stress ranges to prevent fatigue distress of cracked pretensioned or post-tensioned concrete girders.

ACI 318-83 [3] states that in unbonded construction subject to repetitive loads, special attention shall be given to the possibility of fatigue in anchorages and couplers.

The Commentary on the Building Code Requirements refers to the *ACI Fatigue Committee 215* report [4] "for a more complete discussion on fatigue loading". In this report a maximum tendon stress range of 4% of the nominal tension strength f_{pu} of the prestressing steel is recommended. This would be equal to 10.8 ksi for GR 270 steel. The recommendation applies to strand, bars, or wires prestressed between 0.40 f_{pu} and 0.60 f_{pu}.

ACI Guideway Committee 358 recognizes the more severe conditions for curved, post-tensioned tendons and recommends a maximum stress range of 0.025 f_{pu} for these cases [5]. Otherwise they recommend 0.040 f_{pu}, as does the ACI Fatigue Committee 215.

2.4.2 West-Germany. DIN 4227/part 2 recommends the following values for the allowable tendon stress range [12]:

- for strand and wire tendons : 110 N/mm^2 (16.0 ksi)
- for threaded bars : 140 N/mm^2 (20.3 ksi)

2.4.3 CEB-FIP Provisions. The European Model Code for Concrete Structures includes fatigue recommendations in an appendix [7]. If no test results are available it recommends a maximum stress range Sr:

- for prestressing tendons (without bond due to deformed shape) : 200 MPa (29.0 ksi)

- for prestressing tendons (with bond due to deformed shape) : 150 MPa (21.8 ksi)

These values have to be modified by a factor of safety equal to 1.25, and a coefficient to account for the radius of curvature of the tendon. Hence the allowable stress range becomes

all Sr $\leq$ Sr / 1.25 x (1 - 1.5 x d x r),

where d is the diameter of bar, wires, or strands in the tendon in meters, and r is the radius of curvature, also in meters. For 0.5 in. diameter strand and 3.50 m radius of curvature the allowable stress range would equal 16.2 ksi in bonded tendons.

A comprehensive state of the art report on fatigue of conctrete structures was published by CEB in June 1988 [32]. One chapter is dedicated to the fatigue of reinforcing and prestressing steel and also treats the problem of fretting fatigue in partially prestressed concrete members. The tests by Cordes and Lapp-Emden, Muller, and Rigon and Thurlimann are presented [9,18,26].

Two general fatigue models are proposed; one for ordinary fatigue, the other for fretting fatigue of prestressing steel. The latter model is based on the tests mentioned above. In Figure 2.15 both models are presented. Note that no endurance limit is indicated, neither for ordinary fatigue nor for fretting fatigue. If the tendon is subjected to less than N_1 load cycles the same model is used for ordinary fatigue and fretting fatigue.

Figure 2.15   Proposed fatigue models by CEB general Task Group 15 [32]

CHAPTER 3

TEST PROGRAM

3.1 Development of Test Specimens

3.1.1 Girder Specimen. In actual bridge structures, post-tensioned concrete is frequently used in girders in both superstructure and substructure applications. These girders generally make use of curved tendon layouts, both to increase the tendon eccentricity near supports and midspan and to provide inclined tendon shear capacity. Thus realistic girder specimens for laboratory tests should include some tendon duct curvature. In addition, girder specimens should be large enough to simulate, at a realistic scale, a number of strands in a single tendon so that there is a possibility of strand interaction. In order to provide a baseline reference for important variables and to provide a realistic check for the results determined from reduced beam test specimens, a series of tests of simply supported post-tensioned beams were carried out by Diab [11] and Georgiou [15] as part of this overall program.

While a girder specimen best duplicates the conditions in an actual structure, it has drawbacks that make monitoring of some of the important parameters difficult. Particularly, accurate determination of the tendon force is a major problem. The level of prestress in a girder varies substantially along the tendon, due to seating losses at the anchorage device and due to friction forces between strand and duct. Time effects of relaxation, creep, and shrinkage cause

further prestress losses. Estimation of these parameters is subject to quite appreciable uncertainties, even under controlled laboratory conditions. Unfortunately, the influence of the effective prestress level on the tendon stress range is very significant for conventional girders, as is shown in Figure 3.1. This figure illustrates the behavior in terms of tendon stress of two otherwise identical girders, A and B, subjected to the same load cycling from 10 kips to 42 kips. Girder A, with high losses, has an effective prestress level of 160 ksi. Under the load increment of 32 kips it has a stress increase of 30 ksi. In contrast, Girder B which has lower losses and an effective prestress level of 170 ksi would have a substantially lower tendon stress increase of 25 ksi for the same load range.

Furthermore, usually a small amount of passive (non-prestressed) longitudinal reinforcement is present in girders. The tensile stresses acting on a girder cross section are distributed to passive and active (prestressing) reinforcement according to the bond characteristics and cross section areas of the reinforcement. This makes it difficult to accurately determine the stress range in the prestressed tendon.

A difficulty of another nature is the cost and complexity of girder specimens. Fatigue and fretting fatigue tests usually show substantial scatter in the test results, and

34
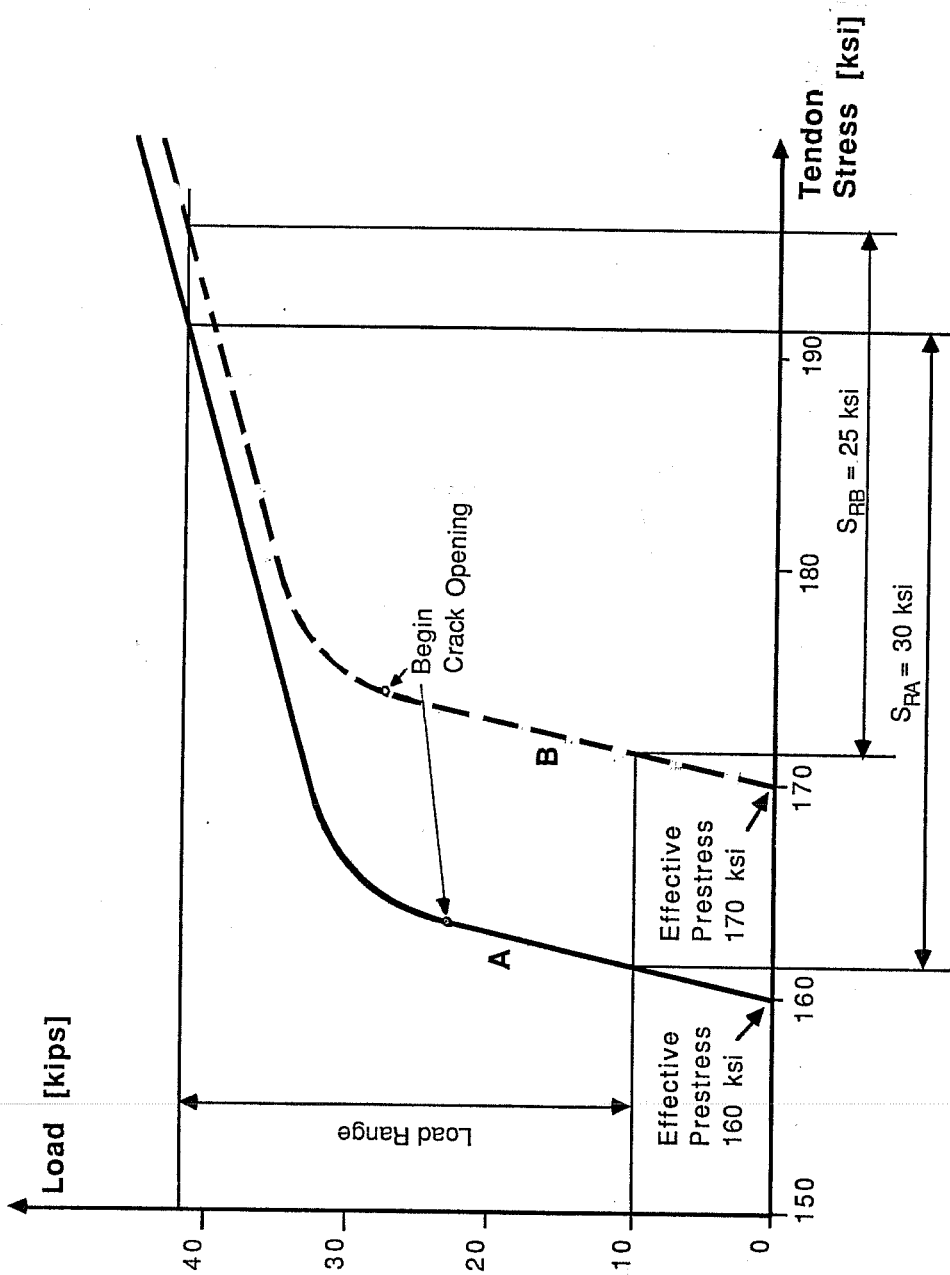
Figure 3.1   Influence of Prestress Level

a large number of data points is required for a reliable evaluation. Therefore, a smaller specimen is desirable to generate enough data points at low cost and within a short time period.

3.1.2 Reduced Beam Specimen.

3.1.2.1 General. To avoid the problems addressed above Oertle, Thurlimann, and Esslinger developed a "reduced beam" specimen [19]. Its essential principles are illustrated in Figure 3.2, which shows the University of Texas version of the reduced beam.

Significant differences between the reduced beam specimens and actual girders are the concentration of the large girder compression zone at a steel hinge in the reduced beam cross section and elimination of non-prestressed reinforcement across the critical cross section. Upon complete cracking of the remaining concrete zone, only the prestressing tendon carries tension forces. With the measured ram force known, the tendon force can be accurately determined from a simple equilibrium equation (see Fig. 3.2b).

The reduced beam specimen reproduces accurately the following important aspects of fretting fatigue in post-tensioning tendons: Debonding and slip of strand on duct or other strands occurs in the vicinity of the crack, the tendon force is sharply increased at the crack, and lateral and friction forces act on the strand.

However, there are some differences between girders and reduced beams, and their influence has to be considered:

- In girders the cracks close completely after each load cycle. For reduced beams it is essential to keep the crack open in order to maintain a statically determined tendon force.

- The strain and stress distribution in the compression zone of the critical cross section of reduced beams differ from the conditions in girders, due to the introduction of the steel roller assembly.

- No concrete tensile zone is available in completely cracked reduced beams.

- The critical cross section of the reduced beams is subjected to a bending moment without any shear force. For actual structures, frequently large tendon curvatures occur near locations of concentrated loads, such as interior supports of continuous beams, to balance these loads. Hence, very often the bending moment is accompanied by a shear force at such locations (Fig. 3.3).

As will be shown, these differences do not alter the test results significantly. Thus, the reduced beam specimen is a valuable tool for fretting fatigue tests of prestressing tendons in post-tensioned concrete.
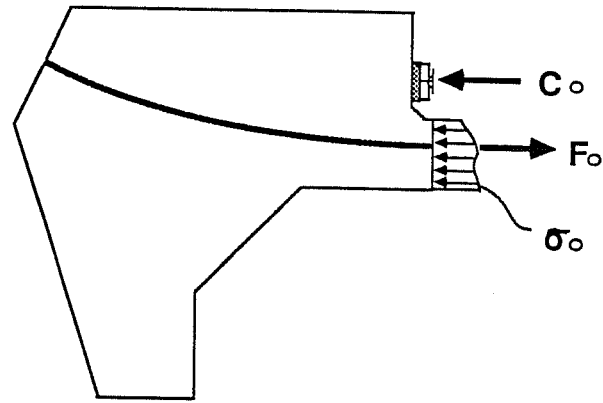
(a) Crack closed
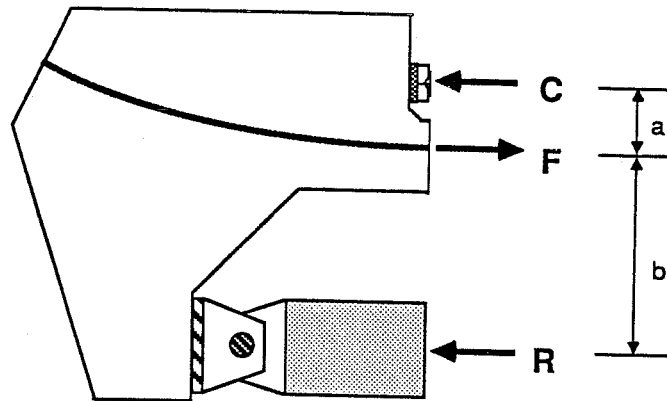
(b) Crack open

Tendon force, $F = R(a+b)/a$

Figure 3.2   Principle of Reduced Beam Specimen (from Yates [31])
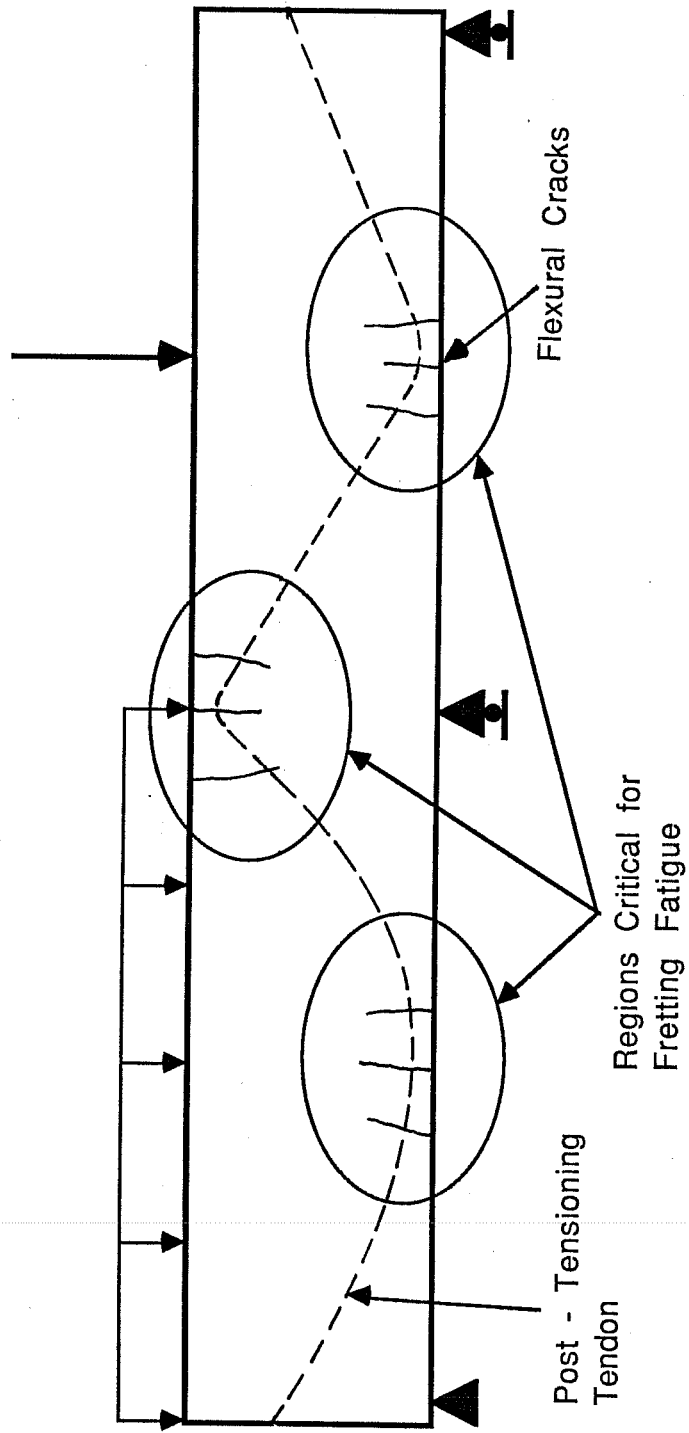
Figure 3.3   Critical Zones for Fretting Fatigue
in Girders (after Yates [31])

3.1.2.2 Single Strand Reduced Beams. The size of the reduced beam specimen depends directly on the tendon force to be accommodated. The smaller the tendon, the smaller and more economical the reduced beam can be.

The single strand reduced beam tests described by Yates in Reference 31 facilitated a quick and fairly economical generation of data points. An important objective of the single strand reduced beam tests was to generate a larger number of data points, in order to facilitate an evaluation of the fretting fatigue behavior of post-tensioning strand. Therefore only two parameters were considered in the single strand tests: Stress range and duct material. However, when using only one strand, some important aspects of fretting fatigue in post-tensioning tendons are excluded, such as the possibility of strand to strand rubbing. Thus, an investigation of reduced beam specimens with multiple strand tendons was necessary.

3.1.2.3 Multiple Strand Reduced Beams. The multiple strand reduced beams described by Wollmann in Reference 34 are based on the same basic idea as the single strand reduced beams. However, in order to accommodate the larger tendon forces, the overall dimensions of the specimen had to be adjusted, larger prestressing jacks and rams were required, and handling became more difficult due to the increased size and weight.

When using a multiple strand tendon, group effects, such as fretting between individual strands and local distribution of contact pressure between multiple strands in the tendon are reflected in the test results. It has been shown that the local lateral pressure between individual strands as well as the contact pressure between strand and duct are sensitive to duct size, and to the number, diameter, and arrangement of the strands [31].

The multiple strand reduced beam tests had different objectives. First, they were to verify the applicability of the single strand reduced beam test results. Second, in addition to stress range and duct material further important parameters - tendon curvature and strand coating - were investigated. This investigation was limited in scope, since the increased size and cost of the specimen did not allow fabrication and testing of a sufficiently large number of specimens for a comprehensive statistical evaluation. Once the group effects of multiple strand tendons are understood, the single strand reduced beam can be used to facilitate a quantitative evaluation of more parameters.

3.2 Design of Test Specimens

3.2.1 Design Criteria. The choice of tendon size, dimensions of the specimens, and auxiliary reinforcement was based on several design criteria:

-   In girder and multiple strand reduced beam specimens, the tendon should be as small as possible, but yet consist of enough strands to achieve a group effect.

- The prestress level should be close to the level in actual structures.

- Cracking of the critical cross section must be possible without yielding of the prestressing tendon.

- Failures away from the critical cross section had to be prevented.

Dimensions and details of the girder specimens which evolved from this criteria are shown in Figures 3.4 and 3.5. All but one of the girders tests were as shown in Figure 3.4. Dimensions and details of the single strand reduced beam specimens which met all of the criteria except for the group effect of strands are shown in Figure 3.6. Dimensions and details of the multiple strand reduced beam which evolved from these criteria are shown in Figure 3.7. For two specimens the tendon layout was slightly changed in order to reduce the curvature, as indicated by the dashed line in Figure 3.7.

3.2.2 Auxiliary Reinforcement. In the girder, a small amount of non-prestressed longitudinal reinforcement was provided in all specimens. Since the presence of such passive reinforcement complicates the determination of the tendon stress range, it was kept to a minimum. Presence and amount of longitudinal passive reinforcement was not a parameter in this study. Shear and confining reinforcement were provided to meet basic ACI and AASHTO requirements. Basic stirrup sizes were #3 bars spaced at 4 in. on center in the vicinity of the load points.

The load arms of the reduced beam specimens were prestressed to control cracks and prevent failure away from the critical cross section. Additional passive reinforcement was required to control cracks occurring at the transition from beam to load arms. Design of this reinforcement for the larger multiple strand specimens was based on a simplified strut and tie model, shown in Figure 3.8. Compression struts are shown by dashed lines while tension ties are shown as solid lines. To avoid fatigue failure, calculated stress ranges in the passive reinforcement were limited to 25% of yield stress. The design followed general principles presented in the excellent paper by Schlaich, Schafer, and Jennewein on detailing using the strut and tie model [27].

Further local confining reinforcement was provided to control anchorage splitting forces as required. The arrangement of the auxiliary reinforcement for the multiple strand specimens is illustrated in Figure 3.9.

3.3 Materials

3.3.1 Prestressing Strand. The primary tendons were composed of 0.5 in. diameter, Grade 270, low relaxation seven wire strand. This strand complied with ASTM A416 specifications. It was taken from four different spools, denoted A, B, C, and D below. All spools were stored inside the laboratory to prevent corrosion.
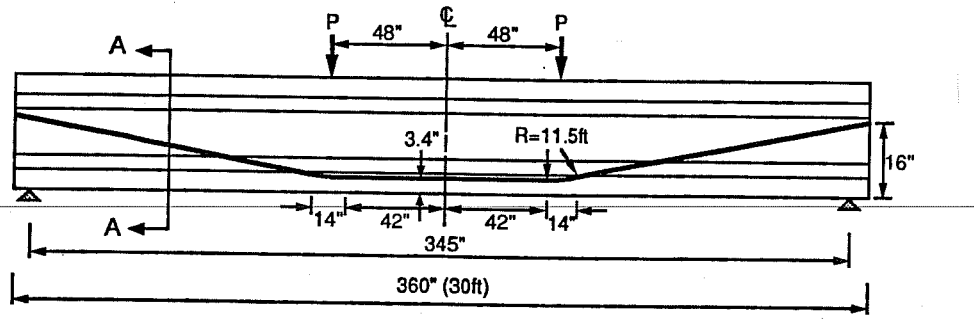
a) Elevation
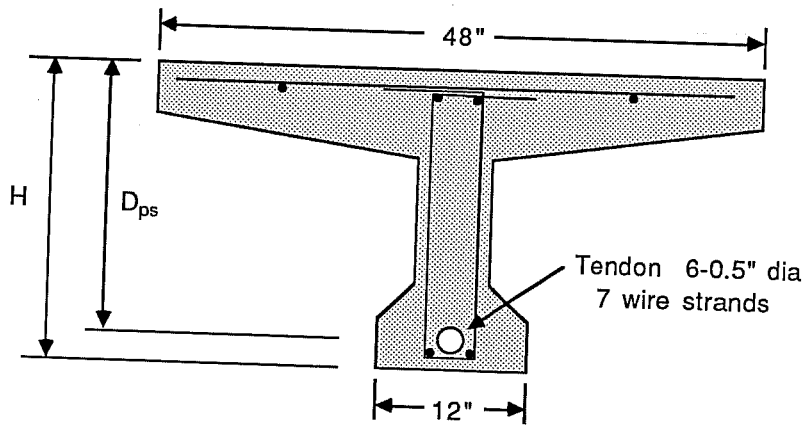
H = 24 in.
D_{ps} = 0.86 x H

SECTION AREA = 408 sq. in.
MOMENT OF INERTIA = 21,831 in.^{4}

b) Midspan Section

Figure 3.4   UT primary girder test specimen [31]

a) Elevation

H = 24 in.
D_{ps} = 0.86 x H

SECTION AREA = 408 sq. in.
MOMENT OF INERTIA = 21,831 in.^{4}
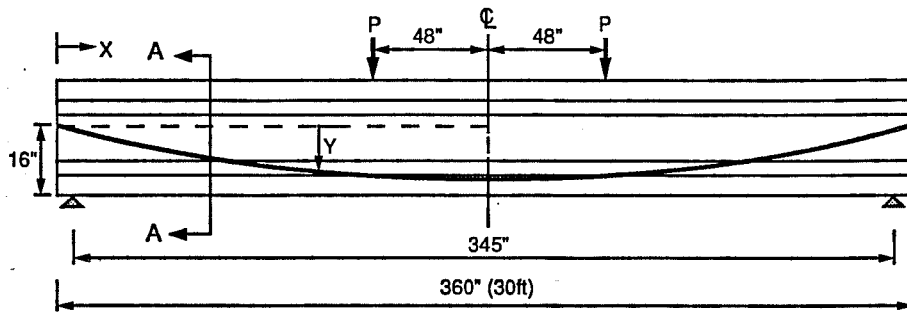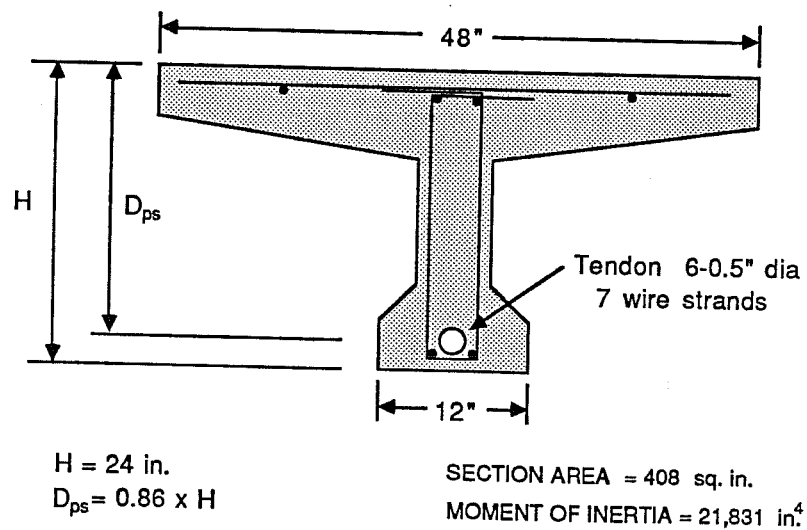
b) Midspan Section

Figure 3.5   UT secondary girder test specimen [31].

42
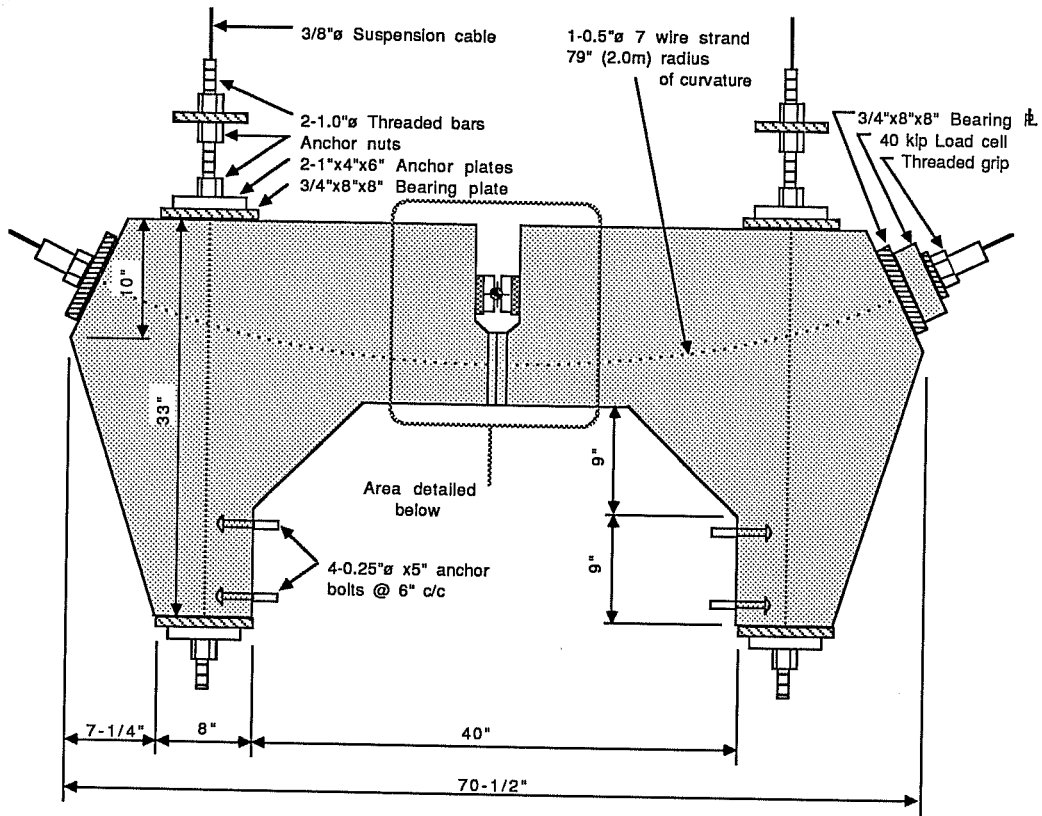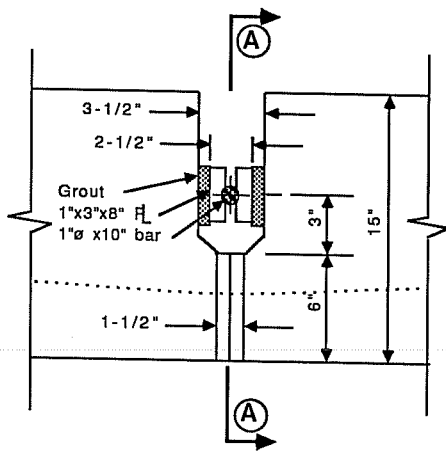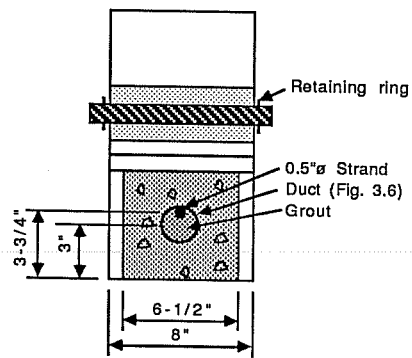
Figure 3.6   Dimensions and details of single strand reduced beam specimen [31]
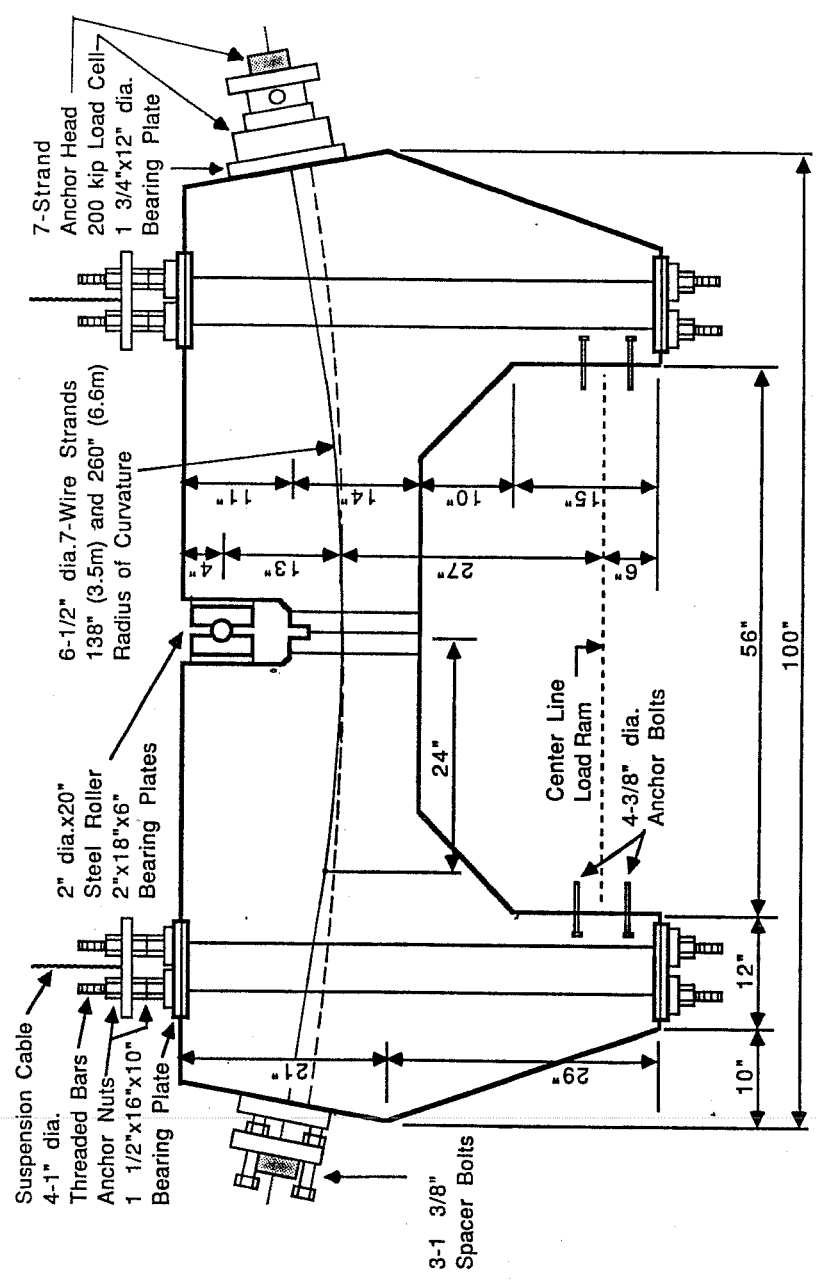
Figure 3.7 Dimensions and details of multiple strand reduced beam specimens [34]

44
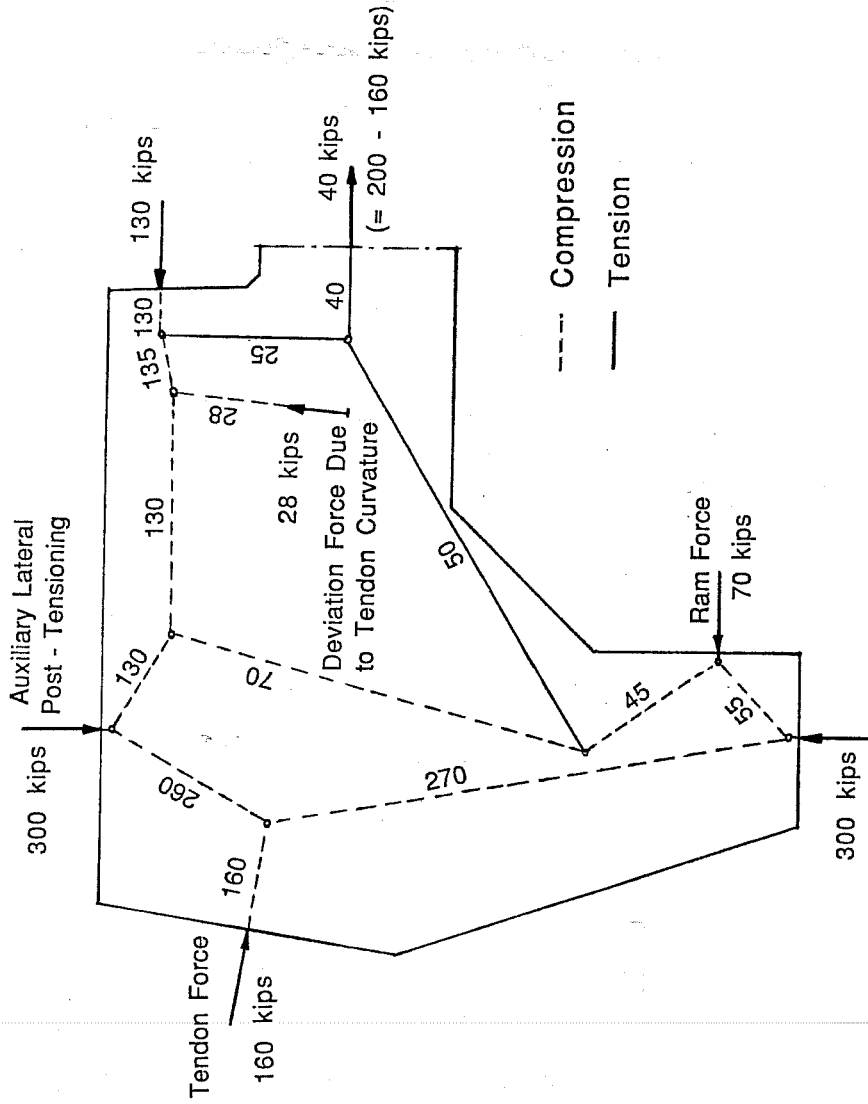
Figure 3.8 Strut and tie model [34]
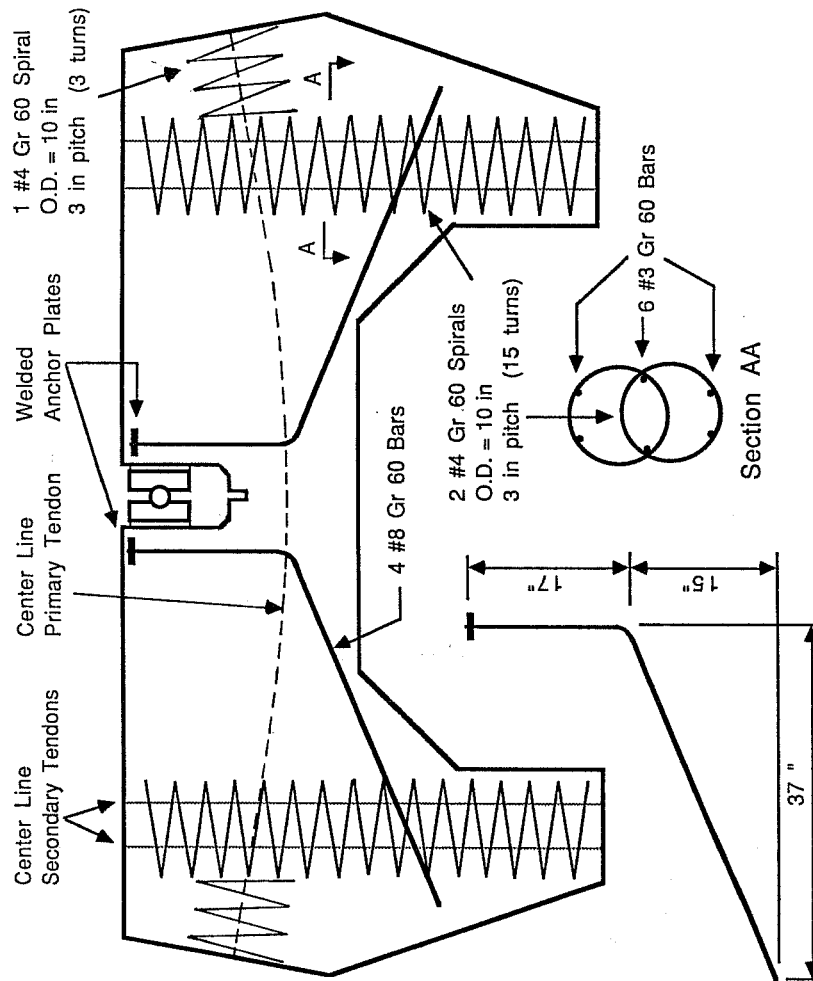
Figure 3.9 Auxiliary reinforcement [34]

Strand A was used in previous projects at Ferguson Structural Engineering Laboratory, including Paulson's work [22], Overman's beams [21], and was also used for some of the single strand reduced beams [31] and some of the multiple strand reduced beams [34]. Strand B was from the same supplier as A, and was used for the remainder of the single strand reduced from specimens and the girders tests of Diab [11].

Strand C was manufactured by a different supplier who provided material for laboratory use when the reel of strand A was used up. It was used for some of the multiple strand reduced beam specimens and for the girder tests of Georgiou [15].

Strand D also was used in a previous project at Ferguson Laboratory [24]. It is a recently developed epoxy coated strand. The epoxy coat was about 0.04 in. thick and impregnated with a grit of crushed glass to improve its bond characteristics. More information on this subject can be found in Reference 10.

Strand in air fatigue tests were performed on samples of all strands to obtain information on their fatigue characteristics. In Figure 3.10 the results of these tests are plotted. Runouts and grip failures were excluded from the figure. The general strand in air failure zone as defined by Paulson [22], based on an evaluation of over 700 fatigue tests shown in Figure 2.3, is indicated by the dashed lines. The new data points all fall within this area, and there is no indication of a significant difference in the fatigue behavior of the four types of strand when tested in air.

3.3.2 Duct. Two types of duct were used for the tendons of all specimens:

- galvanized folded metal duct

- polypropylene corrugated plastic duct.

Both types were purchased from a well known post-tensioning supplier. The actual dimensions are shown in Figure 3.11.

3.3.3 Grout. The same grout mix, complying with TSDHPT Standard Specifications, was used for all specimens:

- 1 bag Portland Cement, Type I

- 5 1/2 gallons water

- 0.94 lbs Interplast (expansion admixture).

The grout strengths were determined at beginning of the fatigue tests from compression tests of three 2 in. cube specimens and are listed in Table 3.1.

3.3.4 Concrete. Actual concrete strengths were determined from compression tests of 6.0 x 12.0 in. cylinders before prestressing and at beginning of the fatigue tests. The results are listed in Table 3.1.
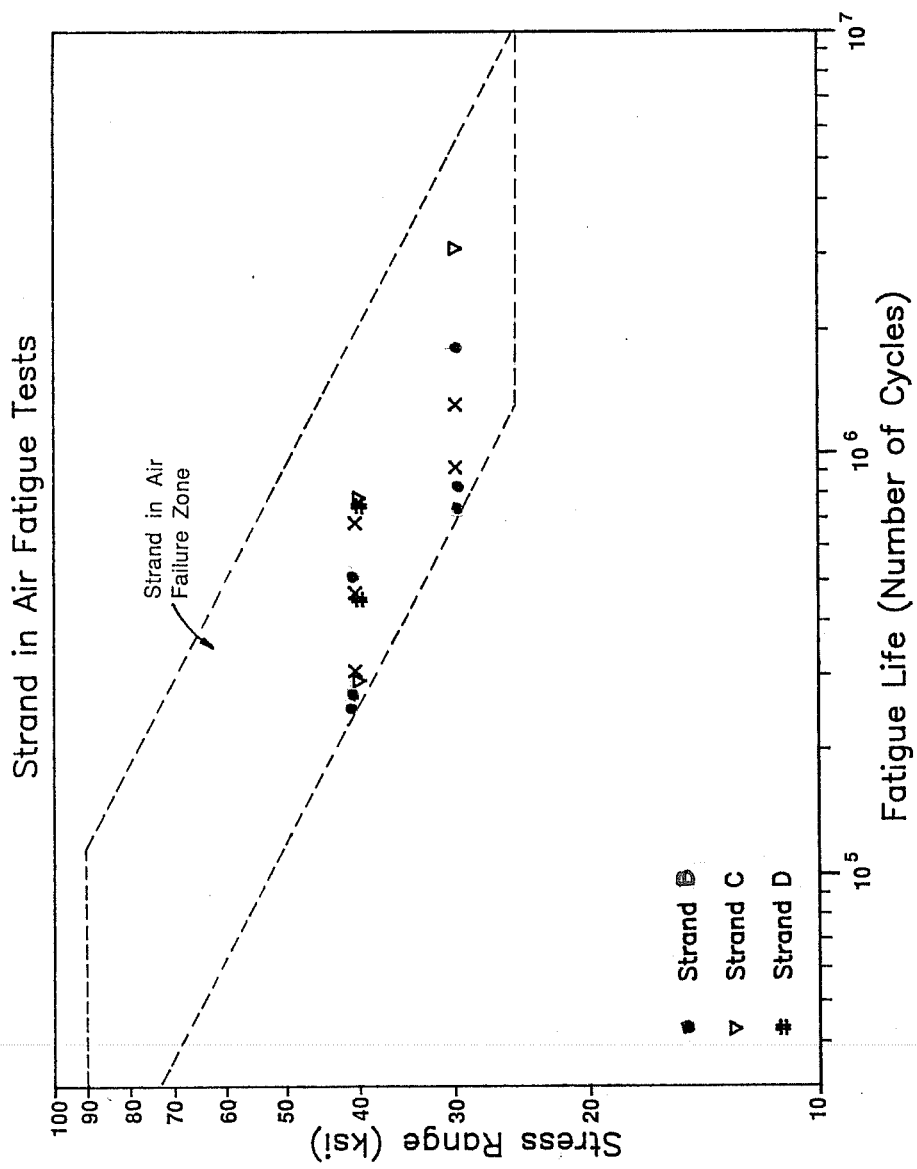
Figure 3.10 Strand in air test results

2.75 "

0.55 "

t = 0.03 "

2.0 " I.D.

2.2 " O.D.

Folded Seam

Longitudinal Section   Transverse Section

Metal Duct

0.42 "

t = 0.06 "

2.0 " I.D.

2.5 " O.D.

Longitudinal Section   Transverse Section
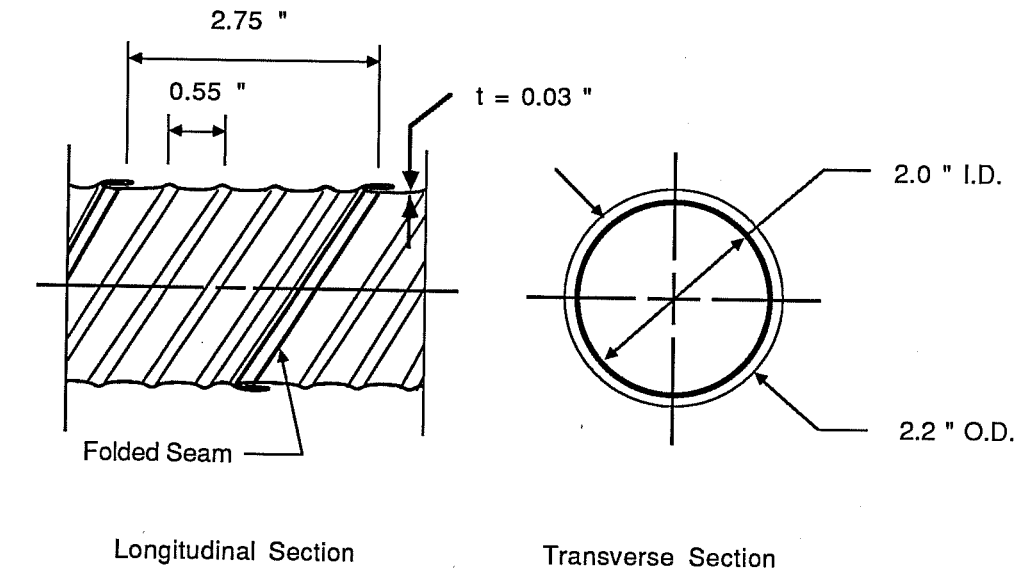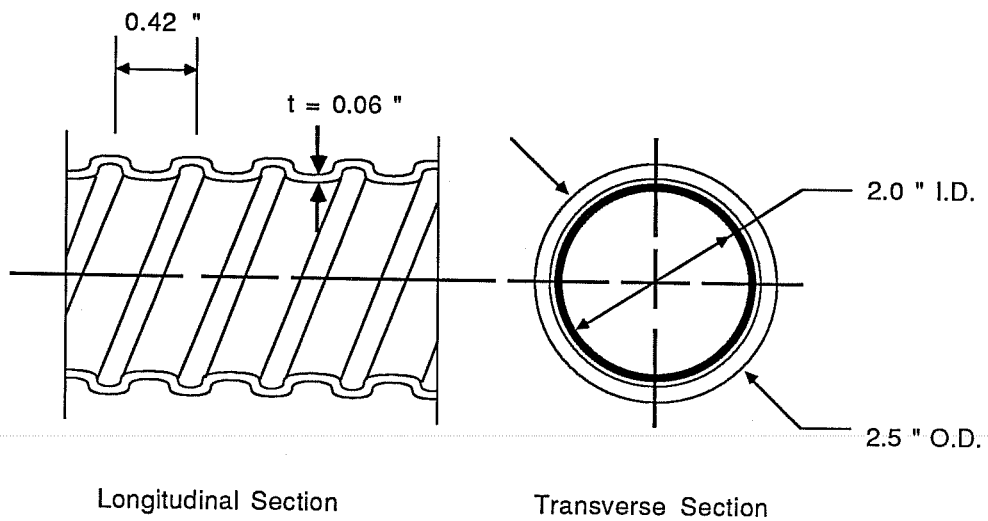
Plastic Duct

Figure 3.11a   Measured dimensions of post-tensioning ducts for single strand reduced beam specimens [31]

2.75 "

0.55 "

t = 0.03 "

2.13 " I.D.

Folded Seam

2.32 " O.D.

Metal Duct

0.42 "

t = 0.06 "

2.0 " I.D.

2.5 " O.D.
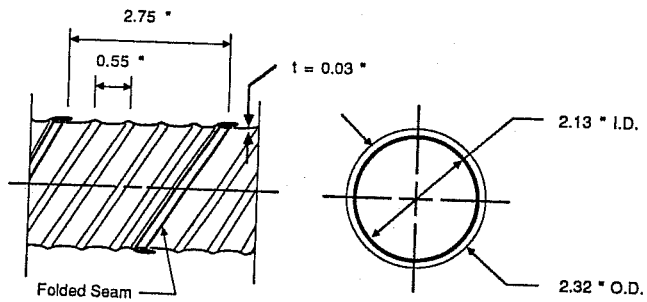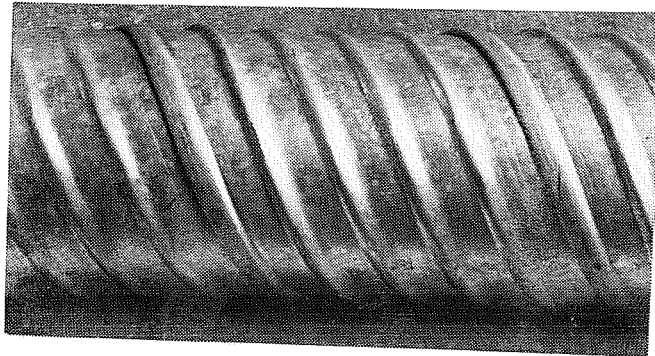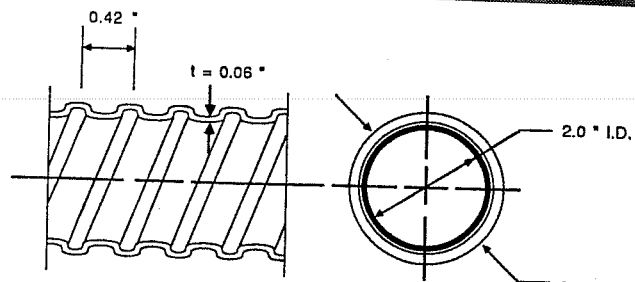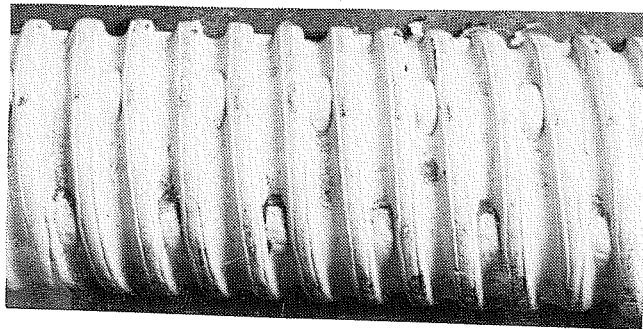
Plastic Duct

Figure 3.11b   Measured dimensions of post-tensioning ducts for girders and multiple strand reduced beams [34]

Table 3.1   Concrete and Grout Strengths

Specimen	Concrete Strength* (psi)	Grout Strength* (psi)
Girders		
GD-M-1-47-0.23	7800	3600
GD-M-2-32.5-0.30	7600	2800
GD-M-3-23-0.32	8800	3200
GD-M-4-25-2.10	5400	2700
GD-M-5-30-0.80	6400	3200
GD-P-6-40-0.49	6700	2700
GD-P-7-30-1.30	6600	2900
GD-P-8-30-0.70	7200	N/A
Single Strand Reduced Beams		
M-1-40-0.00	270	N/A
M-2-40-0.29	353	2240
M-3-30-0.32	3200	2560
M-4-30-0.47	3710	1940
M-5-20-1.27	2550	2340
M-6-18-NF	2600	2940
M-7-30-0.84	3050	2890
M-8-22-4.52	3140	2930
M-9-25-0.80	5410	2300
M-10-19-1.50	6460	3390
M-12-25-1.01	5140	2560
P-11-30-1.84	5040	1950
P-13-40-1.11	4600	2590
P-14-25-3.54	4410	2760
Multiple Strand Reduced Beams		
M6-1-40-0.10	4200	N/A
M6-2-30-0.49	4700	2000
M6-3-20-(0.62)	4400	2700
P6-4-30-0.37	4200	3000
M6-5-20-1,02	4400	2500
P6-6-30-0.50	4800	2500
C6-7-30-0.69	4800	2400
Q6-8-30-0.26	4500	2500
Q6-9-30-0.38	4500	3000

*at beginning of testing

3.3.5 Auxiliary Reinforcement. The load arms of the reduced beam specimens were prestressed with two or four secondary tendons per arm. Each tendon was composed of a 1.0 in. diameter, Grade 150, threaded prestressing bar in a 1.5 in. diameter electrical metal conduit. The tendons remained ungrouted.

For the passive reinforcement of all specimens ASTM A615 Grade 60 steel was used.

3.4 Fabrication

3.4.1 Concrete Placement. All specimens were cast in wooden forms. Careful attention was paid to bending and alignment of the conduit for the primary tendon. A steel barrel was used as a guide for bending, and the radius of curvature was repeatedly compared to a prefabricated template. Particular efforts were made to achieve constant curvature in the curved sections.

Alignment was monitored using several control markers on the formwork, and the exact position of the primary tendon at the critical cross section was recorded after installment. Figures 3.12 and 3.13 show the formwork for a reduced beam specimen shortly before concrete casting and a typical casting procedure, respectively.

Concrete was delivered from a local ready-mix plant and was placed directly from the truck. Consolidation was achieved by vibration with 3/4 in. and 1-1/2 in. roundhead internal vibrators. Nine 6.0 x 12.0 in. test cylinders were fabricated for each specimen. About two hours after casting the specimen was covered with wet burlap and plastic for at least 24 hours.

3.4.2 Prestressing Procedure. In the reduced beam specimens, about one day before prestressing, the steel hinge assembly was installed and grouted with hydrostone.

The secondary threaded bar tendons were stressed first to achieve an initial prestress force of about 75 kips in each tendon. One bar was stressed at a time, and a stressing sequence was chosen to minimize tensile stresses in the concrete due to eccentricity of the bars. The prestress force was monitored with a hydraulic pressure gage and verified after stressing by measuring the elongations of the threaded bars (Figure 3.14).

Immediately after stressing of the secondary tendons was completed the strands of the primary tendon were stressed. Several measures were taken to facilitate careful control and monitoring of the tendon force. In order to reduce prestress losses in the very short tendons due to slip at seating of the anchor wedges, a special bearing plate assembly was devised for the live end of the tendon of the multiple strand reduced beams, shown in Figure 3.15. A standard seven strand anchor head sits on a primary bearing plate which is supported by three spacer bolts. These bolts can be adjusted to compensate for seating
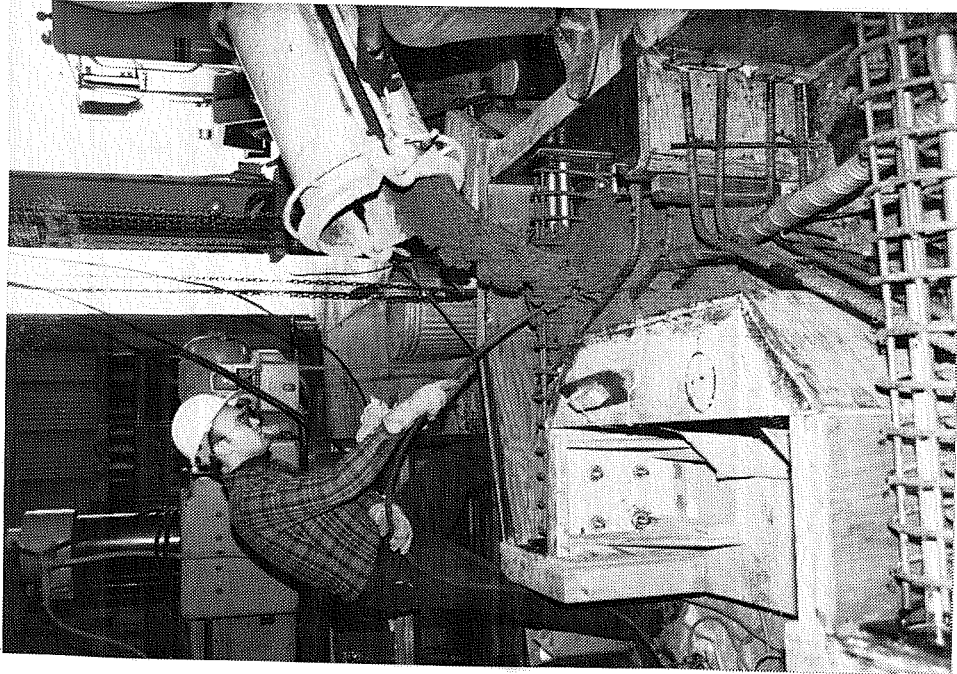
Figure 3.13   Typical casting procedure.
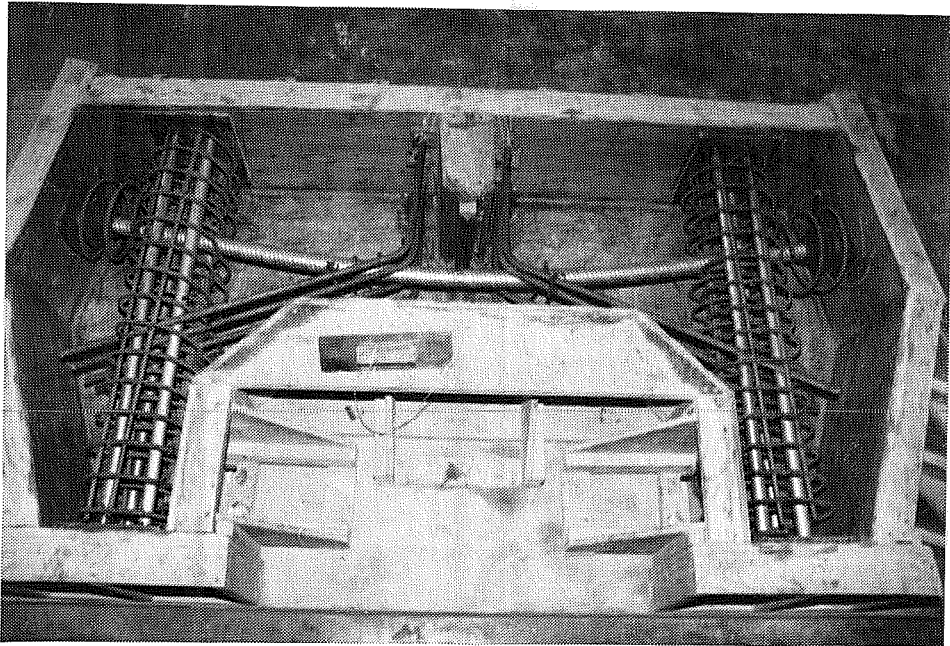
Figure 3.12   Formwork ready for casting
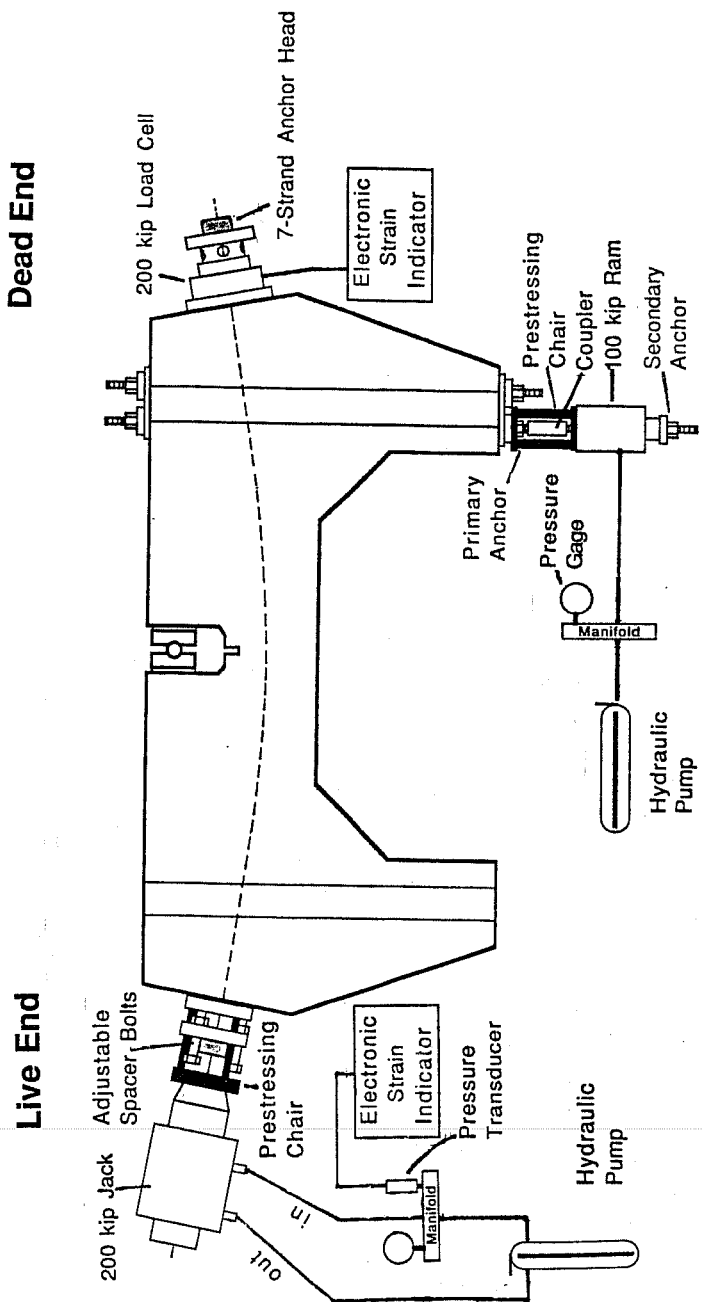
Figure 3.14 Post-tensioning setup

loss and stressing elongation. A secondary steel plate distributes the bearing stresses on the concrete.

The main tendon prestressing procedure involved three steps. First, the strands were stressed individually to about 0.2 f_{pu}, beginning with the strands on the inside of the curvature, to firmly seat the anchor wedges (Fig. 3.16). Most of this initial prestress was lost after release of the jacking force due to wedge slip in the seating process.

In a second step a 200 kip jack was used to stress all six strands simultaneously to 0.70 f_{pu} (Fig. 3.17). The wedges and anchor head held firmly together, due to the initial seating in the first step. Therefore the elongations of the strands caused the entire wedge - anchor head assembly to separate from the primary bearing plate. Thereupon the spacer bolts were adjusted to achieve close contact of plate and anchorhead again.

Release of the jacking force induced further anchor wedge slip and corresponding prestress losses. In the final step the tendon again was jacked to 0.70 f_{pu}, and the spacer bolts had to be readjusted to ensure a snug fit of the anchor head. Release of the jacking force now induced virtually no further wedge slip and no seating prestress losses.

The device worked very well. In fact, it was necessary to reduce the jacking force to 0.65 f_{pu} for the sixth and subsequent multistrand reduced beam specimens. The prestress losses were much smaller than anticipated, which lead to difficulties in cracking the test cross section of some of the early multiple strand reduced beams.

Stressing of the coated strands caused some initial problems. At higher stress levels the epoxy coat was ripped off at the anchor wedges, so that the desired tendon force could not be reached. The problem was eliminated by removing the epoxy coat in the anchorage zone with rotating wire brushes, to allow the chucks to bite into steel. Special chucks with deeper teeth have been used successfully for coated strands but were not available for the current tests.

The prestressing forces were monitored at the jack with a hydraulic pressure gage and an electronic pressure transducer. At the dead end of the tendon a 200 kip Interface load cell was installed. All equipment was calibrated at Ferguson Laboratory before first application.

A special assembly of bearing plates and a short, thick- walled steel cylinder with wall openings was developed to allow cutting of the tendon at the dead end and recovery of the load cell after testing of the specimen. The dead-end assembly is shown in Figure 3.18.

Similar procedures to minimize post-tensioning seating losses were used with the single strand reduced beams using a lock nut on the threaded barrel of the single strand line and chuck. In the girder tests, shims were inserted under the anchor head to perform
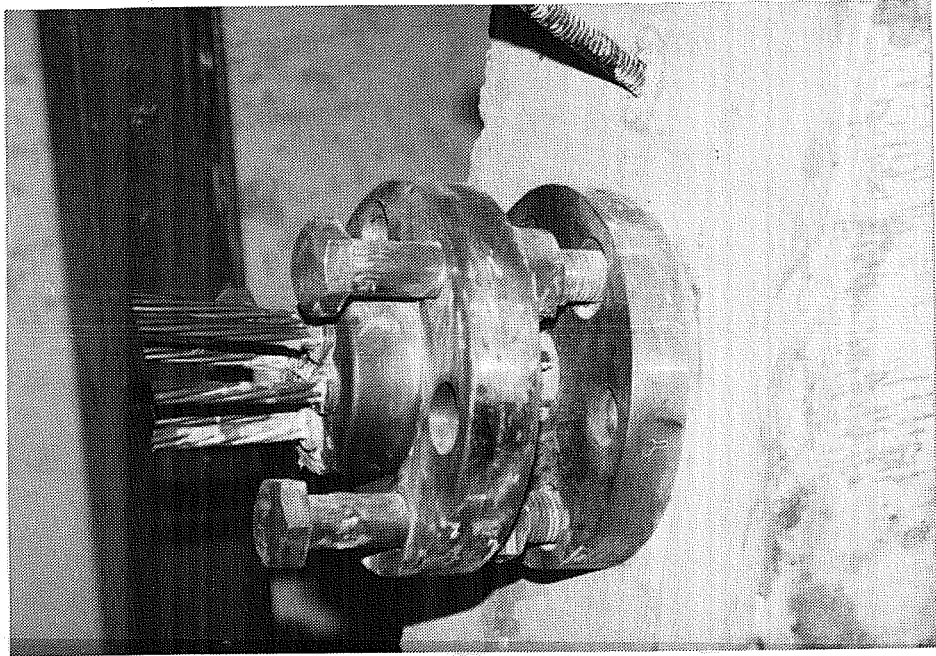
Figure 3.15 Live end
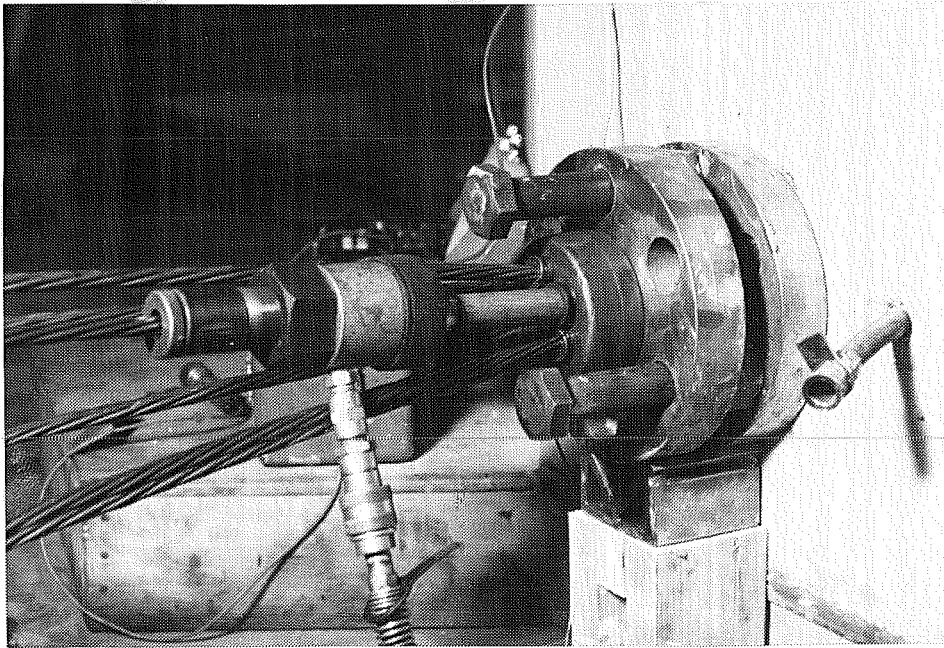
Figure 3.16 Individual stressing of strands
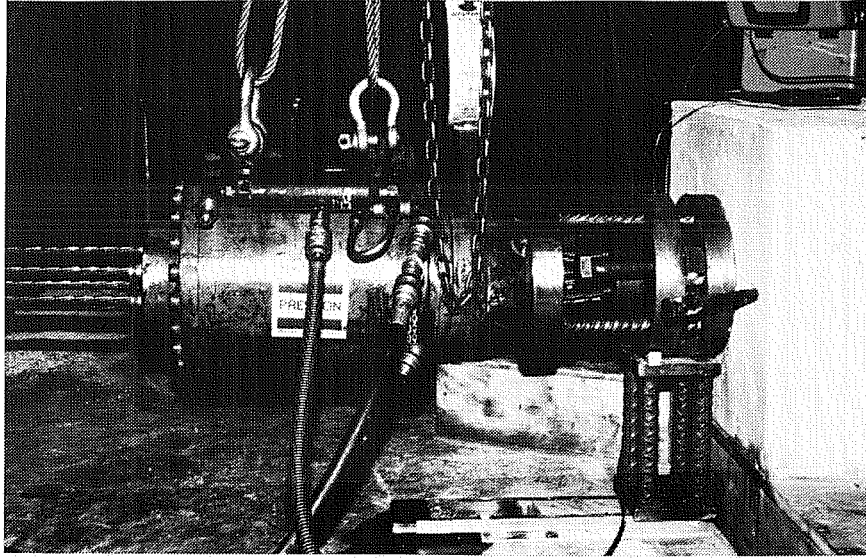
Figure 3.17   200 kip prestressing jack
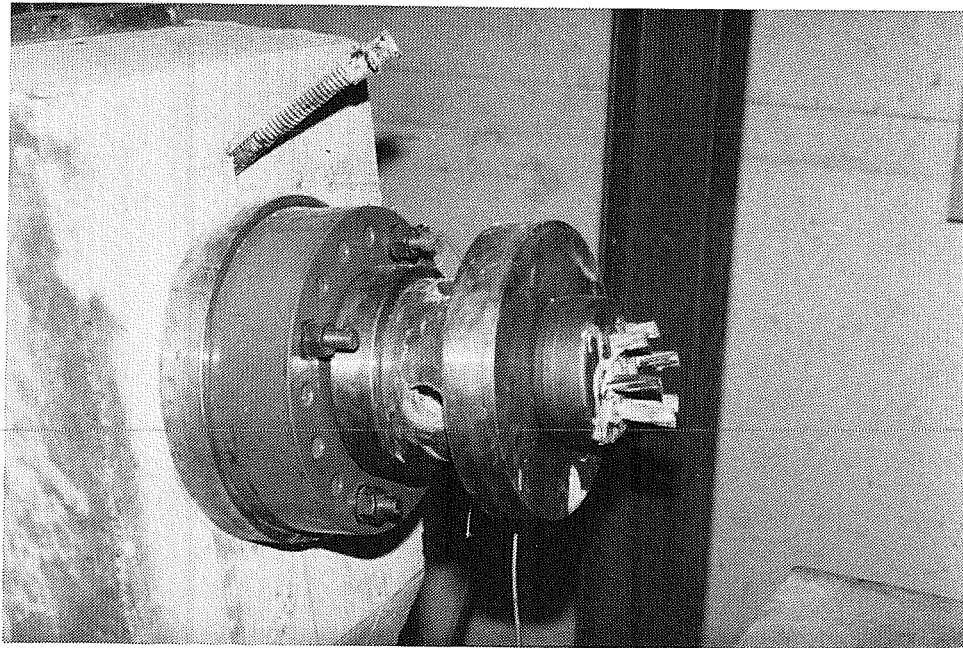
Figure 3.18   Dead end

the same function as the spacer bolts. With the small lengths involved in all specimens, it was essential to attempt to minimize these seating losses.

For the single strand reduced beams, strain gages were applied on the strands at different locations to allow additional monitoring of the prestress force [31]. This procedure was abandoned for the multiple strand tendons after unsuccessful attempts for the first three specimens. The majority of the strain gages were lost during feeding of the strands into the duct or during the prestressing procedure.

The specimens were grouted immediately after stressing or on the following day. A grout mixture as described in Section 3.3.3 was mixed and pumped into the tendon with a commercial grouting machine. Examination of the tendons recovered from the expired specimens consistently showed a very satisfactory grout quality.

3.4.3 Installation of Specimens. After grouting, the specimens were transported to the test frame with an overhead crane. The grout was allowed to cure for at least seven days before beginning testing. During this period the ram and potentiometers for measurement of crack width and displacement were installed, and the control system was calibrated.

In many cases frequent load cell readings were taken to monitor prestress losses in the primary tendon, which were found to be very small. Specimens ready for testing are shown in Figures 3.19 and 3.20.

3.5 Test Procedure

3.5.1 Reduced Beam Tests

3.5.1.1 Test Equipment. The primary test equipment used was an MTS closed loop servo control system. A schematic representation of this equipment is shown in Fig. 3.21 and a photograph of most of the actual equipment is shown in Fig 3.22. A larger ram and load cell were used for the multiple strand specimens. The hydraulic pressure was supplied by an MTS pump. An MTS accumulator with a MOOG servo valve controlled the hydraulic pressure applied to the ram. The forces exerted on the specimen by the ram were monitored with load cell read continuously on an MTS peak detector. The entire system was installed to provide controlled loads that were independent of displacement.

Several fail-safe mechanisms were utilized in conjunction with the test equipment. The factors which could lead to engagement of a fail-safe mechanism were:

- hydraulic fluid temperature in the pump

- hydraulic fluid level in the pump
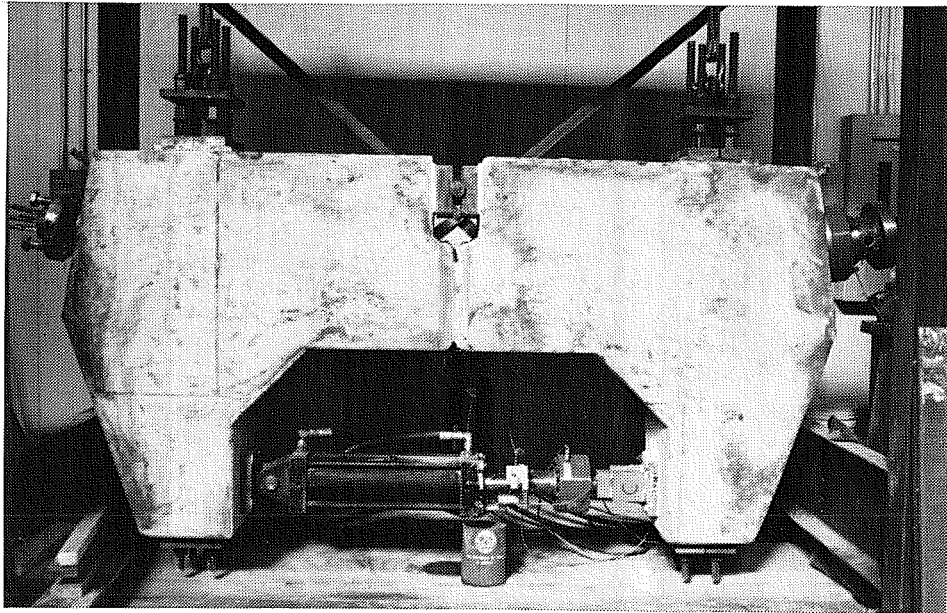
Figure 3.19   Specimen reading for testing
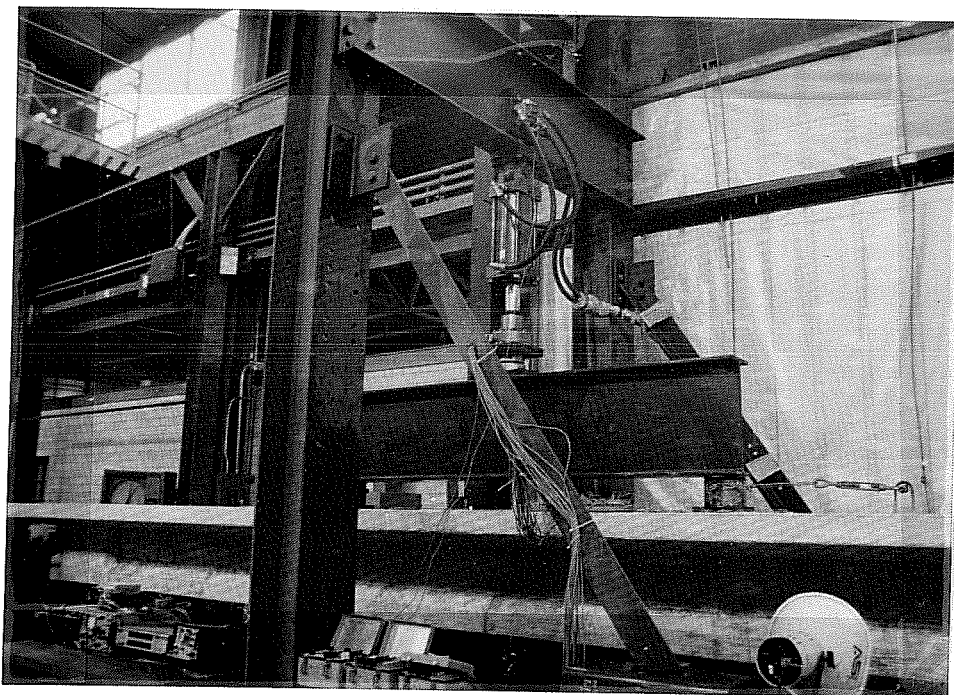
Figure 3.20   Test setup for girders

60
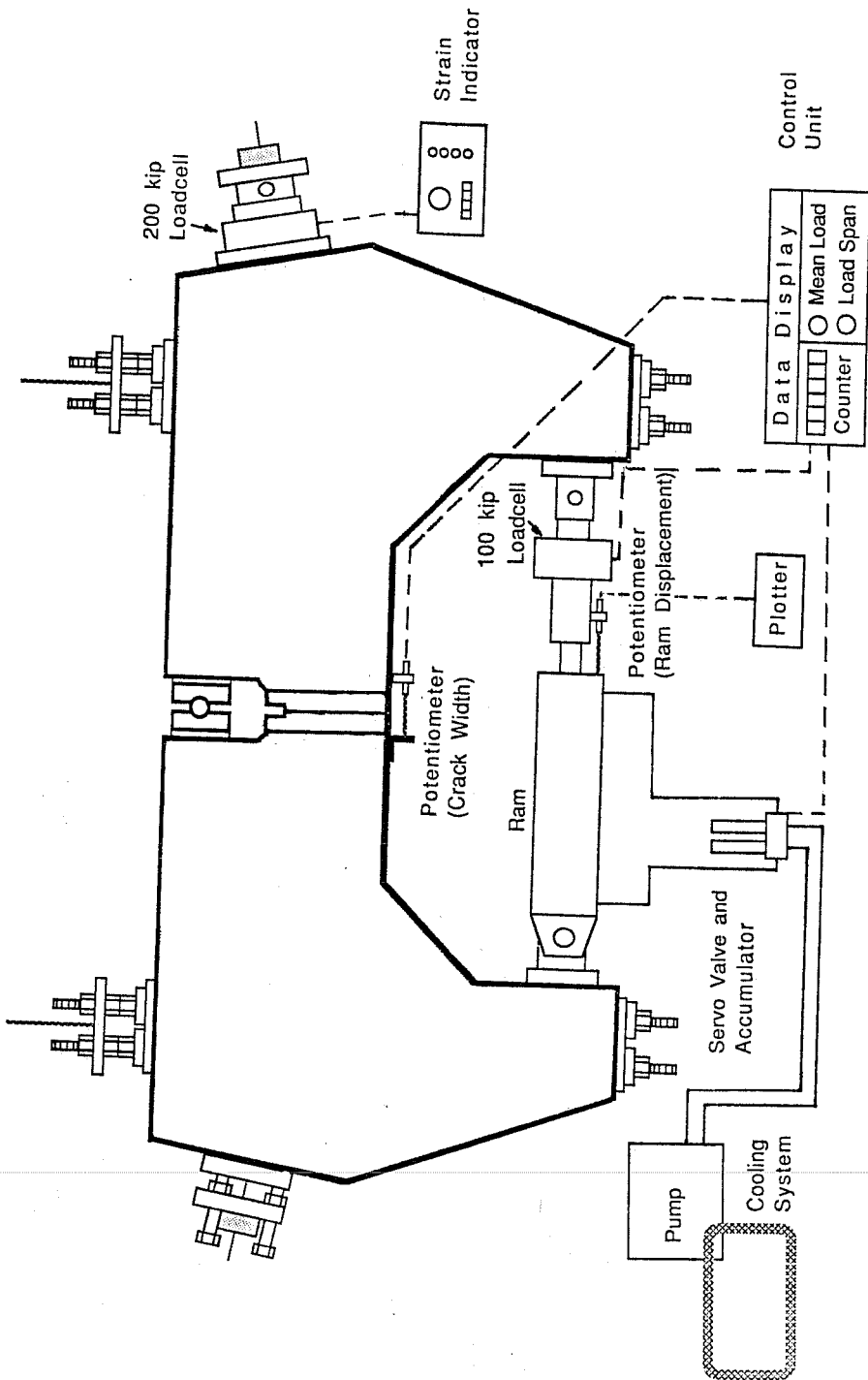
Figure 3.21 Load control and measurement systems
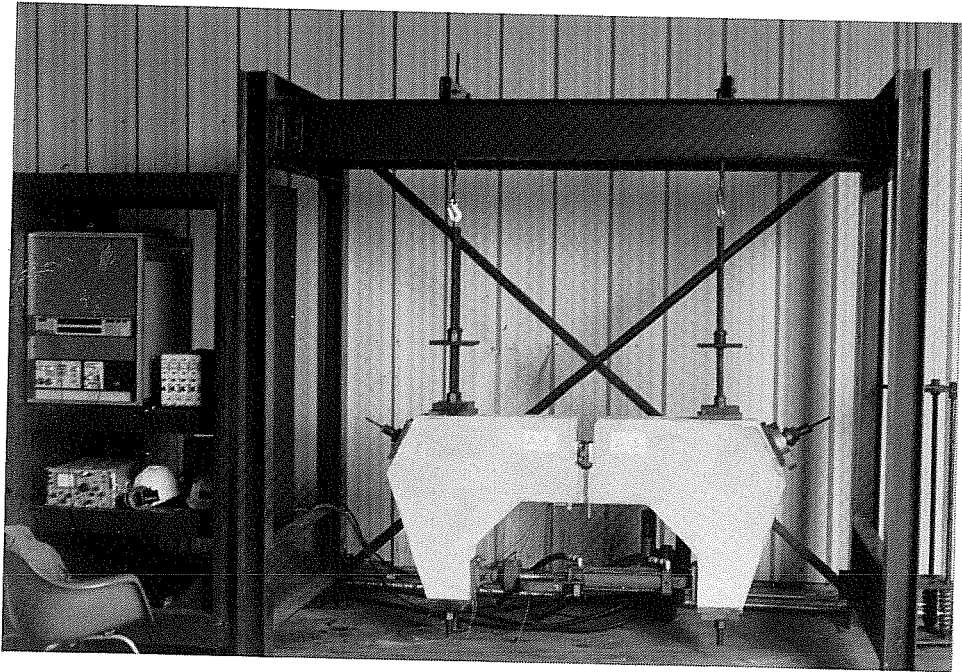
Figure 3.22   Test set-up for reduced beams

- loss of electrical power
- upper load level
- lower load level
- sudden change in specimen stiffness
- ram extension
- cycle number

When any of these factors exceeded a preset limit, the test equipment and cycle counter would shut down automatically. Thus, once the test was started and the limits were set, the test could run continuously without the presence of the operator.

3.5.1.2 Static Cycles.

The reduced beams were slowly loaded and unloaded in three to four initial static load cycles, in order to crack the test cross section and to determine the initial stiffness of the specimen.

For some of the early multiple strand specimens difficulties in propagating the crack through the entire cross section were encountered. For subsequent specimens the concrete zone was reduced by adding crack formers or increasing their size, which eliminated the problem.

A typical load - ram displacement plot for a completely cracked reduced beam is shown in Figure 3.23. Above the transition zone the crack is fully open and the tendon force becomes statically determinate, as discussed in Section 3.1.2. The cyclic test range was maintained in this fully cracked region.

3.5.1.3 Cyclic Loading.

The lower load level for cyclic loading was set to 2% to 10% above the full decompression load as obtained from the initial cycles. The upper load level was determined by the desired tendon stress range for the particular specimen. Stress ranges between 18 and 40 ksi were investigated. The load frequency was constant for each specimen and held between 1.5 and 6.5 Hertz.

Cyclic loading was interrupted occasionally for additional static cycles to monitor and record the changes in the specimen stiffness. Fatigue fractures of wires of the tendon were often audible and could be determined from substantial decay in specimen stiffness and substantial decrease in the full decompression load with subsequent cycles. The compression ram load limits were maintained constant even after fatigue failure of wires was noted, so that the effective stress in the remaining strands and wires increased as failures occurred. This accelerated the fatigue damage with subsequent cycles. Testing usually was terminated when the upper load level of the cyclic loading caused yielding of the remaining wires in the tendon.
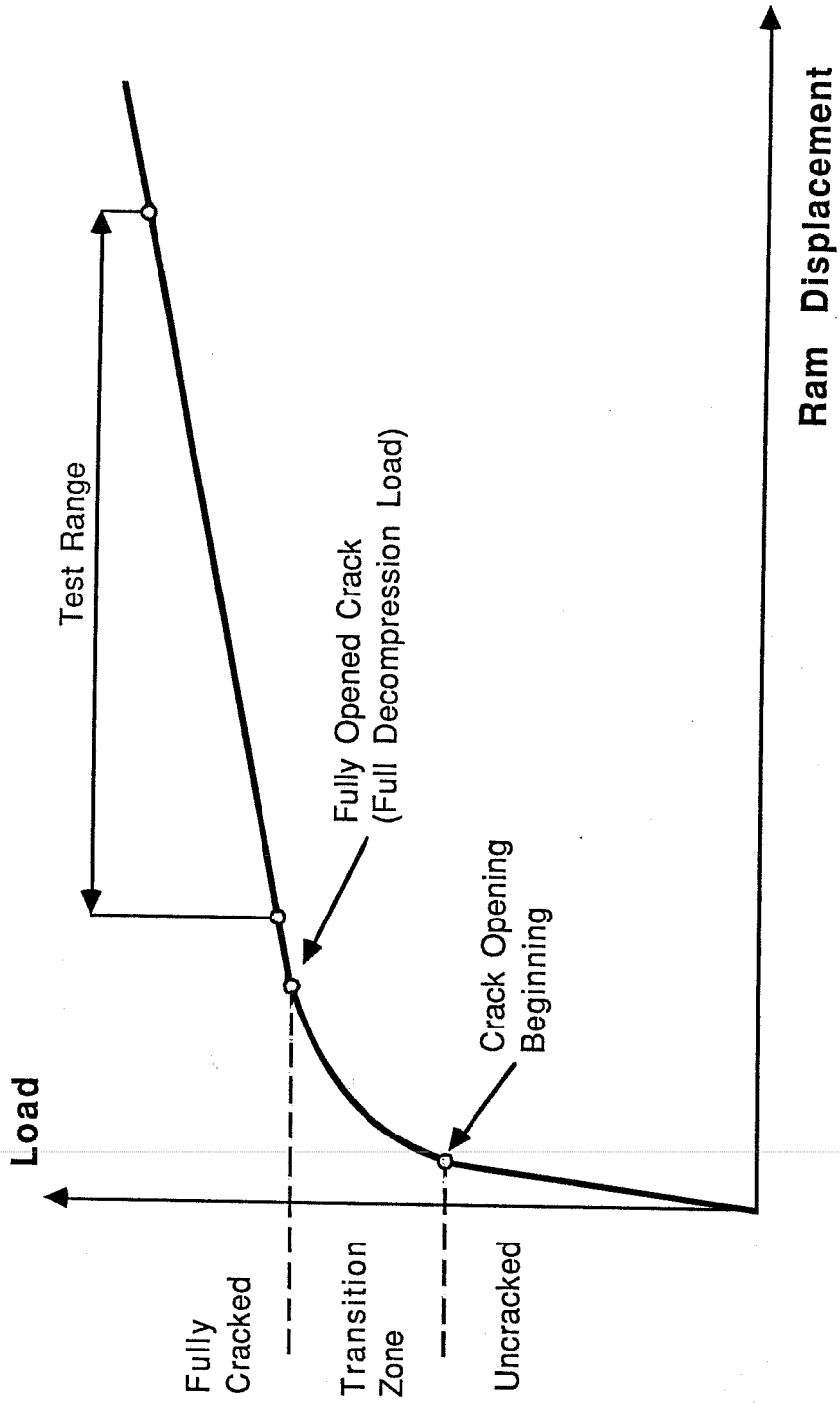
Figure 3.23   Typical load - ram displacement response

64

3.5.1.4 Post-Mortem Investigation.

The specimens were removed from the test frame after expiration and transported outside the laboratory. The post-mortem investigation generally was conducted within one or two days, and the specimens were covered with plastic during this period to avoid environmental influences.

The specimens were carefully opened with a jackhammer to gain access to the tendon. A 30 to 40 inch-long section of the tendon around the test cross section was recovered. The duct was opened along two longitudinal cuts and was then removed from the tendon. Short pieces of duct were left on the ends of the tendon to avoid disturbing the arrangement of the strands. The condition of grout, duct, and strands, and the location and initiation of wire fractures were carefully examined and recorded.

3.5.2 Girder Tests.

3.5.2.1 Loading Frame and Testing Bed.

The loading frame consisted of two steel columns and a cross beam to form a bent. The columns were bolted to the testing floor and braced diagonally to the floor to provide stability.

The specimen was supported at each end on steel pedestals. A 9 x 15.5 x 1-in. neoprene pad was placed between the specimen and each pedestal. Lateral support was provided by two knee braces on each pedestal. Longitudinal movement was restrained by a steel angle bolted to the knee braces at each end of the specimen.

3.5.2.2 Hydraulic System.

A closed loop control system was utilized to maintain a constant load range during fatigue testing. The system consisted of a Pegasus Servo System Module and Hydraulic Accessory Module, and a MOOG servovalve.

Two Shore Western hydraulic pumps, with a total capacity of 60 gpm, were used during testing. An 85 kip Nopak ram was used to apply the loading.

The ram was pin connected to the cross beam of the loading frame and to a spreader beam. The spreader beam transferred load to the specimen through two "cup & dish" assemblies that were positioned 4-ft. each side of midspan. The spreader beam was braced to a load-frame column to provide lateral stability of the ram and the spreader beam. A 7 x 7 x 1-in. neoprene pad was placed under each dish to accommodate differential movement between the top flange of the girder and the bottom flange of the spreader beam. Movement of the spreader beam in the longitudinal direction of the girder was restrained by 5/16-in. diameter airplane cables attached to the beam pick-up loops [11].

3.5.2.3 Determination of Effective Prestress.

The effective tendon stress was determined using an analytical method based on the specimen's response to static load. This method is referred to as the decompression load method. The prestress force was also well documented at the time of post-tensioning. However, experience indicated that appreciable prestress losses occurred between the post-tensioning operation and the start

of testing. Thus the magnitude of the cyclic loads was determined based on an effective tendon stress estimated from the observed decompression load.

3.5.2.4 Test Procedure.

The beams were cracked during initial static load cycles prior to cyclic loading. The cyclic fatigue loading was interrupted periodically and additional static load cycles were applied. After clear indications of fatigue failure of a number of wires, an ultimate load cycle was applied. After failure, the tendon was recovered and opened for inspection.

CHAPTER 4
DESCRIPTION OF TEST RESULTS

4.1 Introduction

Many aspects of the general behavior were common to all specimens. These general test results are presented in the following section. More specific results, reflecting the influence of the principal parameters of this study, are reported in Section 4.3.

Throughout this and the following chapters the reduced beams will be identified by an alpha-numerical label. The composition of this label is illustrated in Figure 4.1. The specimens were organized in four groups:

1) Group M comprises specimens with uncoated strands in metal duct. If the first indicator is M, it is a single strand tendon with a radius of tendon curvature equal to 2.0 m (78.8-in.). If the first indicator is M6, it is a multiple 6 strand tendon with a radius of tendon curvature equal to 3.50 m (138 in.).

2) For the specimens of Group P only the duct material is different. Plastic duct instead of metal duct was used.

3) The single specimen of Group C had a tendon composed of epoxy coated strands and a metal duct. The tendon curvature was the same as for the multiple strand specimens of Group M.

4) For the two multiple strand reduced beam specimens of Group Q the radius of tendon curvature was changed to 6.60 m (258 in.), in order to achieve a lower nominal contact load. Otherwise the specimens were similar to those of Group M.

The girder tests are identified by a similar alpha-numeric label. The composition of this label is illustrated in Fig. 4.2. The specimens were generally identical in construction except that for two girders plastic duct was used in place of metallic duct. Also, one girder had a parabolic tendon layout while all of the remaining girders had constant radius curves near the load points with straight ducts in between and outside the curved sections.

4.2 General

4.2.1 Reduced Beams.

4.2.1.1 **Nominal Contact Load.** Yates discussed in Reference 31 the significant influence of the contact loads between strands and duct and between individual strands
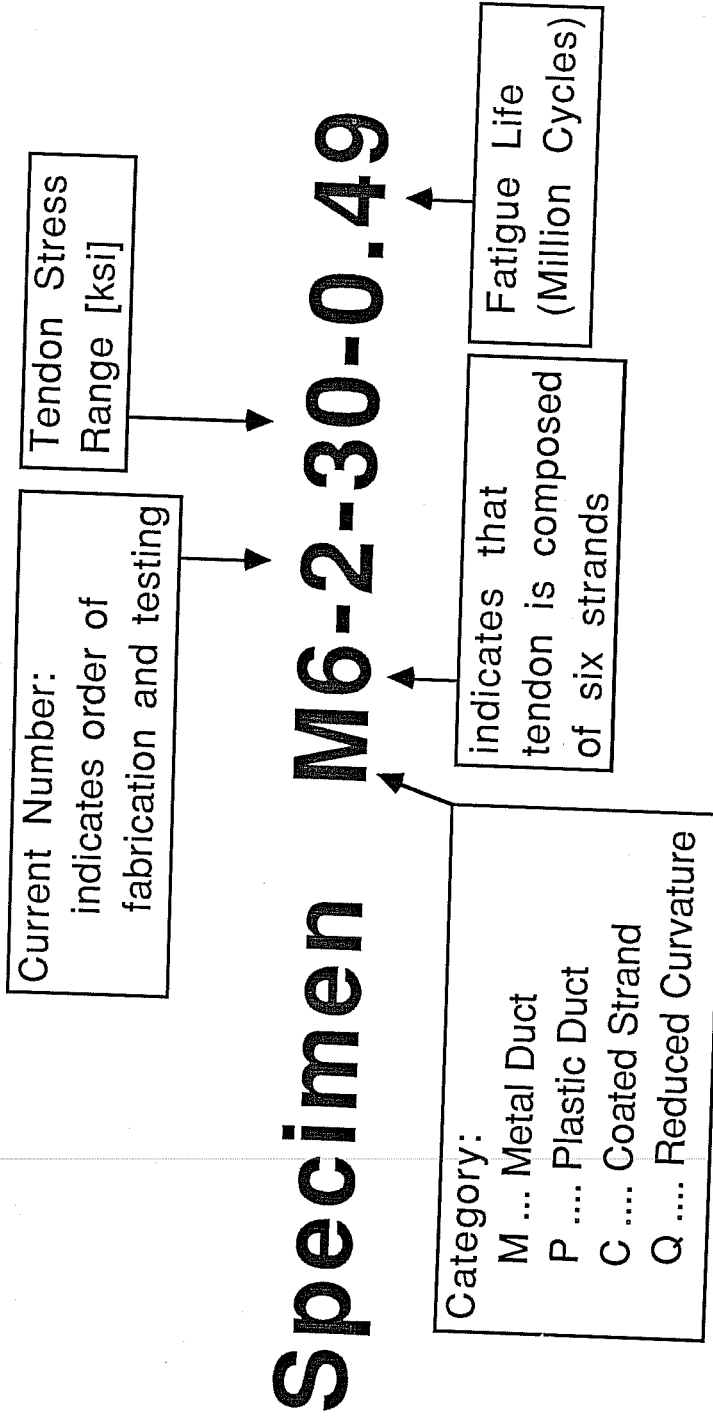
Figure 4.1 Alpha-numerical label for reduced beams.

Girder	Current Number: Indicates order of fabrication and testing	Tendon Stress Range (ksi)

Specimen G D — M — 1 — 47 — 0.23

Category D-Draped Tendon	Category M-Metal Duct	Fatigue Life
Category P-Parabolic Tendon	Category P-Plastic Duct	(million cycles)

Figure 4.2   Alpha-numerical label for girders

on the fatigue performance of post-tensioning tendons. Based on earlier suggestions by Oertle and Thurlimann [20] he suggested a method to compute nominal values for these contact loads, which is illustrated in Figure 4.3. It was pointed out in Section 2.2.4 of the present study that the actual local values will be considerably higher. However, these nominal values can be used to obtain a general idea of the effects of contact load variation.

In Table 4.1 the radii of tendon curvature, the mean tendon forces, and the nominal contact loads as computed by this procedure for the reduced beams are listed. Since the contact load varies with the fluctuating tendon force under cyclic loading, average contact loads based on the mean tendon forces are given.

4.2.1.2 Load – Crack Width Response. Plots of ram load versus crack width were obtained during the initial load cycles, and several times during the test. They provided important information on crack width, prestress level, and stiffness of the specimens.

A schematic load - crack width response for the multiple strand reduced beams is shown in Figure 4.4. The actual plots are included in Refs. 31 and 34. Note that the crack width was measured as change of distance between two points on either side of the crack, approximately two inches apart. Therefore these measurements include elongations of the compressed concrete fibers before crack opening.

The behavior is approximately linear below the first crack opening load and becomes nonlinear in a transition region, where the crack remains partially closed. Upon full opening of the crack (labelled "full decompression" in Figure 4.4), the load - crack width response becomes linear again, and the tendon force now is statically determinant. Finally, the prestressing steel yields and ultimate capacity of the specimen is reached.

As discussed in Chapter 3 and indicated in Figure 4.4, with these specimens it is important to keep the test loads above the full decompression load in order to maintain
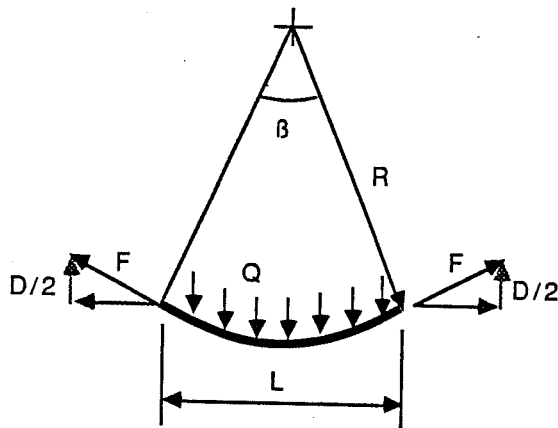
$D = F \times \sin \beta$

$D \approx F \times L/R$ (small angles)

$Q = D/L \approx F/R$

where   F = Tendon force
         R = Radius of curvature
         D = Total vertical force
         Q = Distributed vertical load

a) Estimation of Lateral Load, Q

$q_2 = K_2 \times Q$

$q_1 = K_1 \times Q$

$q_3 = K_3 \times Q$
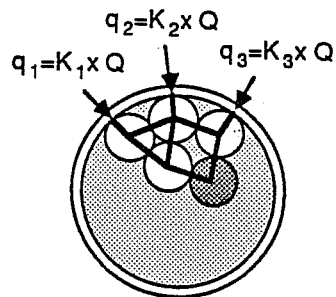
Assumptions:
* Each strand generates equal vertical load, f
* No tangential friction exists between strands
  or strands and duct
* Strands can be idealized as circles

—— Dark lines indicate
      direction of forces

Procedure

1) Assume stable geometry
2) Determine inclination of all forces (indicated by dark lines above)
3) Calculate statically determinant forces starting with outermost
   strand (shaded strand above)

b) Estimation of K Factors

Figure 4.3   Estimation of local contact load (from Yates [31])

Table 4.1 Nominal Contact Loads for Reduced Beam Specimens

	Specimen	Radius of Tendon Curvature (cm)	(in)	Mean Tendon Force (kips)	Nominal Contact Load (kips/ft)
Multiple Strand					
Metal Duct	M6-1-40-0.10	350	138	168.8	7.5
	M6-2-30-0.49	350	138	172.3	7.6
	M6-3-20-(0.62)	350	138	178.4	8.1
	M6-5-20-1.02	350	138	181.7	8.1
Plastic Duct	P6-4-30-0.37	350	138	179.0	7.9
	P6-6-30-0.50	350	138	166.9	7.4
Coated Strand	C6-7-30-0.69	350	138	169.3	7.5
Reduced Curvature	Q6-8-30-0.26	660	258	168.7	4.0
	Q6-9-30-0.38	660	258	172.2	4.1
Single Strand					
Metal Duct	M-1-40-0.00*	200	79	27.5	4.2
	M-2-40-0.29	200	79	27.5	4.2
	M-3-30-0.32	299	79	26.7	4.1
	M-4-30-0.47	200	79	30.6	4.7
	M-5-20-1.27	200	79	27.2	4.2
	M-6-18-NF**	200	79	27.7	4.2
	M-7-30-0.84	200	79	26.8	4.1
	M-8-22-4.52	200	79	26.5	4.1
	M-9-25-0.80	200	79	27.2	4.2
	M-10-19-1.50	200	79	27.7	4.2
	M-12-25-1.01	200	79	26.4	4.1
Plastic Duct	P-11-30-1.84	200	79	28.0	4.3
	P-13-40-1.11	200	79	28.5	4.3
	P-14-25-3.54	200	79	27.2	4.2

* premature failure due to equipment malfunction
** runout at 6.5 million cycles

72
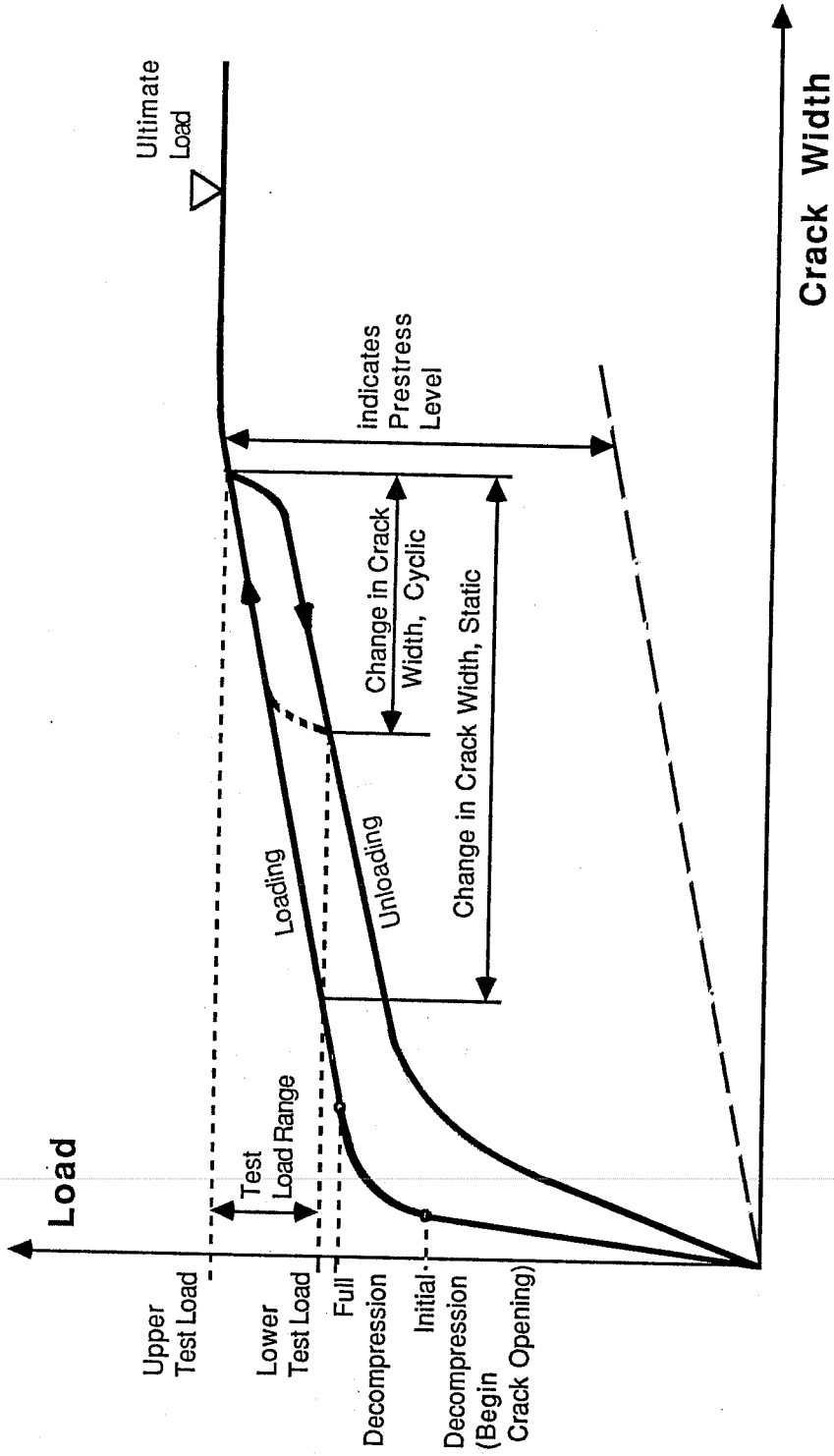
Figure 4.4   Schematic load - crack width response

a statically determinant tendon force. Table 4.2 lists information on final decompression loads, and lower and upper tendon stresses for the reduced beam tests.

Another item of information obtained from the load - crack width response is the actual level of prestress in the specimens. The dashed line in the lower portion of Figure 4.4 indicates the theoretical load - crack width response if no prestress force were present. It simply is a shift of the actual response above the full decompression load in such a way, that it passes through the origin of the graph. The prestress level can be readily determined from the magnitude of this shift. Table 4.3 shows a comparison of the prestress levels as calculated from jacking force, load cell readings, and load - crack width response for the multiple strand reduced beams. As indicated in the table the prestress levels listed were determined at different times during and after stressing. The prestress level obtained from the load - crack width response probably gives the best estimate of the effective prestress in the specimens at beginning of the tests.

For the single strand reduced beams the effective tendon stresses were also monitored by strain gages mounted on the strand. Table 4.4 lists a comparison of the prestress levels in the single strand reduced beams as calculated from load cell readings, strain gage readings, and from an analytical method based on measured decompression moment described by Yates in Reference 31.

Wire fractures caused a loss of prestress force, which changed the load - crack width response, as illustrated in Figure 4.4. Due to the reduced prestress level the crack opening load drops, and the crack widths are larger than at earlier load cycles.

Both single strand reduced beams and multiple strand reduced beams exhibited hysteretic behavior, as indicated in Figure 4.5. Due to this hysteresis the change in crack width during cyclic loading is much smaller than during static loading. In the course of a test the crack widths varied, but after a few thousand cycles the variations were small until the first wire fractures occurred. Wollmann reports in Reference 34 numerical values of crack widths and changes in crack widths for his multiple strand reduced beams.

Yates reported a slight increase of crack width at constant load during static load cycles for his single strand reduced beams [31]. This creep was also observed for the multiple strand reduced beams, but usually became dormant after a few percent of crack width increase for both types of specimen.

4.2.1.3 Stiffness History.

Another important indication of wire fractures was the appreciable decrease in stiffness accompanying the loss of prestress. As a measure of the specimen stiffness, the crack width at a specified load was taken. Stiffness history is a plot of these crack widths versus number of cycles.

The stiffness histories for the reduced beams exhibited the three phases which were also found to be typical for girder tests (Fig. 2.1). Large initial stiffness losses due to

Table 4.2   Full Decompression Loads and Test Tendon Stresses for Reduced Beams

Specimen	Full Decompression Ram Load (kips)	Full Decompression Tendon Stress (ksi)	Lower Test Tendon Stress (ksi)	Upper Test Tendon Stress (ksi)
Multiple Strand				
Metal Duct				
M6-1-40-0.10	48	157	164	204
M6-2-30-0.49	54	169	173	203
M6-3-20-(0.62)	60	180	189	209
M6-5-20-1.02	56	176	188	208
Plastic Duct				
P6-4-30-0.37	61	177	180	210
P6-6-30-0.50	50	162	167	197
Coated Strand				
C6-7-30-0.69	46	147	169	199
Reduced Curvature				
Q6-8-30-0.26	46	155	169	199
Q6-9-30-0.38	50	161	173	203
Single Strand				
Metal Duct				
M-1-40-0.00	N/A	N/A	159.5	199.5
M-2-40-0.29	5.4	156	159.5	199.5
M-3-30-0.32	5.7	150	159.2	189.2
M-4-30-0.47	6.4	169	184.8	214.8
M-5-20-1.27	5.0	166	168.0	188.0
M-6-18-NF	4.6	133	172.0	190.0
M-7-30-0.84	5.5	159	160.0	190.0
M-8-22-4.52	5.5	159	162.0	184.0
M-9-25-0.80	5.0	144	165.0	190.0
M-10-19-1.50	5.5	154	171.8	190.8
M-12-25-1.01	5.0	144	160.0	185.0
Plastic Duct				
P-11-30-1.84	5.0	146	168.0	198.0
P-13-40-1.11	5.5	159	166.0	206.0
P-14-25-3.54	4.5	128	165.0	190.0

Table 4.3   Prestress Levels for Multiple Strand Reduced Beams

	Specimen	From Jacking Force (ksi)	From Load Cell Reading* (ksi)	From Load - Crack Width Response** (ksi)
Metal Duct	M6-1-40-0.10	165	174	124
	M6-2-30-0.49	165	N/A	155
	M6-3-20-(0.62)	165	146	144
	M6-5-20-1.02	N/A	176	153
Plastic Duct	P6-4-30-0.37	165	N/A	153
	P6-6-30-0.50	147	155	152
Coated Strand	C6-7-30-0.69	147	130	126
Reduced	Q6-8-30-0.26	147	155	144
Curvature	Q6-9-30-0.38	147	148	135

N/A Not Available
* immediately after release of jacking force
**beginning of testing

Table 4.4   Prestress Levels for Single Strand Reduced Beams

Specimen	Loadcell[1]	Strain Gage[2]	Calculated
M-1-40-0.00	N/A	152	167
M-2-40-0.29	159	167	165
M-3-30-0.32	137	N/A	148
M-4-30-0.47	160	167	N/A
M-5-20-1.27	148	N/A	140
M-6-18-NF	148	N/A	146
M-7-30-0.84	150	N/A	147
M-8-22-4.52	144	N/A	161
M-9-25-0.80	150	171	149
M-10-19-1.50	153	162	166
M-12-25-1.01	145	178	153
P-11-30-1.84	158	131	158
P-13-40-1.11	145	N/A	164
P-14-25-3.54	N/A	N/A	134

[1] Reading at start of testing
[2] Reading at times of grouting (center gages only)
N/A Not Available
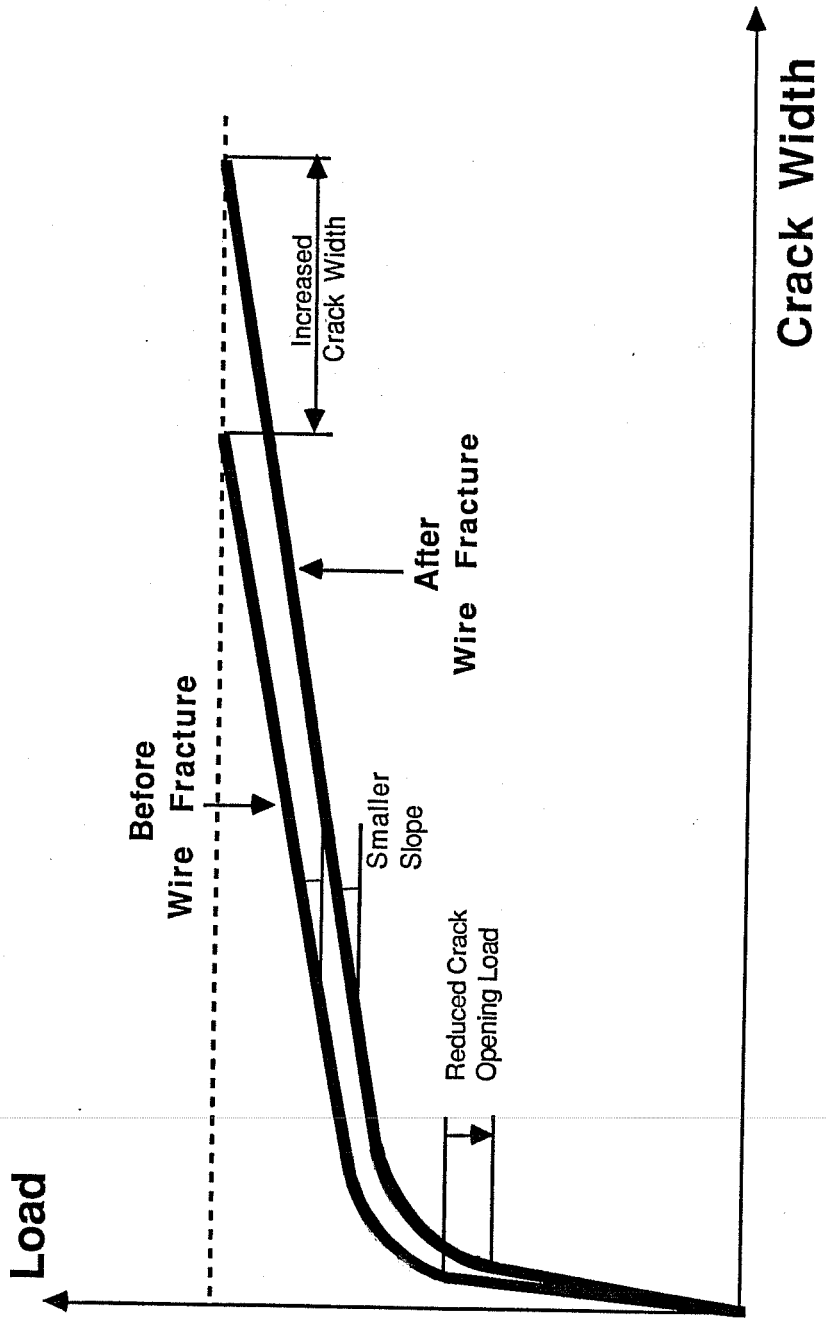
Figure 4.5   Change of load - crack width response after wire fractures

debonding and crack propagation are followed by a phase of slow stiffness decrease. The third stage is initiated by the first wire fracture and is characterized by large and rapid stiffness losses.

Figure 4.6 illustrates the difference in the stiffness histories for single strand and multiple strand reduced beams. Fracture of a single wire in the mono strand specimens reduced the tendon cross section by about 14%, and the stiffness decreased dramatically (Fig. 4.6a). For the multiple strand reduced beams and for the girder specimens with six strands in the tendon, fracture of the first wire reduced the tendon cross section by only 2.5%. The decrease in stiffness therefore is more gradual (Fig. 4.6b). However, subsequent wire fractures occurred at a very fast rate, and the transition from the stable phase with fairly constant stiffness to the final stage with rapid deterioration of the tendon never required more than 50,000 to 100,000 cycles for the multiple strand reduced beams. Since the test setup was not sensitive enough to detect single wire fractures and the corresponding small stiffness decrease, the approximate onset of this transition curve was chosen to define their fatigue life.

4.2.1.4 Post Mortem Investigation.

"Post Mortem Investigation" refers to the examination of the tendons recovered from the expired specimens. All specimens suffered one or several duct fractures in the vicinity of the crack. For the plastic ducts these fractures were small and never exceeded two inches in length. The fractures in metal ducts were much larger and occasionally went through the entire sheath.

The grout usually was fractured at several locations in the vicinity of the crack. Several inches away the grout condition was very satisfactory. The grout penetrated the voids between the strands completely except for some small air bubbles which occasionally were enclosed between the top strands and the duct.

The rubbing action and lateral pressure between strands and duct left clear marks on the fretting partners. Usually they were more severe in the vicinity of the crack. Strands in contact with the duct caused longitudinal indentations and wear on the metal ducts and locally rubbed through the plastic ducts (Fig. 4.7). In return, the strands were abraded from the rubbing action on the duct, and in the case of metal ducts both fretting partners showed signs of corrosion. Figure 4.8 shows the severe damage of a tendon due to fretting fatigue failures. A more detailed report of these results is presented in the following sections.

Five types of wire fractures were identified (Fig. 4.9):

1) fractures initiated from fretting between duct and strand,

2) fractures initiated by strand - strand rubbing,

3) fractures initiated by wire - wire fretting within a strand,

4) ordinary fatigue fractures,
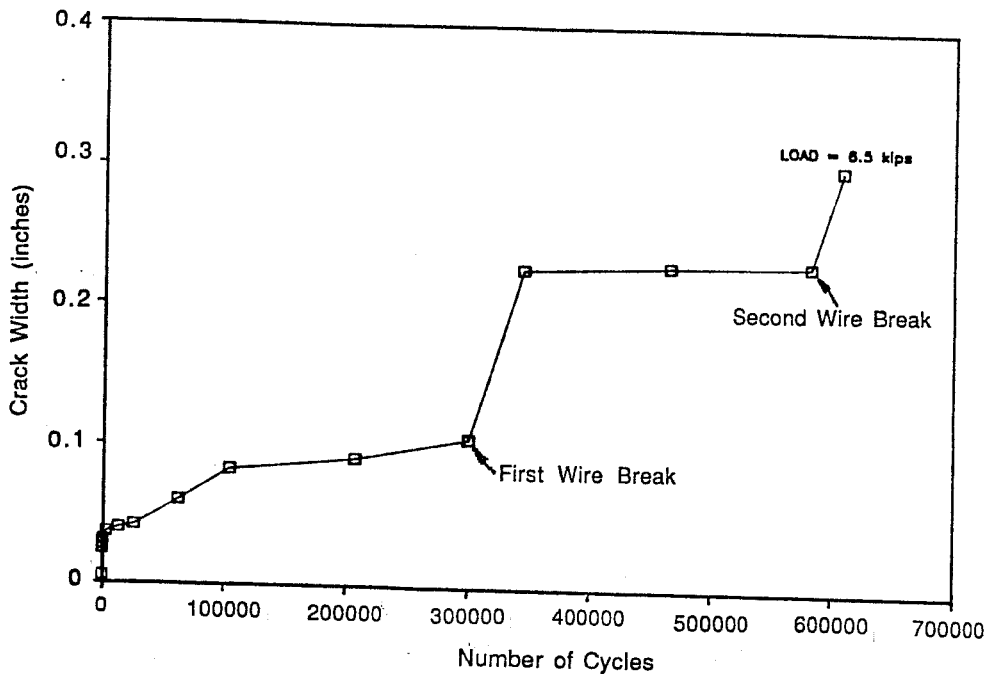
a) Single Strand Reduced Beam
M-3-30-0.32 (from Yates [31])
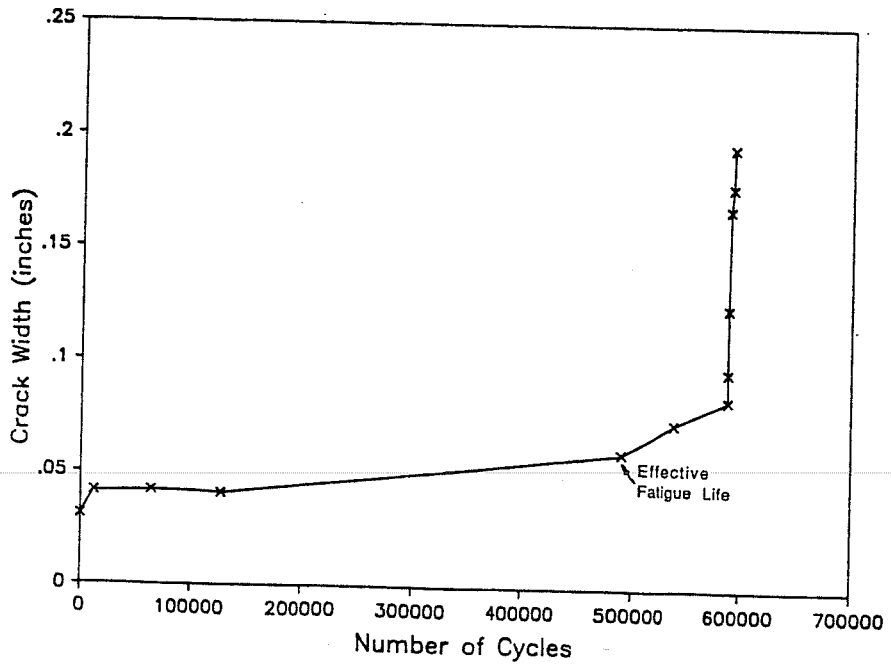
b) Multiple Strand Reduced Beam M6-2-30-0.49

Figure 4.6   Stiffness histories
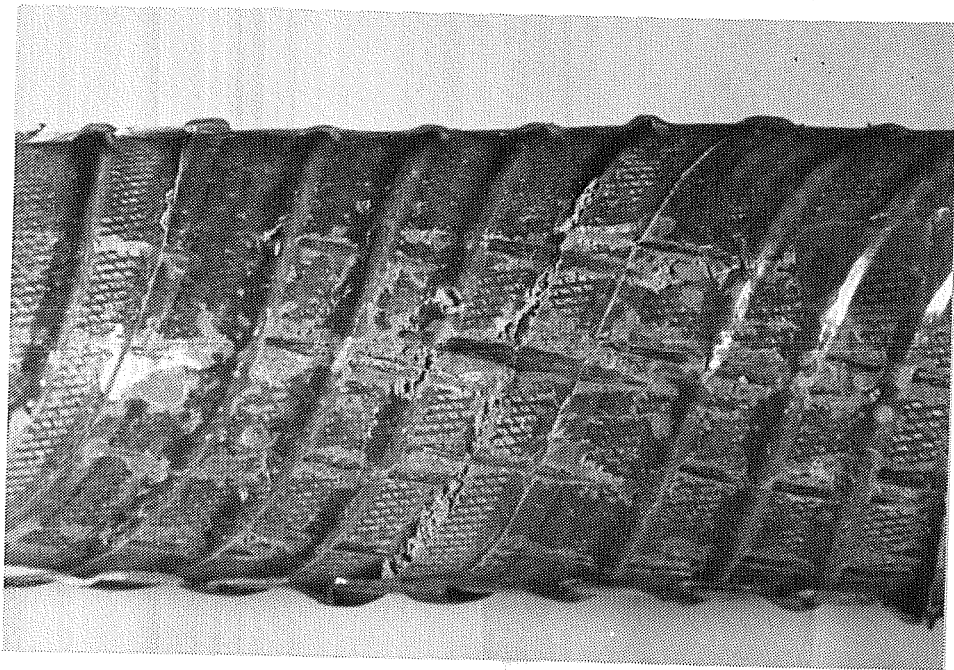
a) Metal Duct
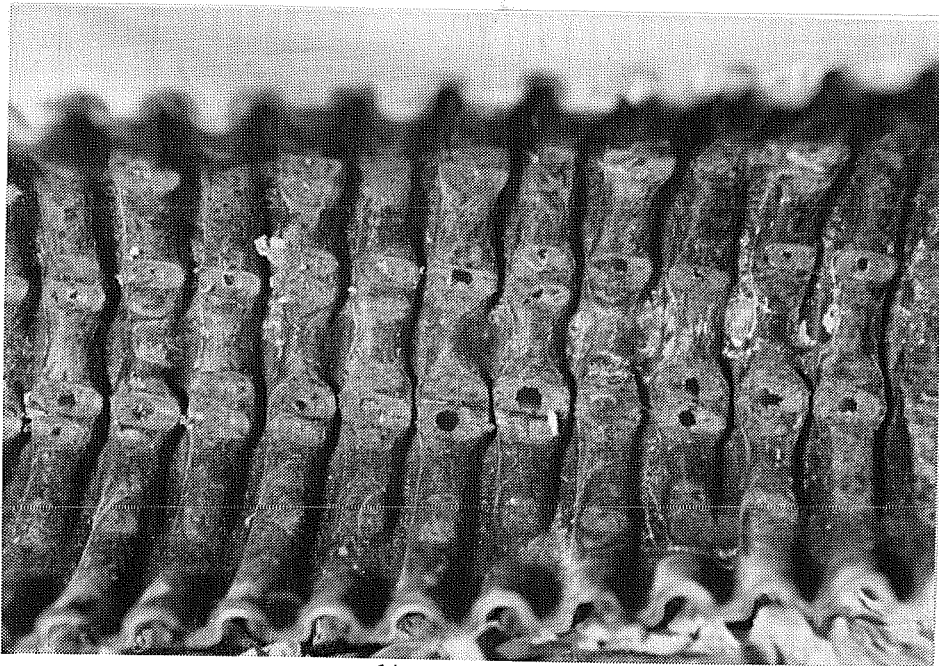
b) Plastic Duct

Figure 4.7 Condition of duct
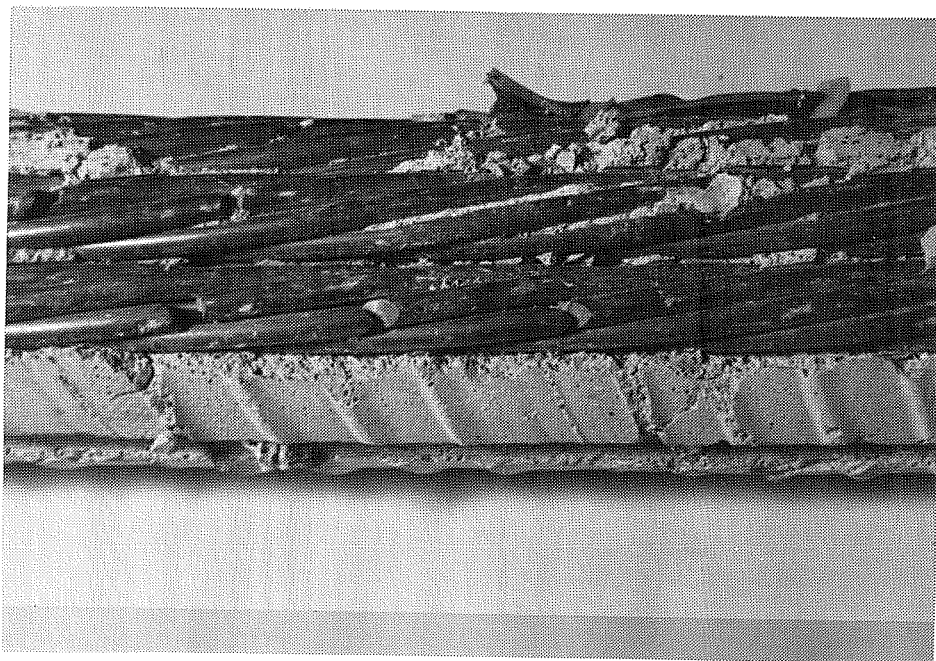
Figure 4.8   Severe tendon damage due to fretting fatigue
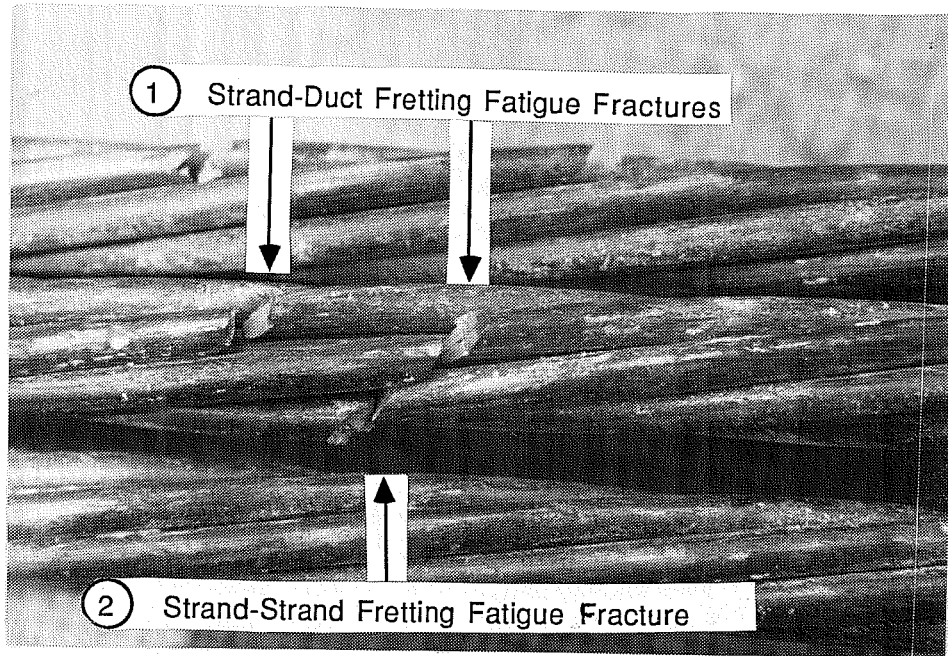
a) Strand - Duct and Strand - Strand Fretting Fatigue
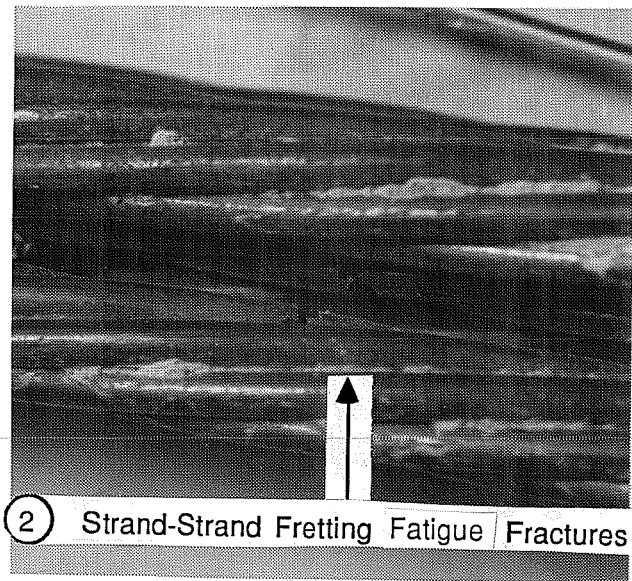
b) Strand - Strand Fretting Fatigue

Figure 4.9   Types of wire fractures
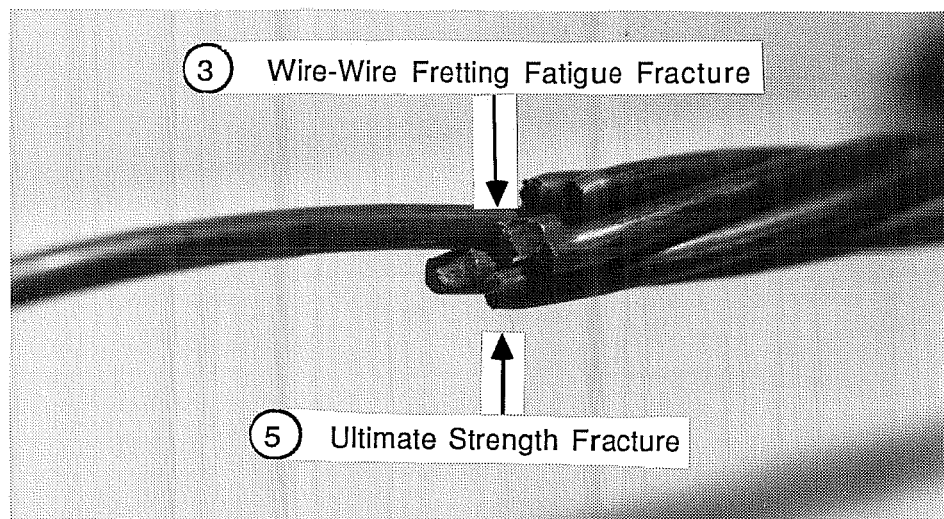
c) Wire - Wire Fretting Fatigue and
Ultimate Strength Fractures
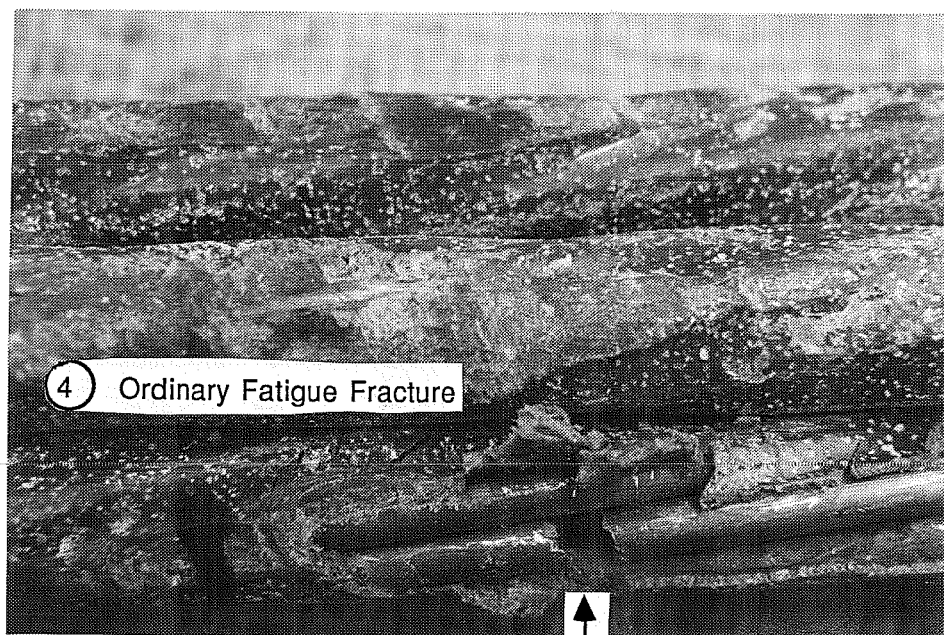
d) Ordinary Fatigue in Epoxy Coated Strand

Figure 4.9 Types of wire fractures (continued)

5) ultimate strength fractures.

All three types of fretting fatigue fractures were characterized by the typical marked inclination of the initial part of the crack, where fretting took place. The section of the crack produced by the fretting fatigue shows a smooth, plane surface. Once the fatigue crack reaches a critical depth, the crack growth becomes unstable and brittle fracture of the remaining wire cross section occurs. This stage generally is characterized by a jagged crack surface.

The test load range was not adjusted after wire fractures, and hence the remaining tendon stress range increased with each wire fracture. This led in some cases to development of ordinary fatigue fractures in some wires subsequent to fractures due to fretting fatigue. The surface of ordinary fatigue cracks does not exhibit the initial inclination of the crack, as is typical for fretting fatigue cracks.

Strength failures were characterized by necking of the wires, and occurred shortly before termination of the tests. Tests usually were terminated when the upper load level of the cyclic loading caused yielding of the prestressing steel.

4.2.2 Girder Specimens

4.2.2.1 Nominal Contact Load. Yates [31] and Wollmann [34] computed the nominal contact load for all girder specimens using the same procedure as outlined in Sec. 4.2.1.1. The values are given in Table 4.5

4.2.2.2 Crack Development. The girder specimens generally developed vertical flexural cracks in the bottom flange extending upward into the webs. The cracks usually occurred at the location of stirrups [11]. In addition, horizontal cracks developed along the bottom flange and were aligned with the non-prestressed reinforcing bars indicating splitting. These cracks were permanent under the load points and were continuous in the constant moment region [11]. They generally developed from flexural cracks during the latter stages of fatigue loading.

4.2.2.3 Stiffness Deterioration. The behavior of the girders was monitored by its response to these periodic static load cycles. The behavior of the beams was typical of that observed for fatigue tests of prestressed concrete beams. The behavior can be divided into three distinct phases. There was an initial gradual deterioration in beam stiffness during the early phases of loading followed by a relatively stable period in which little or no deterioration in beam stiffness occurred. These two phases constituted roughly 90% of the fatigue life of the beams. Finally, there was a fairly rapid deterioration in stiffness which marked the initial fatigue fracture of a wire within the tendon. After a substantial number of wires were broken, an ultimate strength test was conducted on each of the girders. During these tests, most of the flexural cracks in the constant moment region

Table 4.5   Nominal Contact Load for Girder Specimens

Specimen	Radius of Tendon Curvature		Nominal Contact Load
	(in.)	(in.)	(kips/ft)
GD-M-1-47-0.23	350	138	7.3
GD-M-2-32.5-0.30	350	138	7.9
GD-M-3-23-0.32	350	138	7.6
GP-M-4-25-2.10	3450	1360	0.7
GD-M-5-30-0.80	350	138	7.1
GD-M-6-40-0.49	350	138	5.9
GD-P-7-30-1.30	350	138	7.3
GD-P-8-3-0.70	350	138	8.3

remained relatively small while one or two cracks in the vicinity of the drape point opened up considerably. The beams exhibited good ductility during these ultimate strength tests with midspan deflections at failure of up to 11 inches.

4.2.2.4 Post-Mortem Examination. After the completion of testing, the central section of tendon and duct was extracted from each of the girders for a more detailed inspection. The detailed inspection revealed that the majority of fatigue fractures of individual strand wires occurred at the drape points. In the early specimens, a large amount of powdery, reddish debris resembling ordinary rust was present in the vicinity where the fractured wires were concentrated. Photographs of typical damaged areas from one of the girders are shown in Fig. 4.10. The majority of fatigue fractures were initiated at contact points between strands and duct. Most of the fracture surfaces were inclined, similar to the condition described by Rigon and Thurlimann [26].

One final comparison of interest is the typical condition of tendons after testing for the reduced beam specimens and the companion girders reported by Diab [11]. As shown in Figure 4.11, the tendon from the companion girder (with six 0.5-inch diameter strands) generally had a much greater volume of fretting debris and overall signs of corrosion.

4.3 Influence of Parameters

4.3.1 Introduction. One of the objectives of the multiple strand reduced beam test series was to study the influence of some of the important parameters on the fretting fatigue in post-tensioning tendons. Specimens with metal and plastic duct, various tendon curvatures, and epoxy-coated strands were tested in this series. The following sections emphasize test results for the multiple strand reduced beams as reported in Reference 34 since they give a clearer picture when the same general test specimen is used. The test results and trends determined from the single strand reduced beams and the girders are included in Chapter Five of this report. Detailed results for all series are presented in References 11, 15, 31 and 34.

4.3.2 Metal Duct Specimens - Large Curvature. Four multistrand reduced beam specimens with metal ducts with a radius of curvatures of 3.5m (139 in.) were fatigue tested at tendon stress ranges of 20, 30, and 40 ksi. The fretting fatigue lives of these specimens are plotted in Figure 4.12.

Specimen M6-3-20-(0.62) (shown shaded) has to be regarded with reservation. Initially it was accidently tested for two million load cycles with the crack not fully propagated through the concrete cross section. Since the remaining concrete zone could carry tensile stresses the tendon stresses became indeterminant. They were roughly estimated to be equal to 10 to 12 ksi, but may have been somewhat lower or higher. After two million cycles the crack was opened completely by cutting through the uncracked concrete in the tensile zone. For the remainder of the test the crack was kept fully open and a tendon stress
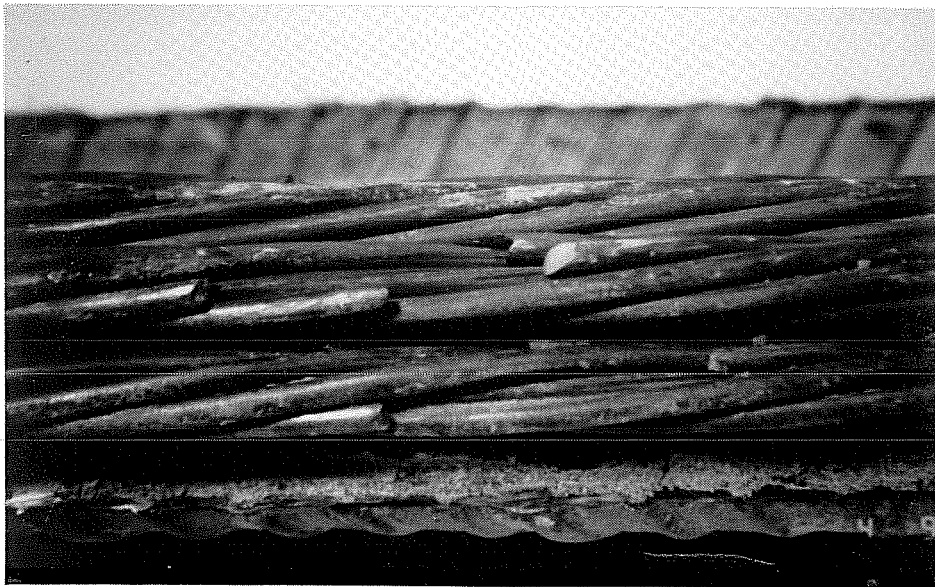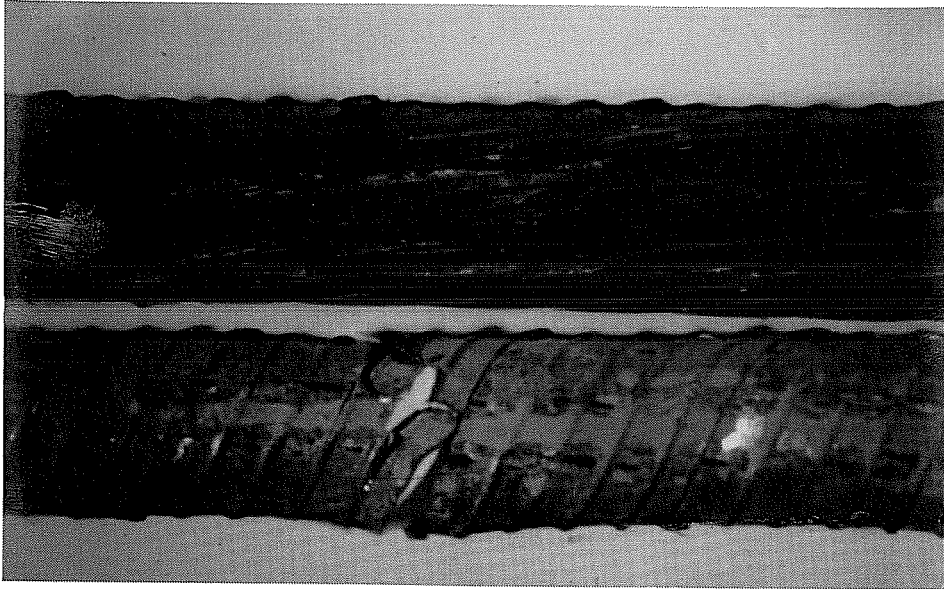
Figure 4.10   Damaged sections of tendon from companion beam
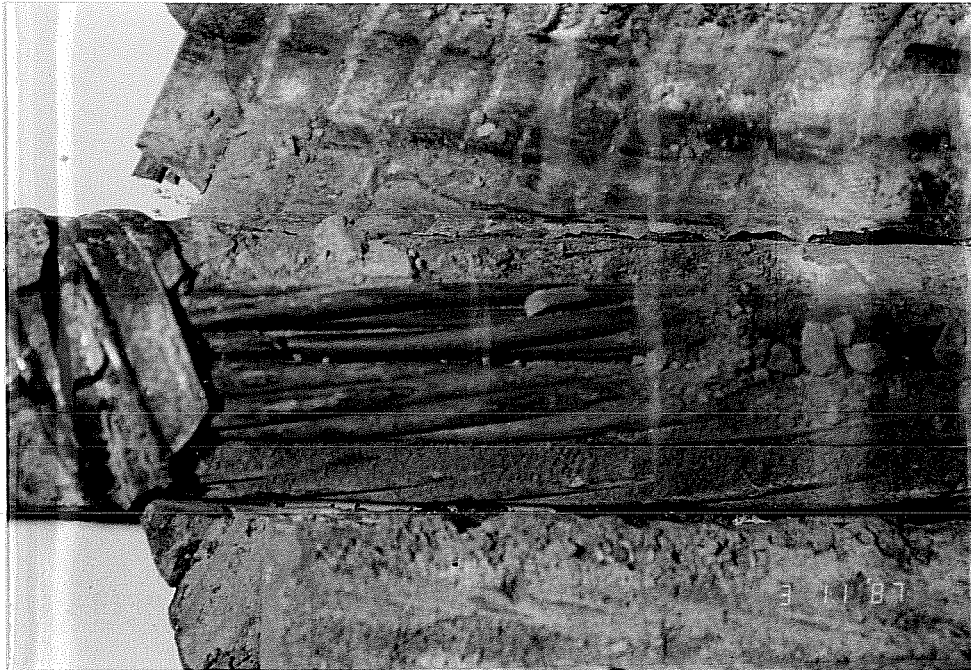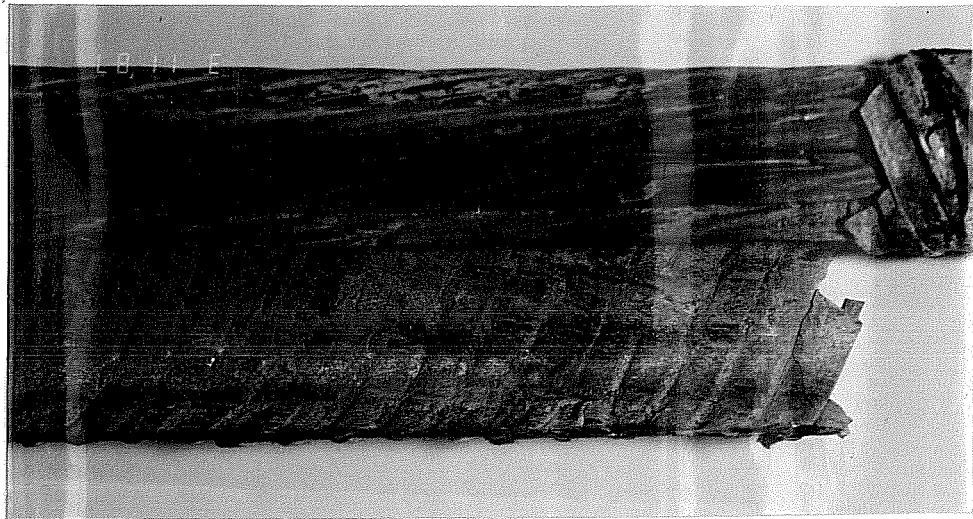
Figure 4.11   Severely damaged tendons from companion beams
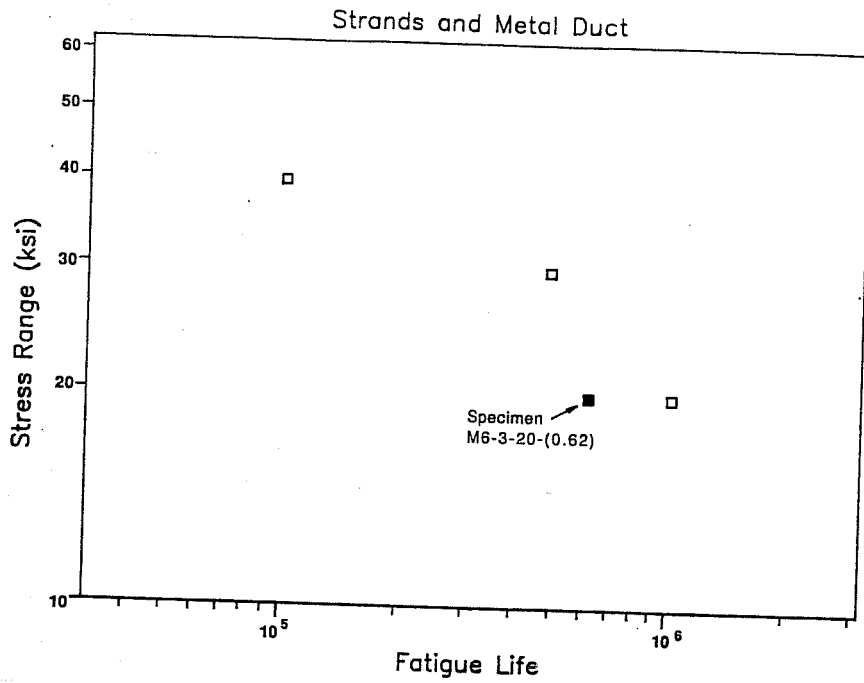
Figure 4.12 Fatigue lives for multiple strand reduced beam with metal duct and large curvature
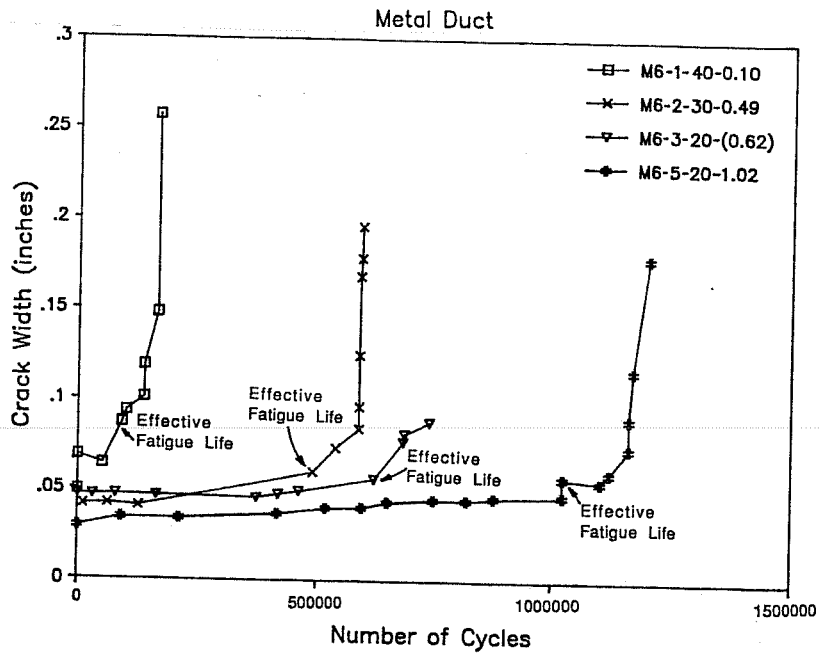
Figure 4.13 Stiffness histories for multiple strand reduced beams with metal duct and large curvature.

range of 20 ksi was maintained. It is hard to assess how much impact the cycles at the lower stress range had on the fretting fatigue performance of this specimen. However, comparison with the second specimen tested at 20 ksi stress range - M6-5-20-1.02 - indicates that some detrimental effect probably occurred, looking at the appreciable difference in fatigue performances (Fig. 4.9). Only the load cycles beyond two million cycles, where the 20 ksi stress range was clearly known, were considered for designation and in the plots of stiffness history and load - crack width response for specimen M6-3-20-(0.62). The last item in the designation label indicating the fatigue life is put in parentheses to call attention to this uncertainty.

The stiffness histories for all four specimens are plotted together in Figure 4.13. The reference crack width for determining the stiffness was measured at a stress 20 ksi above the full decompression stress, which was different for each specimen (Table 4.2). In all cases deterioration of the tendon took place very rapidly once the first wire had fractured.

Post-mortem investigations indicated that the contact pressure between metal duct and strands caused deformations and abrasions of the duct (Fig. 4.8), and the strands were worn at the contact points (Fig. 4.4). Traces of corrosion were found where fretting between strands and duct took place. Abrasions and corrosion were most severe for specimen M6-1-40-0.10, which was tested at the largest stress range (40 ksi) and exhibited the largest crack width and change in crack width due to cyclic loading. Figure 4.15 shows a comparison of ducts recovered from specimens M6-1-40-0.10 and M6-5-20-1.02. The duct damage appears to be related to the stress range.

The majority of wire fractures were induced by fretting of prestressing strands on the duct. However, in three of the four specimens at least one fracture due to strand - strand fretting occurred (Appendix B). Fractures initiating from wire - wire rubbing within an individual strand were found at locations where other wires broke earlier.

Strand - strand and wire - wire fretting did not cause the very clear abrasions as occurred due to strand - duct rubbing. Frequently no signs of abrasion at all could be found, and the only indication of fretting was the characteristically inclined initial part of the fretting fatigue crack.

4.3.3 Plastic Duct Specimens. Two multiple strand reduced beam specimens with plastic duct with a radius of curvature of 3.5m (139 in.) were tested at a tendon stress range of 30 ksi. The results of these tests are shown in Figure 4.13, together with the results of the corresponding metal duct tests. This comparison does not indicate any significant improvement of the fatigue performance with the use of plastic duct. The figure also includes the results for a coated strand tendon and for tendons with reduced curvature, which will be reported on in Sections 4.3.4 and 4.3.5. The lack of significant improvement for the plastic duct specimens was very surprising since reports of tests of single strand reduced beam specimens had indicated substantial improvement in fatigue life when plastic ducts
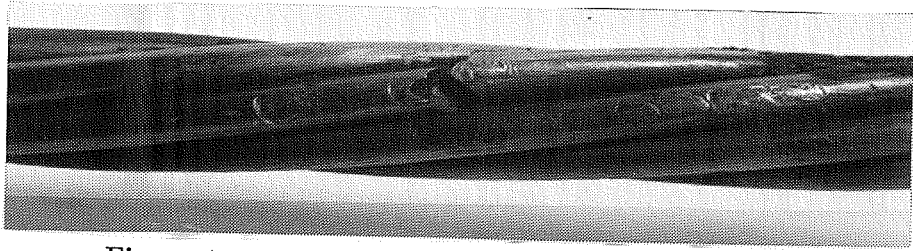
Figure 4.14   Fretting wear from strand - metal duct rubbing
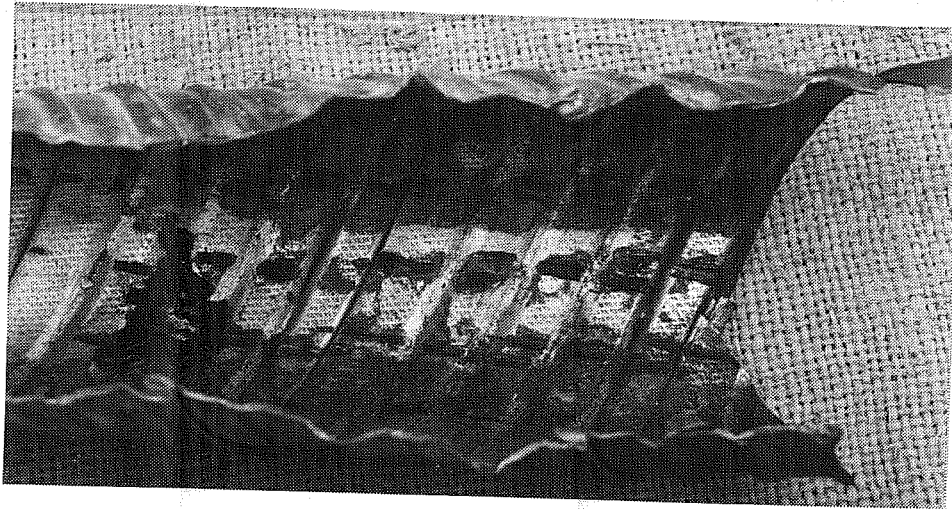
a)   Specimen   M6-1-40-0.10
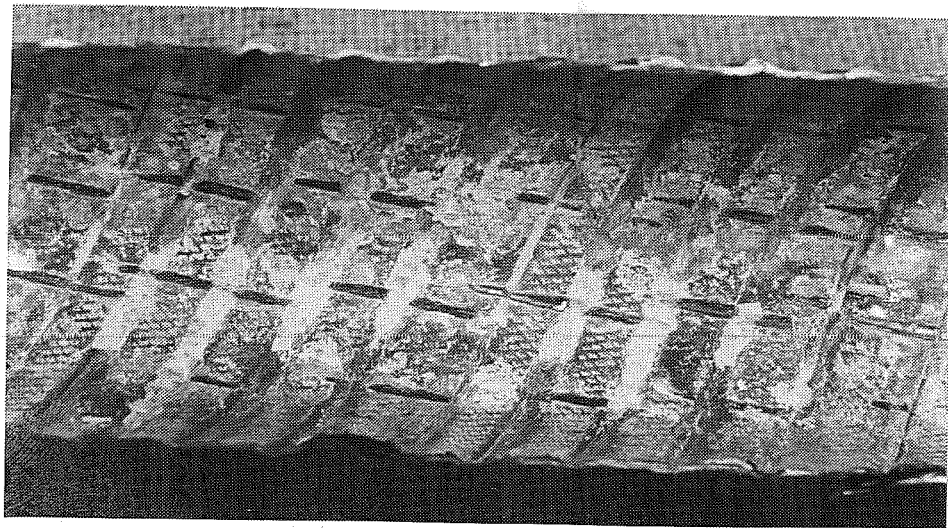
b)   Specimen   M6-5-20-1.02

Figure 4.15   Comparison of duct abrasions

were used [19, 31]. Figure 4.17 shows the dramatic improvement in fatigue life for plastic duct for the single strand reduced beam tests of this study.

Figure 4.18 shows the stiffness histories for the multiple strand specimens with the plastic duct tendons. The increased crack width as compared to the metal duct tests is noteworthy. It may be caused by the smaller coefficient of friction between strands and plastic duct.

The failure of specimen P6-4-30-0.37 at 370,000 cycles occurred considerably earlier than had been expected. Previous research [19,31] with single strand specimens had indicated that use of plastic duct increases the fatigue life significantly. Therefore the test was terminated immediately after the first indications of wire fractures to determine the cause of the premature failure. Failure was verified as caused by strand to strand rubbing between strands in the outer layer and strands in the inner layer of the multistrand tendon.

Specimen P6-6-30-0.50 became necessary to verify or disprove the result of specimen P6-4-30-0.37. Figure 4.16 shows that its fatigue life is somewhat higher but still does not exceed the fatigue life of the comparable specimen with a metal duct tendon.

Post-mortem investigations indicated that for both specimens almost all wire fractures initiated from strand to strand fretting in adjacent strand layers. One fracture was caused by wire - wire fretting within a strand. Figure 4.19 shows a typical tendon cross section for the multiple strand reduced beams. Usually four strands, numbered one through four in the figure, were in contact with the duct. Fretting fatigue for the specimens with plastic duct initiated from contact points between the interior strands five and six and the other strands, but not from rubbing of strands one through four against each other or against the duct. Consequently all fractures in strands five and six were located on the inside of the tendon curvature, while fractures in strands one through four occurred on the outside of the curvature (Fig. 4.20).

The plastic duct was rubbed through at several locations. The strands showed very regular surface abrasions and black discoloring in a pattern corresponding with the corrugations of the duct (Fig. 4.21). However, no wire fractures were induced from strand - duct or strand - concrete rubbing.

4.3.4 Metal Duct with Epoxy-Coated Strand Specimens. The tendon of specimen C6-7-30-0.69 was composed of six epoxy coated strands in a metal duct with a radius of curvature of 3.5m (138 in.). It was tested at a tendon stress range of 30 ksi. The result of this test is included in Figure 4.16. The epoxy coating clearly improved the fatigue performance.

The stiffness history for this specimen is shown in Figure 4.22. Its fatigue life was estimated to be 690,000 cycles. However, no data points are available between 420,000 and 690,000 cycles and the stiffness decrease from 420,000 cycles to 690,000 cycles is quite
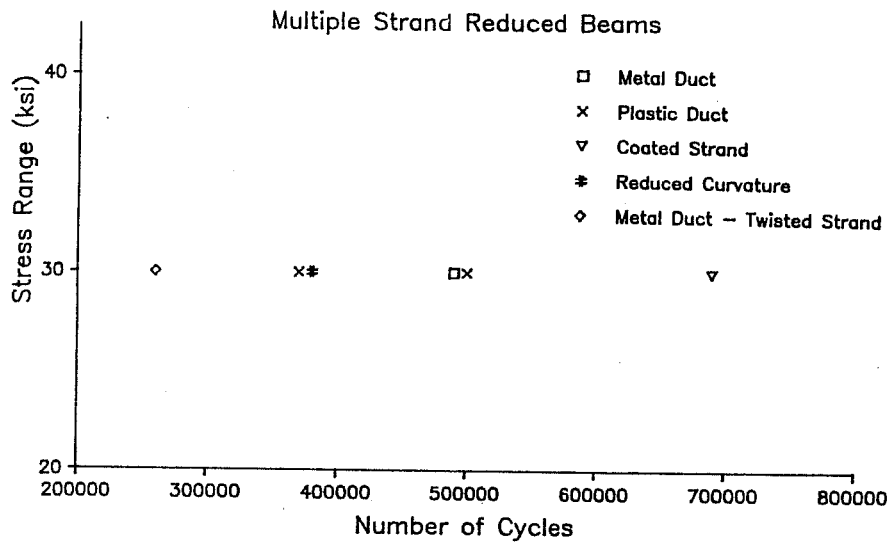
Figure 4.16 Comparison of parameters

94
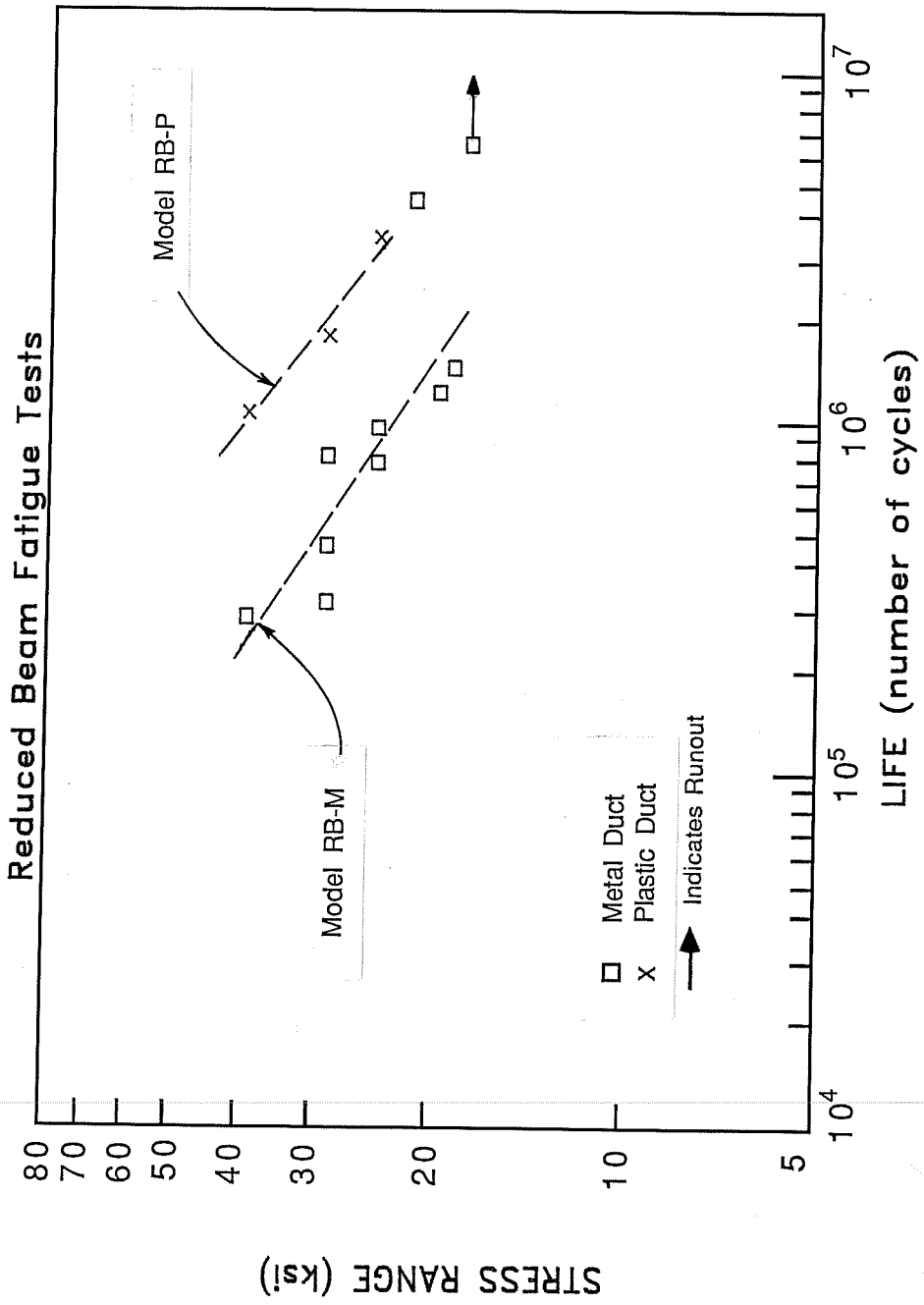
Figure 4.17 Results of single strand reduced beam fatigue tests
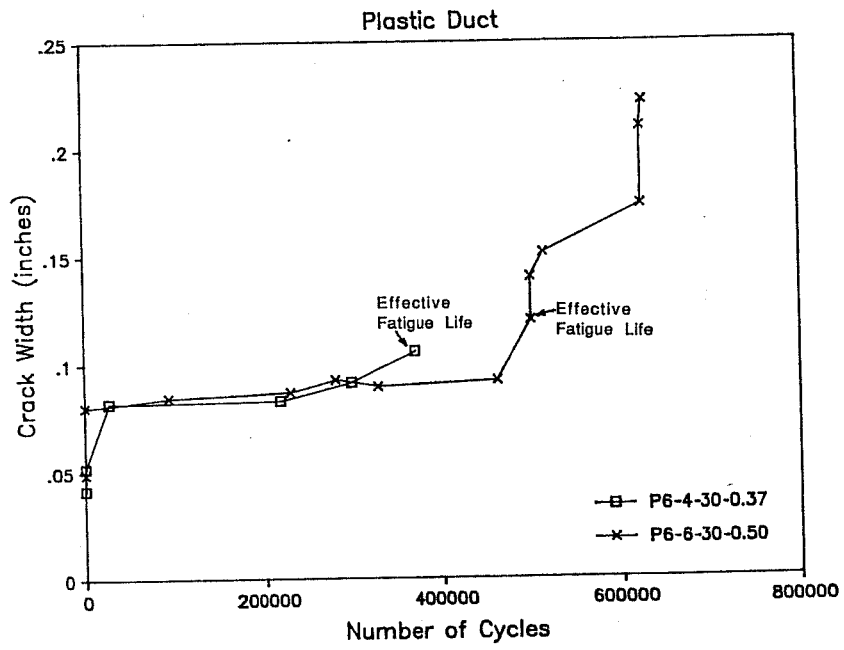
Figure 4.18   Stiffness histories for multiple strand reduced beam specimens with plastic
duct
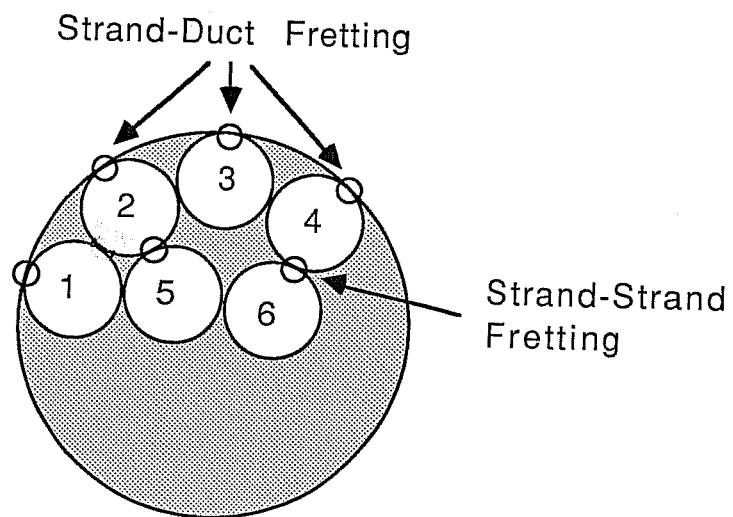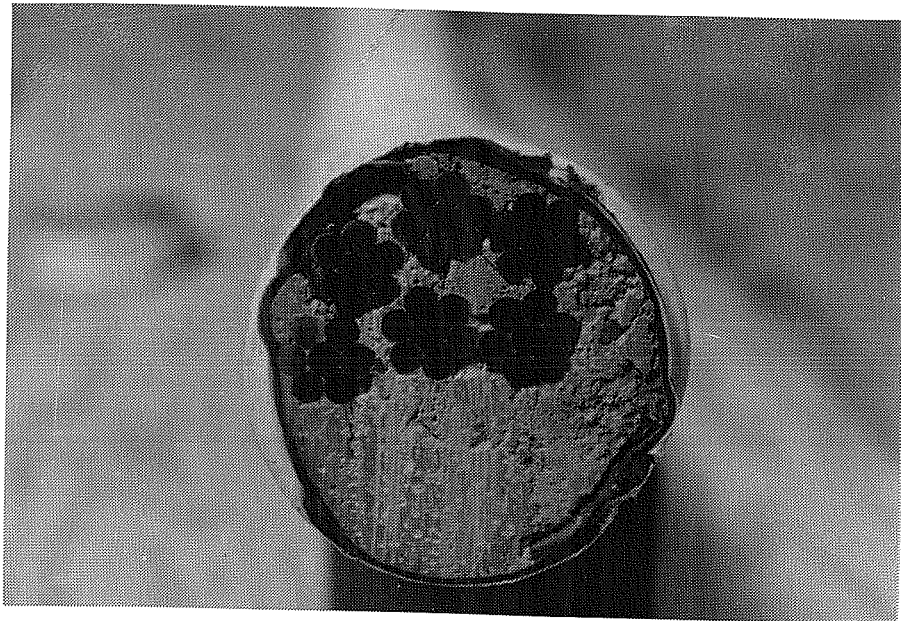
Figure 4.19   Typical strand arrangement
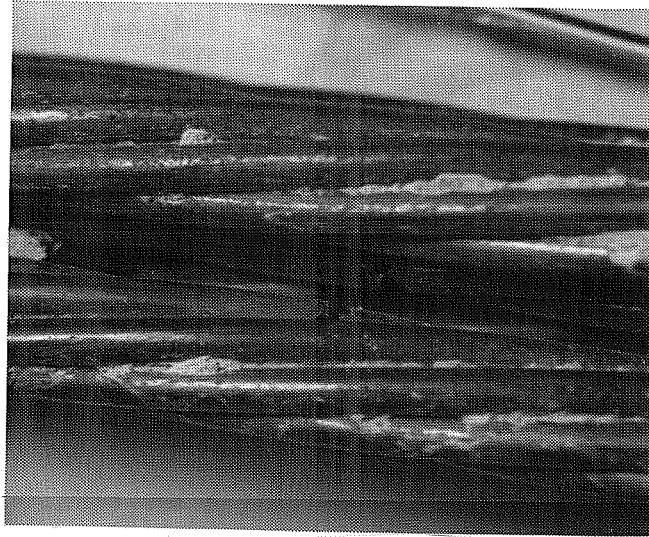
Figure 4.20   Strand - strand fretting fatigue fractures
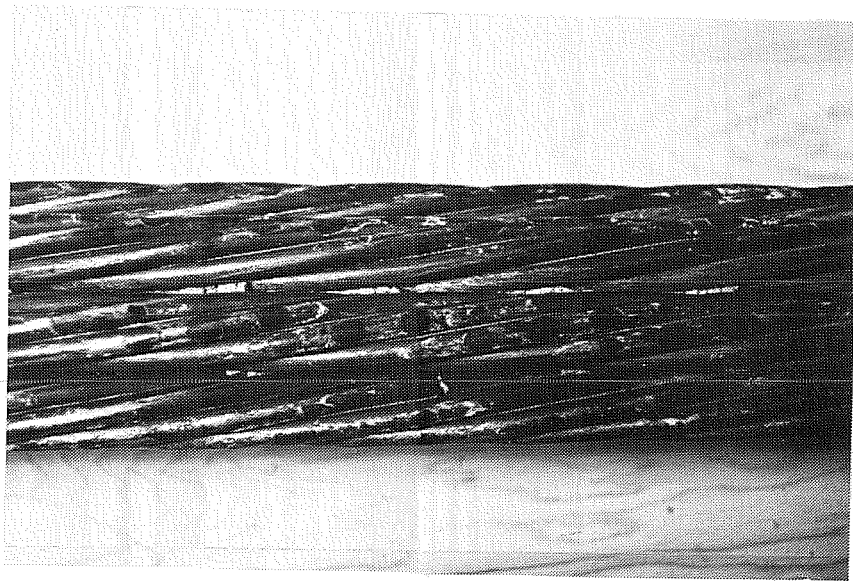
Figure 4.21   Abrasions and discoloring of strands in plastic duct
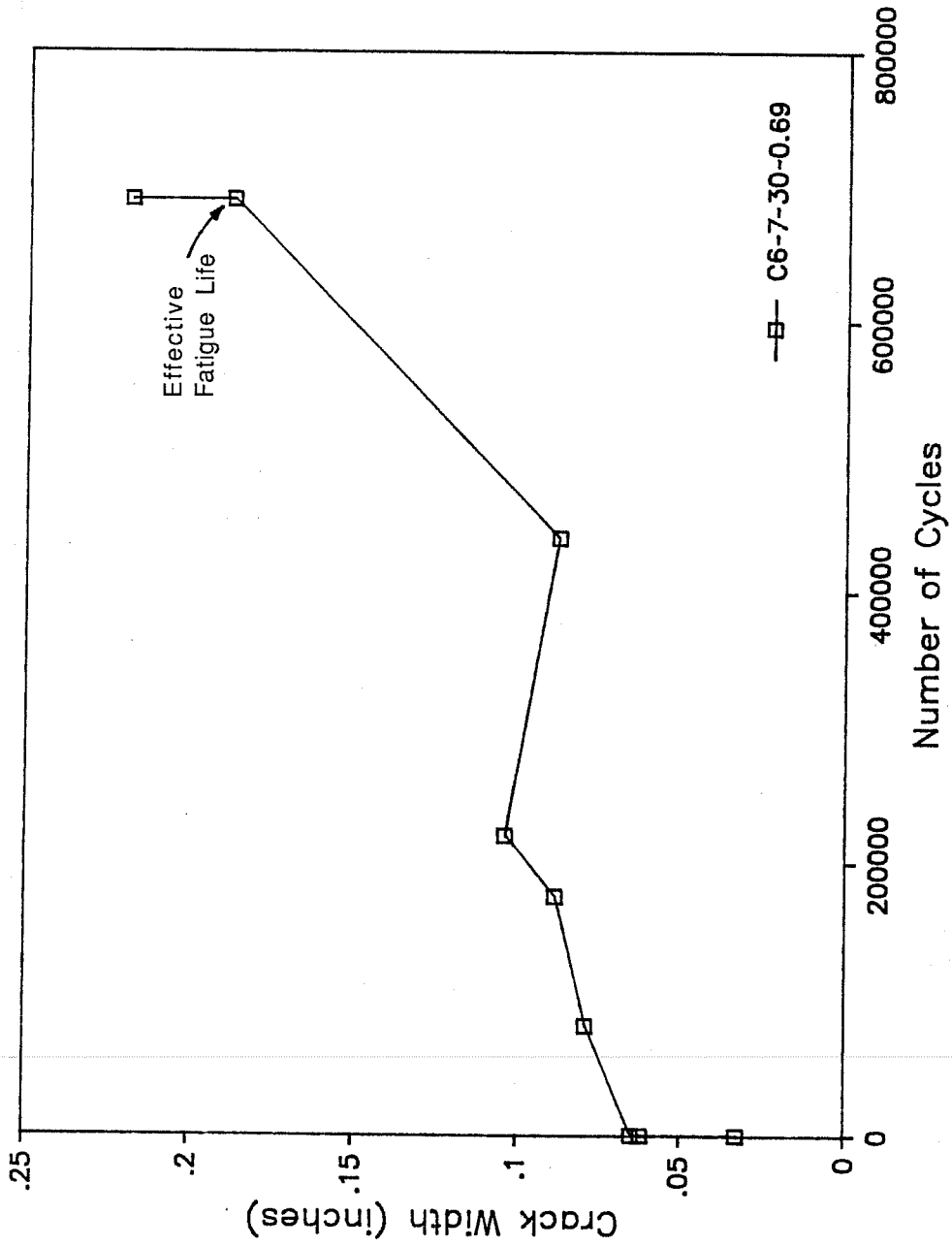
Figure 4.22   Stiffness history for multiple strand reduced beam specimen with epoxy coated strand

appreciable. Hence, the actual fatigue life may have been somewhat lower than indicated. Usually, the test setup was sensitive enough to detect stiffness changes much smaller than those that occurred between 420,000 and 690,000 cycles. It was concluded that either the deflection control was not set accurately enough for this specimen or that several wires fractured simultaneously at 690,000 cycles.

Figure 4.23 shows the epoxy coated strand tendon recovered from the expired specimen. Where strands and duct were in contact, the epoxy coat was deformed and worn, exposing the bare metal of the strand at some locations. Metal on metal fretting with traces of corrosion occurred only at one location where the epoxy was worn away. However, no fracture initiated from this contact.

Most fractures occurred due to wire to wire fretting and were concentrated at two locations. Nine fatigue fractures were found at the crack, and two more were found about four inches away. Where wires were fractured, the epoxy coat showed several cracks and separated easily from the prestressing strand (Fig. 4.24).

Evidence of fretting between individual wires of a strand was found. The oxide film on the surface of the steel was worn away along the very thin line of contact between wires. Abrasions on the duct due to contact with the coated strands were wider and did not cut as deep into the metal as was the case for the tests with uncoated strands in metal duct. The epoxy coat also showed scratches and wear due to strand - strand rubbing, but the blemishes never penetrated below the surface of the coating.

4.3.5 Metal Duct Specimens with Reduced Curvature. For two multiple strand reduced beam specimens the curvature of the tendon was reduced in order to achieve a smaller contact load between strands and metal duct. The strands were uncoated and a metal duct with a radius of curvature of 6.6m (258 in.) was used. A tendon stress range of 30 ksi was chosen for both specimens. The results of these tests are also shown in Figure 4.16.

The stiffness histories for the specimens with reduced tendon curvature are shown in Figure 4.25. The poor fatigue performance of specimen Q6-8-30-0.26 is remarkable and was very surprising. Previous research had indicated that reduced lateral pressure increases the fretting fatigue life. The post mortem investigation of this specimen revealed that two strands were twisted in the tendon, resulting in a severe concentrated contact load between the strands, which probably caused the premature failure (Fig. 4.26).

It was decided to repeat the test, carefully inserting the strands to preclude twisting. The second specimen with reduced tendon curvature showed a substantially better fatigue performance than the first one. However, the beneficial effect of reduced curvature still could not be confirmed. Specimen Q6-9-30-0.39 failed at approximately the same fatigue life as the corresponding specimen M6-2-30-0.49 with larger nominal contact load (Fig. 4.16).
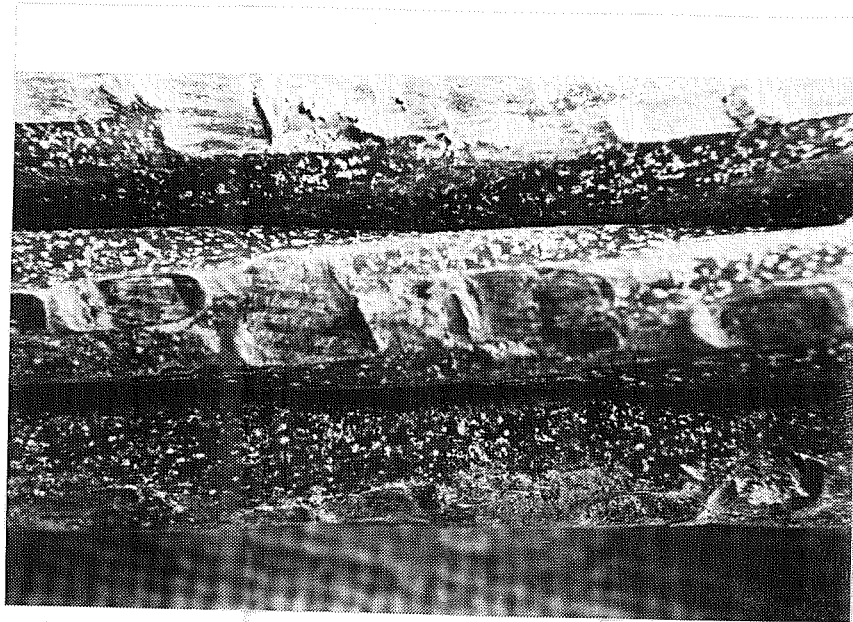
Figure 4.23   Wear and deformation of epoxy coated strand

Figure 4.24   Fractures in epoxy coated strand
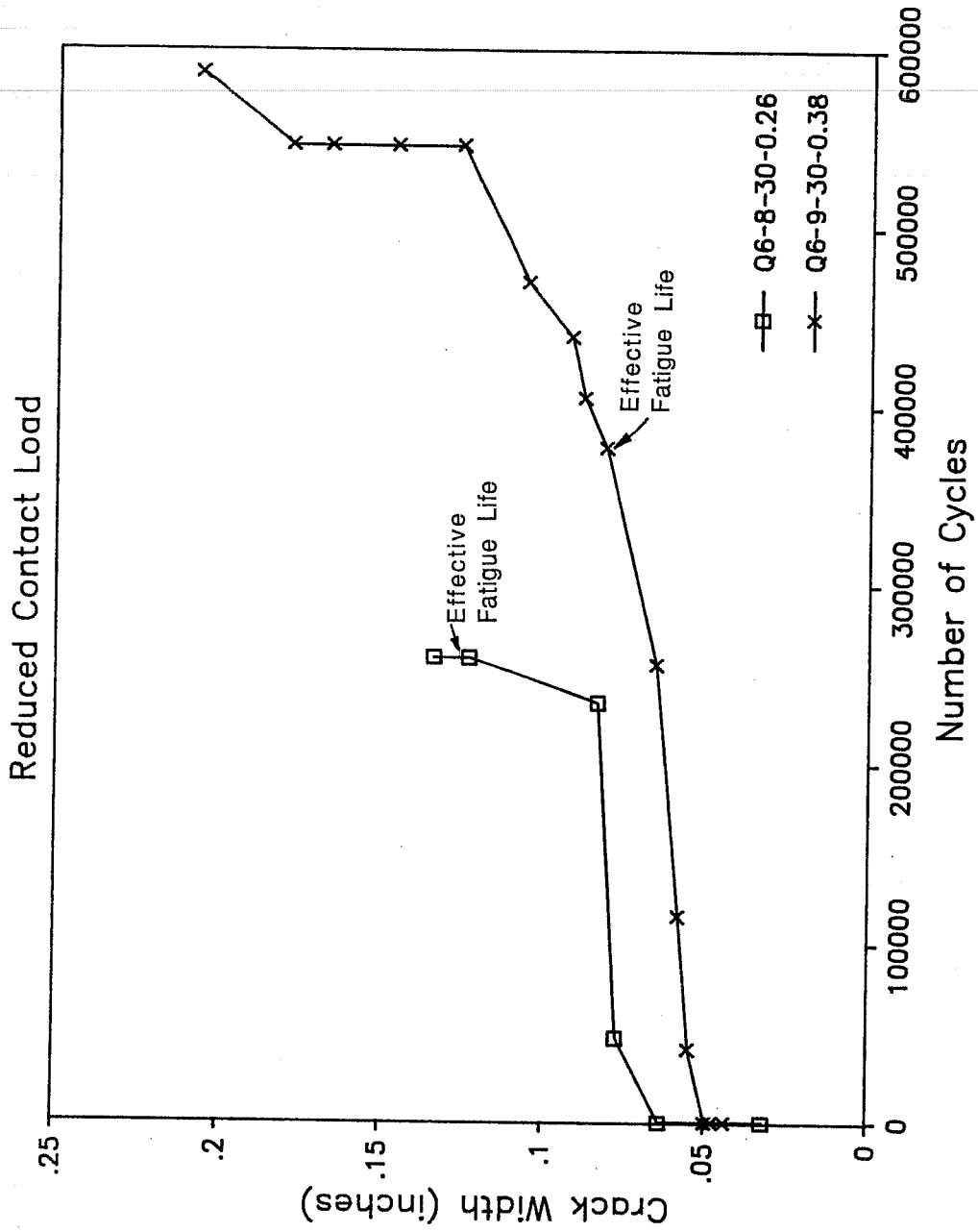
Figure 4.25   Stiffness histories for multiple strand reduced beam specimens with reduced tendon curvature
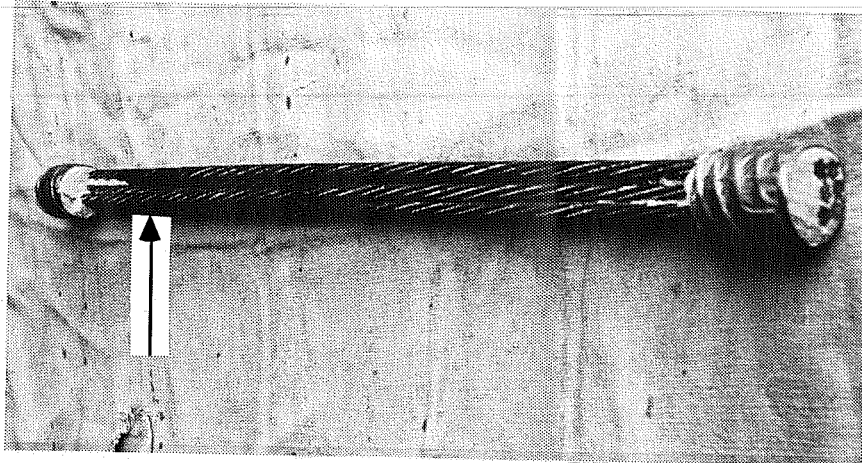
Figure 4.26   Twisted strands in Specimen Q6-8-30-0.26
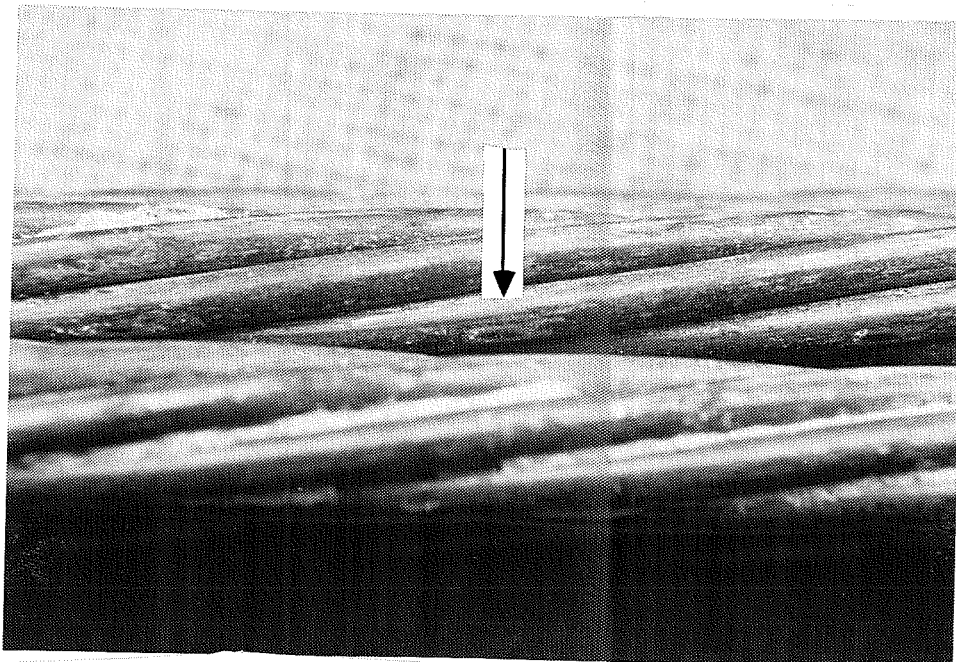
Figure 4.27   Strand-strand fretting

Figure 4.26 shows the tendon recovered from specimen Q6-8-30-0.26. Note the two lower strands which cross each other and thereby generate a locally increased contact pressure between the strands. Consequently all but one of the wire fractures in the tendon were initiated by strand - strand fretting, while one fracture occurred due to strand - duct fretting. Similar to the plastic duct tendons, strand - strand fretting was caused exclusively by the rubbing action of the interior strands against the peripheral strands.

For the second specimen of this Group Q, the parallel alignment of the strands within the tendon was carefully controlled and verified by the post mortem investigation. Fretting fatigue fractures, wear, and corrosion resembled very much those of the specimens of Group M. All fractures were induced by strand - duct or wire - wire fretting, but fretting corrosion due to strand - strand rubbing was found (Fig. 4.27) where interior and peripheral strands touched each other.

CHAPTER 5

COMPARISON AND EVALUATION OF TEST RESULTS

5.1 Introduction

This chapter is devoted to the evaluation and comparison of the test results of this and of previous studies. The following data sets are included in this evaluation and comparison of test results:

- girder tests by Rigon and Thurlimann [26]

- girder tests by Oertle, Thurlimann, and Esslinger [19]

- girder tests by Muller [18]

- University of Texas girder tests by Diab [11] and Georgiou [15]

- reduced beam tests by Oertle, Thurlimann, and Esslinger [19]

- University of Texas single strand reduced beam tests by Yates [31]

- University of Texas multiple strand reduced beam tests by Wollmann [34]

- fretting simulation tests by Cordes and Lapp-Emden [9].

Two comments are necessary at this point. It is difficult to interpret fatigue tests where varied loading histories are used. While most of the studies used constant load ranges throughout the test, Rigon and Thurlimann and Oertle, et al. did not maintain constant stress ranges. Instead they often increased the tendon stress range for their tests if no fractures had occurred at the lower stress range after a few million cycles. They then would continue fatigue testing at this higher stress range [19,26]. Since it is very difficult to assess how much impact the cumulative load cycles at the lower stress range had on the fatigue life, such data points were interpreted as run outs at the lower stress range at the number of cycles when the stress range was increased. Any further loading of the specimens was disregarded. This procedure was recommended by Yates [31].

The second comment refers to the Cordes and Lapp-Emden data points [9]. Their fretting simulation apparatus applied lateral pressure only at a very limited portion of the strand, but fractures were also reported in the free length of the specimen, particularly at higher stress ranges. Since these free length failure data do not represent fretting fatigue failures they were omitted from the following comparison.

In Figure 5.1a the test results for strand type tendons with metal duct are plotted and grouped according to the type of test. The general trend of reduced fatigue life with increased stress range is quite clear. However, many of the girder test results fall

105

Figure 5.1 Test Results for Strand Type
Tendons with Metal Duct
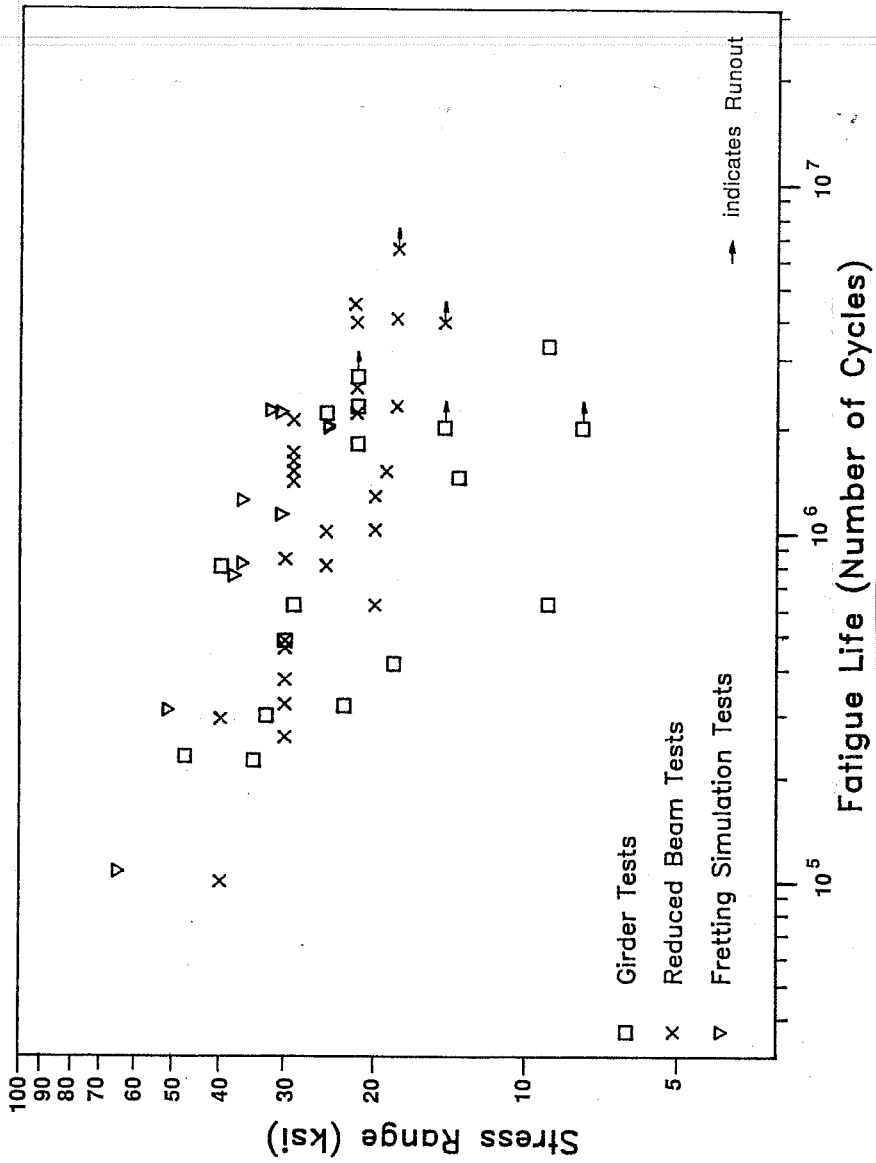
a) Grouped According to Type of Test

significantly below the bulk of the data. Also, the fretting simulation tests tend to show a somewhat better fatigue performance than the girder and reduced beam tests.

Figure 5.1b shows the same data points as Figure 5.1a, but this time they are grouped according to the data sets. This plot reveals that the inconsistent girder test results generally comprise data points reported by Rigon and Thurlimann. Oertle and Thurlimann conducted a follow up study to the Rigon and Thurlimann research program at the same institution. Referring to the Rigon and Thurlimann test series they state in Reference 20:

> Die durchgeführten Versuche waren nicht auf das Studium der überraschend aufgetretenen Reibermüdung ausgelegt. Im besonderen war es nachträglich nicht mehr möglich, die Vielfalt der einwirkenden Parameter (Spannungsamplitude, Hüllrohrmaterial, Krümmungsradius, Querpressung, Gruppenwirkung, usw.) zu separieren. Folglich wäre es auch unverantwortlich gewesen, quantitative Angaben über den Abfall der Ermüdungs - festigkeit infolge von Reibermüdung zu machen.

(Fretting fatigue was not foreseen in the Rigon and Thurlimann study and the tests were not designed specifically for the study of fretting fatigue. In particular, it was impossible to separate the many parameters affecting fretting fatigue (stress range, duct material, radius of curvature, lateral pressure, group effects, etc.) after conclusion of the tests. Consequently it would have been irresponsible to come up with a quantitative evaluation of the decrease of fatigue life due to fretting fatigue in post-tensioned concrete.)

In particular the indirect determination of the tendon stresses via measurements of the elongations of a passive reinforcement bar over a length of 200 mm seems to lead to a significant underestimation of the actual tendon stress concentrations at the cracks [19,26].

Hence, in Figure 5.1c the Rigon and Thurlimann and the Cordes, et al. fretting simulation data points were eliminated. The remaining test results are appreciably more consistent, although the scatter is still large. A similar trend can be shown by a comparison of test results for parallel wire tendons (Figure 5.2). Therefore it was felt that the exclusion of the Rigon and Thurlimann data could be justified.

One important objective of the present study was to compare the fatigue performance of prestressing strand subjected to ordinary fatigue and of strand subjected to fretting fatigue. Paulson, et al. compiled over 700 test results from ordinary strand fatigue tests in a previous study at The University of Texas at Austin [22], shown in Figure 5.3. Most of the data points fall within a clearly defined region (shaded), labelled "Strand in Air Failure Zone" and enclosed by dashed lines in the figure. In Figure 5.4 this strand in air failure zone is compared to the test results of the fretting fatigue tests after elimination of the Rigon, et al. and the Cordes, et al. data. All fretting fatigue data points fall below

108
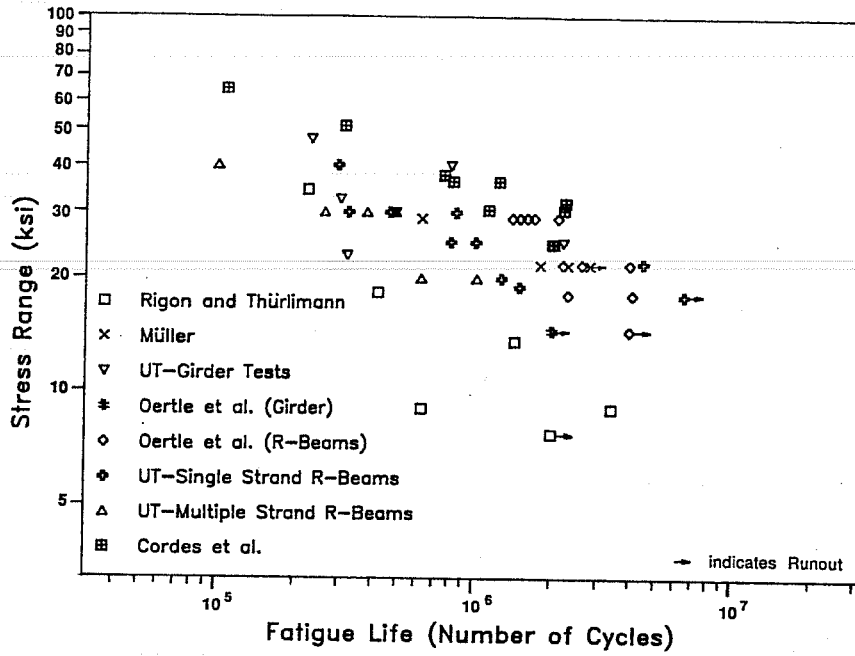
b) Grouped According to Data Sets
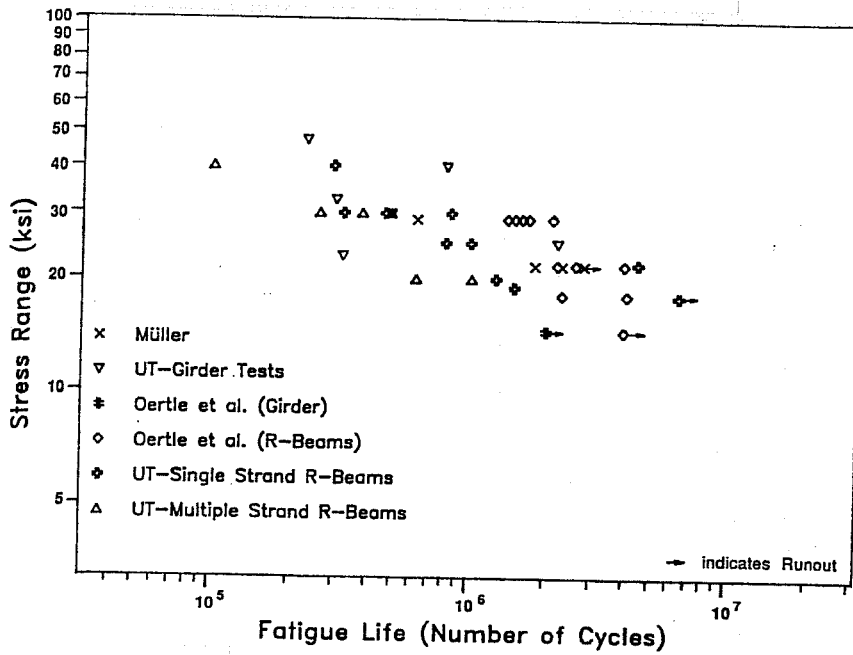
c) Rigon and Thürlimann and Fretting
Simulation Data Sets Eliminated

Figure 5.1   Test Results for Strand Type
Tendons with Metal Duct (cont.)
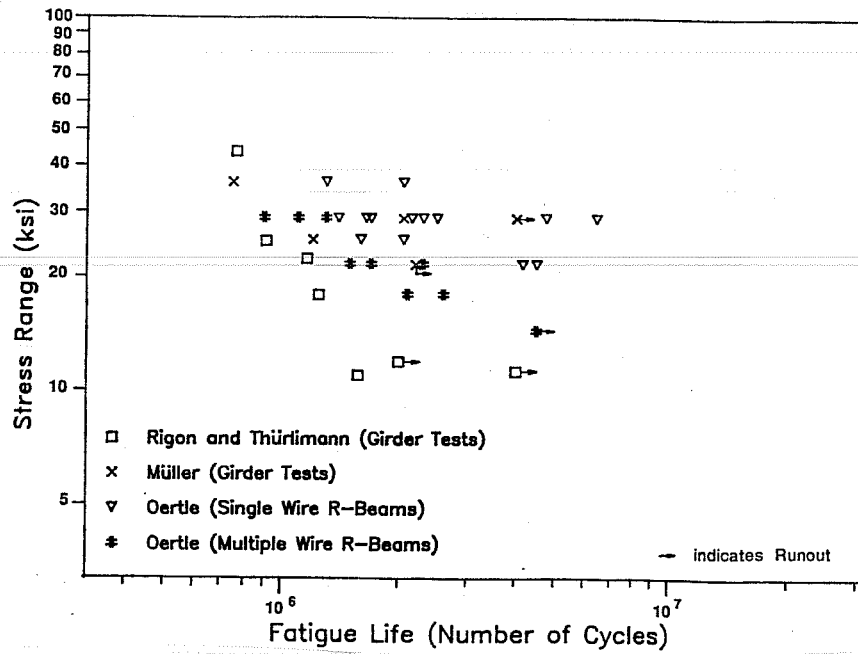
a) Including Rigon and Thürlimann Results
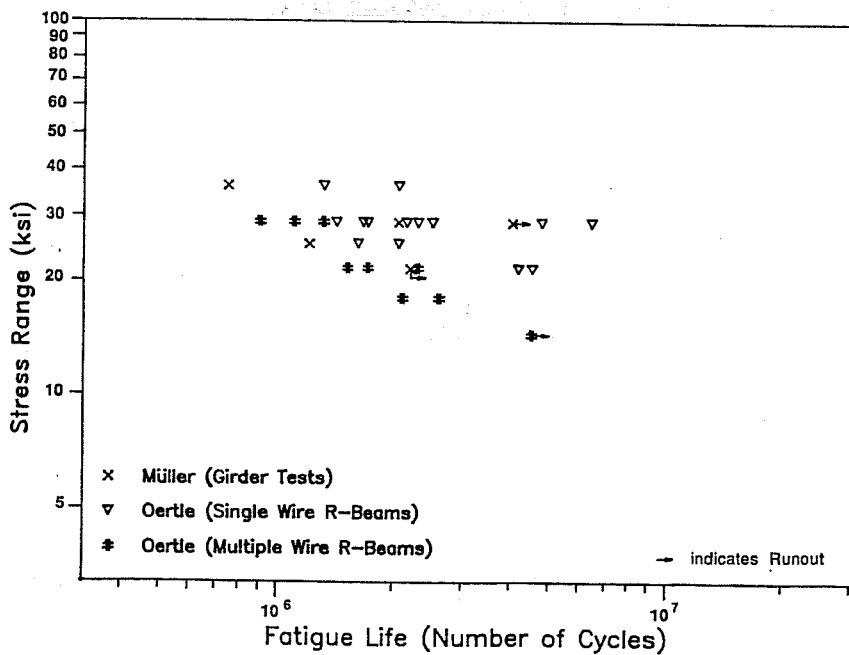
b) Excluding Rigon and Thürlimann Results

Figure 5.2   Test Results for Parallel Wire
Tendons with Metal Duct
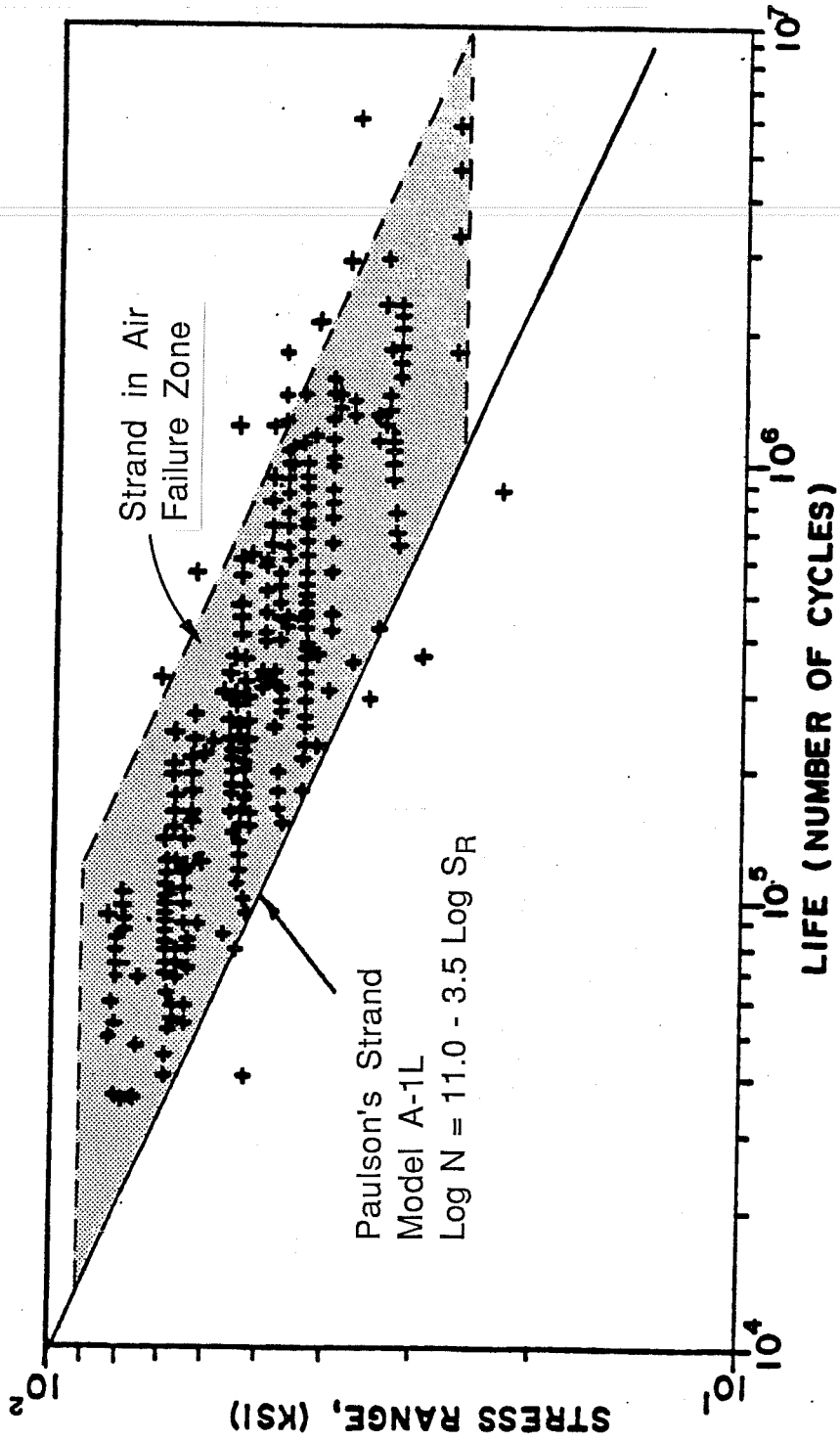
Figure 5.3   Strand in Air Failure Zone (after Paulson [22])
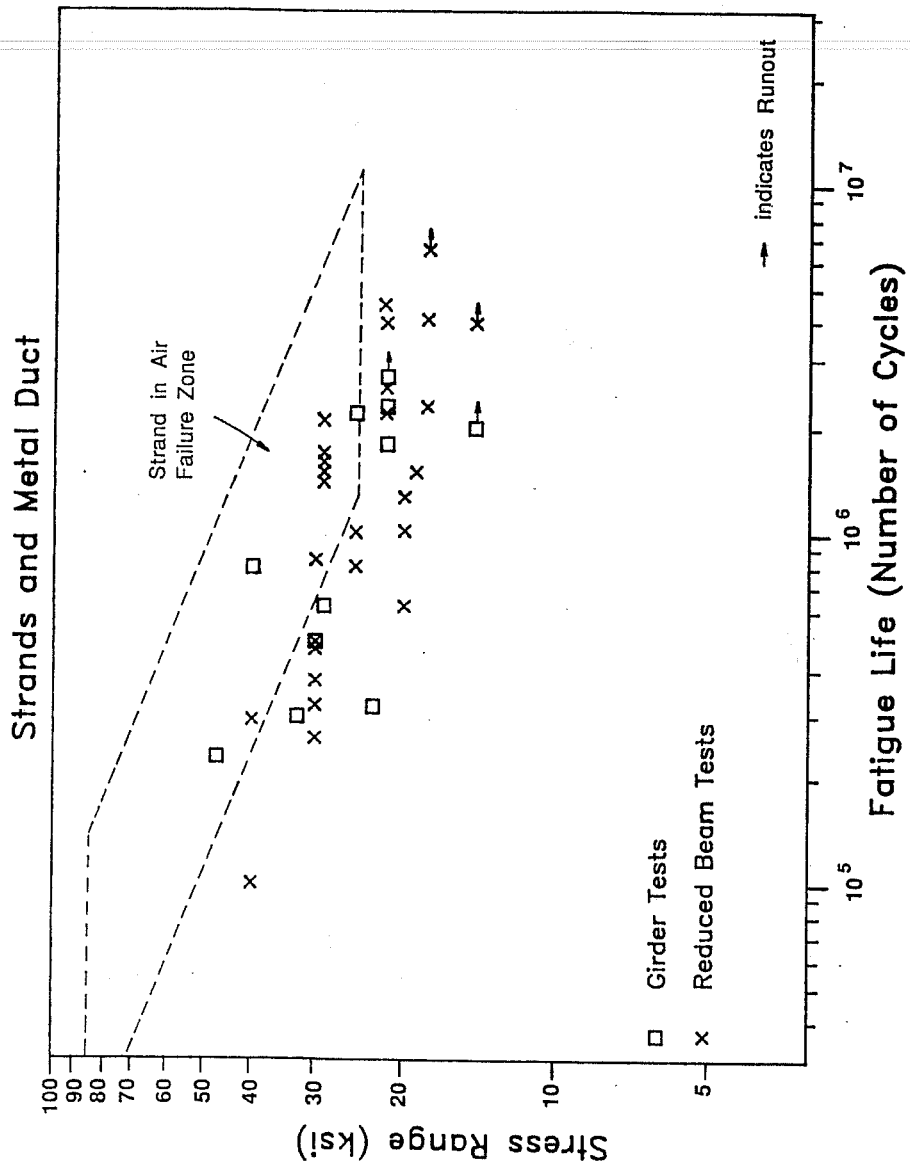
Figure 5.4   Detrimental Effect of Fretting Fatigue

or in the lower portion of the strand in air failure zone, indicating the detrimental effect of fretting fatigue in post-tensioned concrete. In contrast, a similar comparison for fatigue tests of pretensioned girders [21] shows that a lower bound model for strand in our tests also works for strands in pretensioned concrete girders (Figure 5.5).

In Figure 5.6 a fretting fatigue failure zone for post-tensioning strands is compared to the strand in air failure zone. The definition of the fretting fatigue failure zone will be discussed in Section 5.3. It is interesting to note that the scatter of the data is very similar for the strand in air and for the fretting fatigue tests. The width of the failure zone is about equal to log N = 1.0 for both cases, which means that the fatigue lives for different strands tested at the same stress range may vary as much as one order of magnitude. For example, a strand tested in air at a stress range of 30 ksi may fail anywhere between 700,000 and 7.000,000 load cycles. Similarly, a post-tensioning tendon tested at the same stress range may fail anywhere between 200,000 to 2.000,000 load cycles. Because of this considerable scatter of test results, a large number of data points would be required for meaningful parameter studies. Drawing conclusions from relatively few test results must be approached with care. However, the scatter band should be appreciably reduced when strands of similar fatigue characteristics are used in a single test series.

5.2   Significance of Test Results

5.2.1   Applicability of Reduced Beam Specimens.

5.2.1.1   Metal Duct Tendons. Figure 5.7a shows the test results for strand type tendons with metal duct, grouped according to the type of test. The fretting simulation and the Rigon and Thurlimann data points have been eliminated, as discussed in Section 5.1. The results for the remaining girder tests and for the reduced beam tests overlap at all stress ranges, indicating the applicability of reduced beam specimens for fretting fatigue tests of strand type tendons with metal duct. This is also true for parallel wire tendons with metal duct (Fig. 5.7b). The girder test results reported by Muller [18] overlap with Oertle's reduced beam data [19].

5.2.1.2   Plastic Duct Tendons. Only a very limited number of test results with strand type tendons and plastic duct is available, and the majority of the data stem from single strand reduced beam tests [19,31]. After elimination of the Rigon and Thurlimann data, only three girder test results remain, one reported by Oertle, et al. [19], and the other two by Georgiou [15]. Two more data points for multiple strand tendons were reported by Wollmann [34]. The remaining data points were obtained from single strand reduced beam tests and were reported by Oertle, et al. [19] and Yates [31]. In Figure 5.8 these results are presented. The data points are grouped into test results from specimens with single strand and from specimens with multiple strand tendons. Also included in the figure for reference is the strand in air failure zone. While the single strand specimens
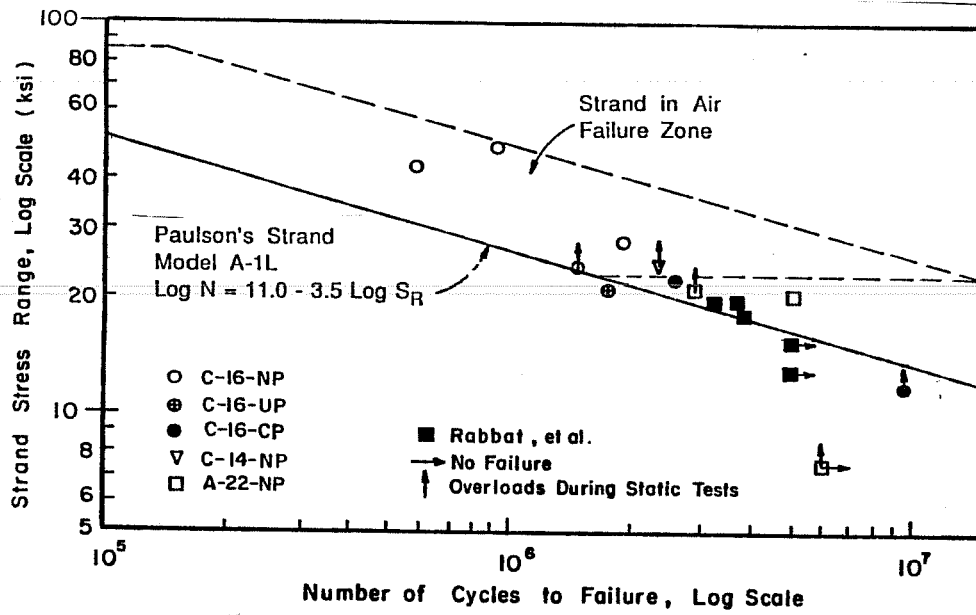
Figure 5.5   Fatigue of strands in pretensioned girders (from Overman [21]).
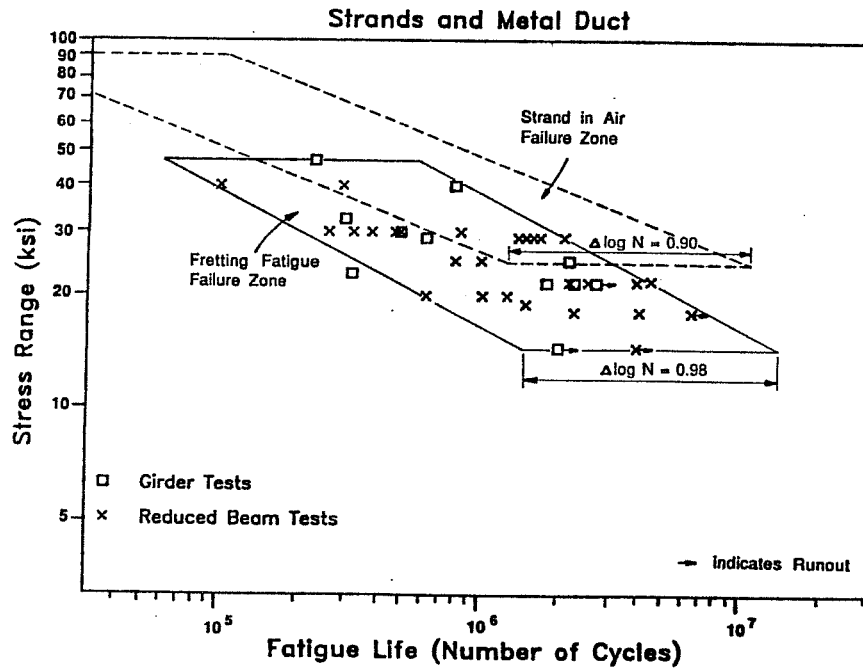
Figure 5.6   Fretting fatigue failure zone.

114
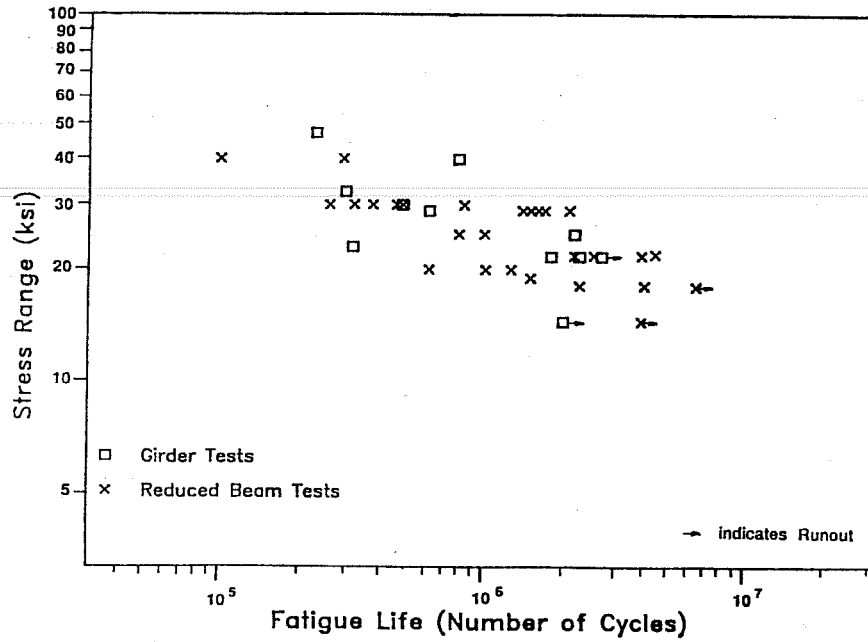
a) Strand Type Tendons with Metal Duct
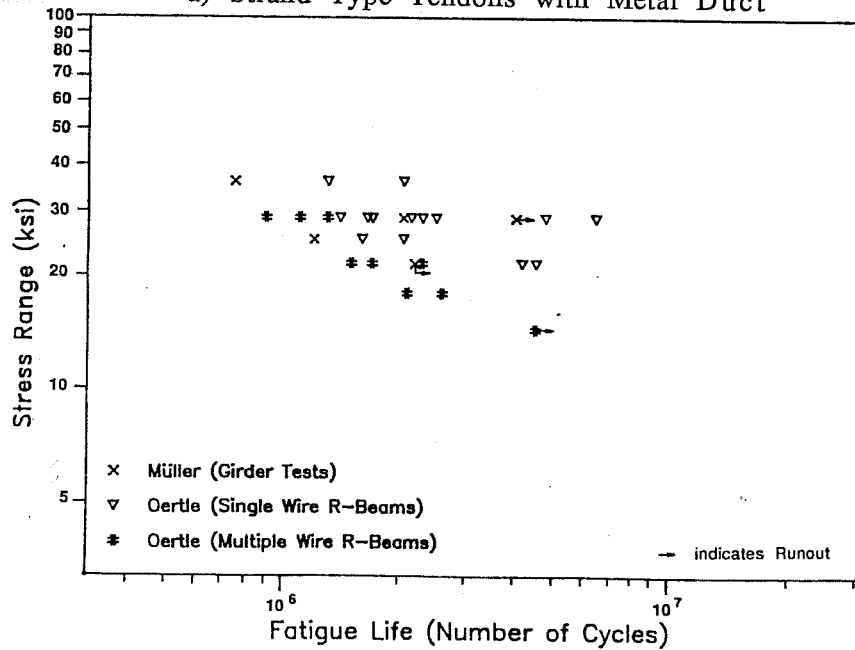
b) Parallel Wire Tendons with Metal Duct

Figure 5.7   Applicability of reduced beam specimens

Figure 5.8   Test results for strand type tendons with plastic duct.

clearly indicate a substantial improvement in the fretting fatigue performance with the use of plastic duct, this trend is not confirmed by the multiple strand specimens, which experienced interlayer strand to strand fretting and had reduced fatigue lives.

Oertle, et al. report in Reference 19 that their girder test with a tendon composed of four strands and a plastic duct had a longer fatigue life than a corresponding girder with a metal duct. But in actuality the girder with the tendon in the plastic duct was tested at a higher stress range and failed earlier than the girder with the tendon in the metal duct, so that a direct comparison is not possible.

The data for multiple strand specimens with plastic duct are extremely scarce, and any conclusions have to be drawn with care. However, it is obvious that single strand reduced beams are not able to model group effects in a tendon, such as fretting between individual strands. This has little influence on tests with metal duct tendons, since the predominant failure mode is strand - duct fretting fatigue and this also occurs in single strand reduced beams. However, with plastic duct wire fractures are induced by fretting between individual strands and this cannot be reproduced in single strand tendons. It is interesting to note that for parallel wire tendons with one or several wires all test results consistently show a beneficial effect of plastic duct [19,26].

5.2.2 Comparison with Actual Structures.
Laboratory tests allow close monitoring and control of many parameters. But they also require consideration of time and monetary constraints, which may result in neglecting some of the parameters affecting actual structures. For the present study these differences concern the environment and the load history.

An item of particular concern has been corrosion of the prestressing steel subsequent to cracking of a girder, due to aggressive agents in the environment (acid rain, seawater, deicing salt). It is unknown how this electro-chemical corrosion may effect fretting fatigue of post-tensioning tendons.

The load history for actual structures is random and irregular. Load distribution, prestress losses, and subsequent crack formation are uncertain. Little information on magnitude and frequency of typical tendon stress ranges is available. Many structures may be subjected to occasional overloads, yet others possibly never have to carry their full service load. At this time no studies concerned with actual service load stress range histories or the evaluation of the effects of irregular loading on the fretting fatigue performance of post-tensioning tendons are available.

5.3 Discussion of Principal Parameters

5.3.1 Introduction. Fretting fatigue of post-tensioning tendons is affected by a large number of interdependent variables, only a few of which have been studied systematically in the past. Because of the complex interactions between these variables, the isolation of individual parameters becomes extremely difficult. Furthermore the influence of some variables is highly nonlinear. Considering the somewhat sparse data available at this time, and the large scatter of fatigue test results, any conclusions have to be regarded with caution. However, this and previous studies have greatly enhanced our understanding of fretting fatigue in post-tensioned concrete, and it is felt that meaningful interim recommendations are possible at this stage of research.

The following sections are devoted to the discussion of some of the important parameters investigated in this and other studies.

5.3.2 Group Effects. Except in unbonded monostrand construction used in slabs, almost all post-tensioning applications use multiple strand tendons. Inclusion of more than one strand in a tendon greatly increases the lateral pressure between strands and duct, depending on the strand arrangement, duct size, and strand diameter. Furthermore, fretting between individual strands becomes a possibility, as was shown by the test results of the multiple strand reduced beams. Apparently the severity of this strand fretting is highly dependent on the strand arrangement. It does not seem to be a problem between strands in one layer, but fractures occurred due to fretting of interior strands against the peripheral strands.

5.3.3 Stress Range. A regression analysis was conducted for the test results of the strand type tendons with metal duct. Runouts were omitted from this analysis. Two characteristic values are available to estimate the quality of the straight line fitting: The correlation coefficient R, and the standard error s′. For a perfect fit R is equal to 1.0 and s′ is equal to 0.0. The mean fretting fatigue life model presented in Figure 5.9 has a correlation coefficient R = 0.68, and the standard error s′ equal to 0.29.

For design purposes a lower limit model is more useful, such as indicated in Figure 5.9. This model represents a 97% confidence limit, which means there is a 97% probability that a test result falls above that line. The data indicate that a stress range of 14.5 ksi or less ensures a fatigue life of at least two million load cycles. However, not enough data is available to verify a true endurance limit. Cordes, et al. point out in Reference 9, that fretting fatigue failures may occur as late as after ten million load cycles.

Finally, a fretting fatigue failure zone for strand type tendons with metal duct is defined in Figure 5.9. It contains 94% of the data evaluated, thus there is a 94% probability that approximately a test result will fall in this zone.
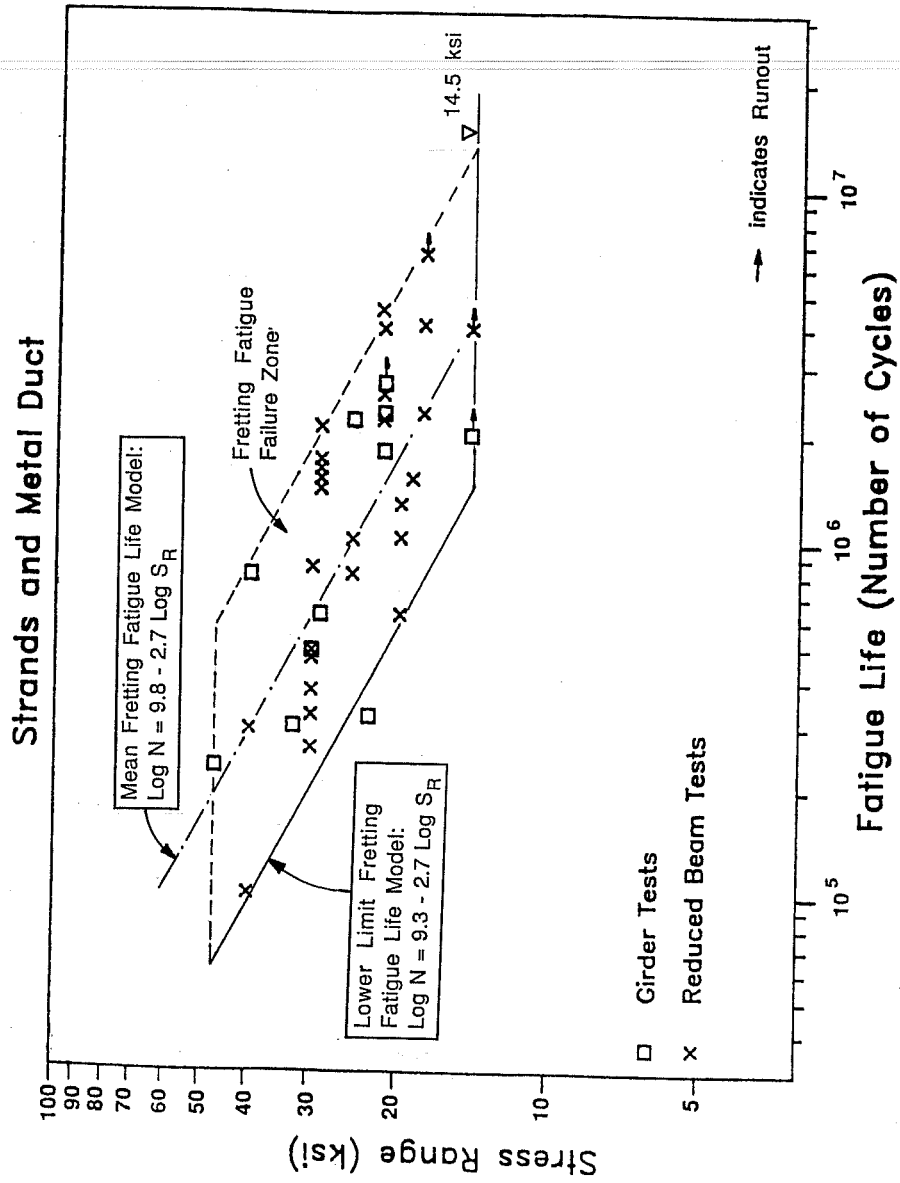
Figure 5.9   Fretting fatigue life models for strand type tendons with metal duct

In Reference 31 Yates suggested a design approach patterned after the current AASHTO recommendations for fatigue stress ranges in steel structures [1] as a way of describing the fretting fatigue life of post-tensioning tendons. In this way the traffic volume and service application can be related to general AASHTO procedures. More specifically, he recommended the use of AASHTO Category D model for redundant load path structures for tendons with a contact load less than ten kips/ft, and the AASHTO category B model for contact loads less than six kips/ft. It should be kept in mind that these AASHTO recommendations were developed for steel structures. Their application to post-tensioned concrete girders is for mere convenience and has no direct physical relationship. In fact, there are very profound differences between ordinary fatigue in steel structures and fretting fatigue in post-tensioning tendons. However, such an indirect procedure has been successfully used in fatigue criteria for cable stays [23].

In Figure 5.10 the lower limit model of the present study and AASHTO Category B, C, and D models are compared. Yates did not exclude the Rigon and Thurlimann data in his study [31] and therefore recommended the Category D model as a lower limit. Figure 5.10 shows that the Category C recommendation approximates more closely the lower limit model of the present study, where the Rigon and Thurlimann data were eliminated.

Yates also recognized the beneficial effect of reduced contact loads and recommended the less conservative AASHTO Category B model for tendons with a mean contact load less than six kips/ft. The influence of the contact load will be discussed in Section 5.3.5.

5.3.4 Duct Material. It was felt that not enough conclusive data was available for a regression analysis for strand type tendons with plastic duct. The data for single strand tendons and multiple strand tendons are in contradiction, and the number of multiple strand tendon tests is extremely limited. In Figure 5.8 the test results for strand type tendons with plastic duct are shown, and in Figure 5.11 the recommended lower limit design model for metal duct tendons is added. The latter figure shows that this design model may also be used for plastic duct multiple strand tendons.

Studies by Rigon, et al. and by Oertle, et al. show that the use of plastic duct undoubtedly improves the fatigue performance of parallel wire tendons. This trend could not be confirmed for multiple strand tendons in the present study. However, the data are extremely scarce, and more research is needed. As pointed out in Section 5.3.2 the strand arrangement within the tendon is critical factor for fretting between individual strands of a tendon, and future research should consider this finding.

The plastic duct used in the specimens of the present study was a corrugated tube with closely spaced inward and outward deformation. Oertle [19] reported development of an improved plastic duct with widely spaced corrugations which are essentially only
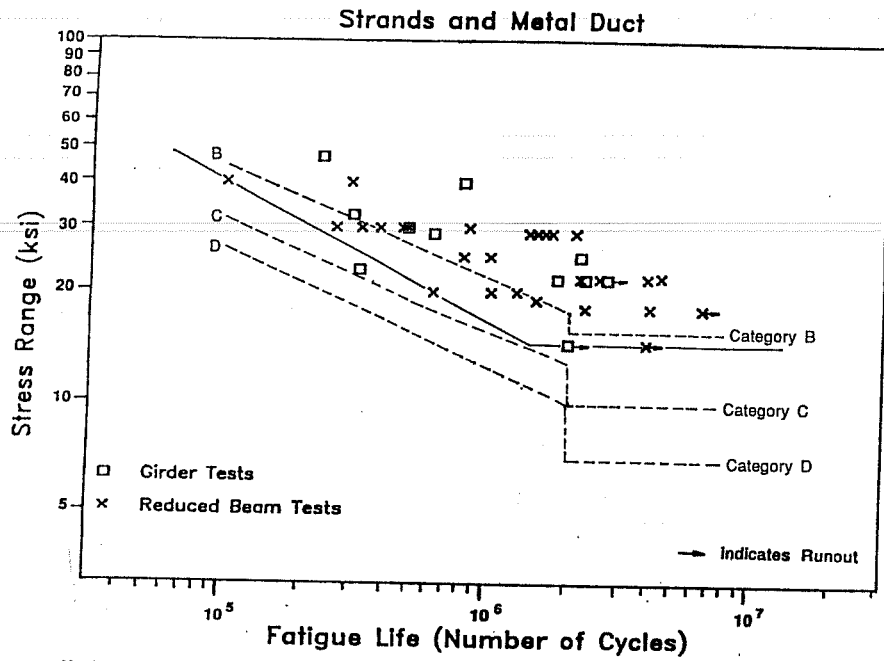
Figure 5.10   Comparison of lower limit fatigue model with AASHTO recommendations for redundant load path
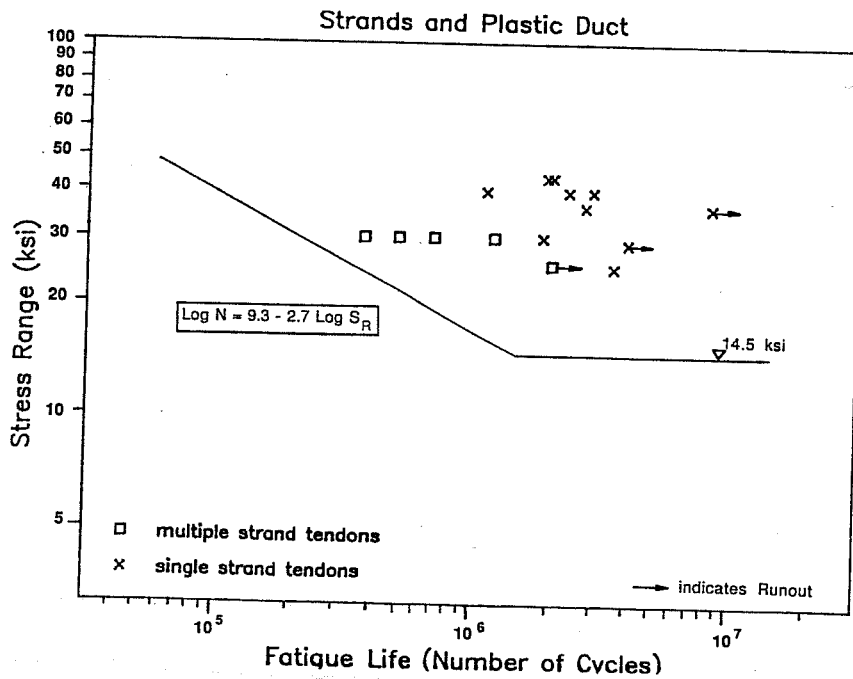
Figure 5.11   Fretting fatigue life model for strand type tendons with plastic duct.

outward. This should result in improved performance in single layer tendons but would probably not control strand-to-strand fretting between layers of strands.

5.3.5 Contact Load. Yates suggested in Reference 31 that the contact load between strands and duct or individual strands has a significant influence on the fatigue performance of post-tensioning tendons. Since the data base was changed by the elimination of the Rigon and Thurlimann data and by addition of the latest test results, a reevaluation of the influence of the contact load became necessary. Yates compiled a listing of test results and contact loads from several studies [31]. An updated version of this listing for the strand type tendons with metal duct is shown in Table 5.1. In Figure 5.12 the test results are organized in five groups according to the lateral load:

1) $q < 1$ kip/ft   (one data point)

2) $4 < q < 5$ kips/ft   (14 data points)

3) $5 < q < 6$ kips/ft   (13 data points)

4) $6 < q < 8$ kips/ft   (eight data points)

5) $8 < q < 10$ kips/ft   (one data point)

Groups 1, 2, 4, and 5 confirm the trend of improved fatigue performance with decreased lateral load. However, the test results of group three contradict this trend. Closer examination of this group reveals that all but one data point originate from the reduced beam tests by Oertle, et al. [19]. The only other inconsistent data point stems from a University of Texas girder test. It shows a surprisingly high fatigue life.

In Figures 5.13a and 5.13b the test results of the single strand reduced beams with metal duct and with plastic duct, respectively, are plotted. In both figures the majority or all of Yates' data fall significantly below the results of Oertle, et al., despite Yates' lower contact load. However if test results of specimens with multiple strand tendons are compared, the general trend of increased fatigue life with decreased contact load is confirmed (Fig. 5.14). A similar trend was identified for parallel wire tendons, as indicated in Figure 5.15.

In Figure 5.16 the test results of both single strand and multiple strand tendons are included and categorized according to contact loads less or greater than six kips/ft. If the division line is drawn at this level of contact load, the reverse trend of the Oertle, et al. data is concealed and a beneficial effect of reduced contact load is indicated again. Therefore it was concluded that another parameter must have offset the detrimental effect of the larger contact load in the reduced beam specimens by Oertle, et al..

In Table 5.2 some of the important variables of the reduced beam specimens by Yates and by Oertle, et al. are listed and compared. Both specimens had the same tendon

Table 5.1 Test Results for Strand Type
Tendons with Metal Duct
(adapted from Yates [31])

Researchers	Tendon Type	Stress Range [ksi]	Fatigue Life [x 1,000]	K-Factor	Contact Load [kips/ft]
Müller [18]	3-0.6 in. dia. 7 Wire Strands	28.9	620	0.65	4.4
		21.7	1,800	0.65	4.3
		21.7	2,300	0.65	4.3
		21.7	2,800 R.O.	0.65	4.3
UT-Girder Tests [11,15]	6-0.5 in. dia. 7 Wire Strands	47	229	0.51	7.3
		32.5	300	0.51	7.9
		23	320	0.51	7.6
		40	800	0.51	5.9
		30	490	0.51	7.1
		25	2,200	0.51	0.7
Oertle, et al. (girder) [19]	4-0.6 in. dia. 7 Wire Strands	14.5	2,000 R.O.	0.69	9.7
Oertle, et al. [19] (reduced beams)	1-0.6 in. dia. 7 Wire Strand	29	1,400	1.0	5.4
		29	1,500	1.0	5.9
		29	1,500	1.0	5.9
		29	1,600	1.0	5.9
		29	1,700	1.0	5.9
		29	2,100	1.0	5.4
		21.8	2,200	1.0	5.6
		21.8	2,600	1.0	5.6
		21.8	4,000	1.0	5.6
		18.1	2,300	1.0	5.6
		18.1	4,100	1.0	5.6
		14.5	4,000 R.O.	1.0	5.7

Table 5.1   Test Results for Strand Type
Tendons with Metal Duct (cont.)
(adapted from Yates [31])

Researchers	Tendon Type	Stress Range [ksi]	Fatigue Life [x 1,000]	K-Factor	Contact Load [kips/ft]
UT-Single Strand Reduced Beams [31]	1-0.5 in. dia. 7 Wire Strand	40	293	1.0	4.2
		30	323	1.0	4.1
		30	467	1.0	4.7
		30	841	1.0	4.3
		25	804	1.0	4.2
		25	1,008	1.0	4.1
		22	4,515	1.0	4.1
		20	1,270	1.0	4.2
		19	1,500	1.0	4.2
		18	6,500 R.O.	1.0	4.7
UT-Multiple Strand Reduced Beams	6-0.5 in. dia. 7 Wire Strands	40	100	0.51	7.5
		30	490	0.51	7.6
		20	(620)*	0.51	8.1
		20	1,020	0.51	8.1
		30	260	0.51	(4.0)**
		30	380	0.51	4.1

R.O.   Runout   *) after full crack opening   **) twisted strand

Figure 5.12   Test results for strand type tendons with metal duct grouped according to contact load.

a) Strand and Metal Duct

b) Strand and Plastic Duct

Figure 5.13   Comparison of single strand reduced beam test results.

Figure 5.14   Comparison of multiple strand reduced beam test results

Figure 5.15   Influence of contact load for parallel wire tendons with metal duct

128

Figure 5.16   Influence of contact load for strand type tendons with metal duct.

Table 5.2   Comparison of Variables for
Single Strand Reduced Beams

	Yates [31]	Oertle, et al. [19]
tendon curvature	2.0 m (254 in)	2.0 m (254 in)
contact load	4.0 - 4.7 kips/ft	5.4 - 5.9 kips/ft
grout strength	2000 - 3400 psi	not available
prestress level	160 ksi (0.60 f_{pu})	140 ksi (0.55 f_{pu})
maximum tendon stress	200 ksi (0.74 f_{pu})	180 ksi (0.71 f_{pu})
tendon	1-0.5 in. dia. 7 Wire Strand 2.0 in I.D. Duct grout area: 2.99 in^2	1-0.6 in. dia. 7 Wire Strand 30 mm (1.2 in) I.D. Duct grout area: 0.87 in^2

curvature and were based on the same principle, as discussed in Chapter Two. The only apparent dissimilarity lies in the tendon size and the strand diameter, as shown in Table 5.2. The ratio of duct diameter to strand diameter is much smaller for the reduced beams tested by Oertle, et al.. However, a much more important difference is revealed upon closer examination of Figure 5.13b. It is striking that the reduced beams with plastic duct tested by Oertle, et al. exhibited a fatigue life better than would be expected for strand in air tests. Yates pointed out in Reference 31 that fractures in single strand tendons with plastic duct are caused by normal fatigue, rather than fretting fatigue. Hence, the comparison of the single strand reduced beam test results in Figure 5.13b indicates that the strand used by Oertle, et al. had superior ordinary fatigue characteristics. The strand in air fatigue properties of their strand are not specifically characterized in their report. The strand used by Yates had been thoroughly characterized in air tests and was within the normal range. This difference in the ordinary fatigue characteristics may also explain the inconsistency of the test results of the single strand reduced beams with metal duct (Fig. 5.13a). However, it should be noted that Rigon and Thurlimann characterized the fatigue properties of the strand used in their study [26] and the strand in air data fell well within the general strand in air failure zone previously defined. The tests conducted by Oertle, et al. were a follow up study to the Rigon and Thurlimann research program at the same institution, but it is unknown if strand from the same spool and from the same manufacturer was used in both studies.

Despite the contradicting trend of the reduced beam test results by Oertle, et al. the indications for a beneficial effect of a decreasing contact load on the fatigue performance are very strong. However, it should be kept in mind that no systematic study of the influence of the contact load by individual researchers is available at this time. Only for the multiple strand reduced beams and girders of the present study were tendon curvature and thus contact load varied, but they failed to clearly reveal the influence of these parameters. More research is necessary to clarify this question.

In Figure 5.17 two fretting fatigue design models are recommended. Model SM-1 is the previously discussed lower limit fatigue model and applies to tendons with a contact load less than eight kips/ft. For contact loads below six kips/ft a less conservative model - SM-2 - is suggested, as indicated in the figure. In Figure 5.18 models SM-1 and SM-2 are compared to the current AASHTO Category B and C recommendations for redundant load path structures which could be safely used to approximate these results.

A method to determine the contact loads in a tendon was suggested by Oertle in Reference 20 and by Yates in Reference 31 and is also illustrated in this study in Figure 4.2. However, the method is involved and cumbersome so that a simpler approach is desirable. An attempt was made to find a simple equation for the K - factor which is required to compute the contact load [34]. The K - factors for typical tendon arrangements were calculated, and the results of these calculations are listed in Table 5.3 and plotted in Figure
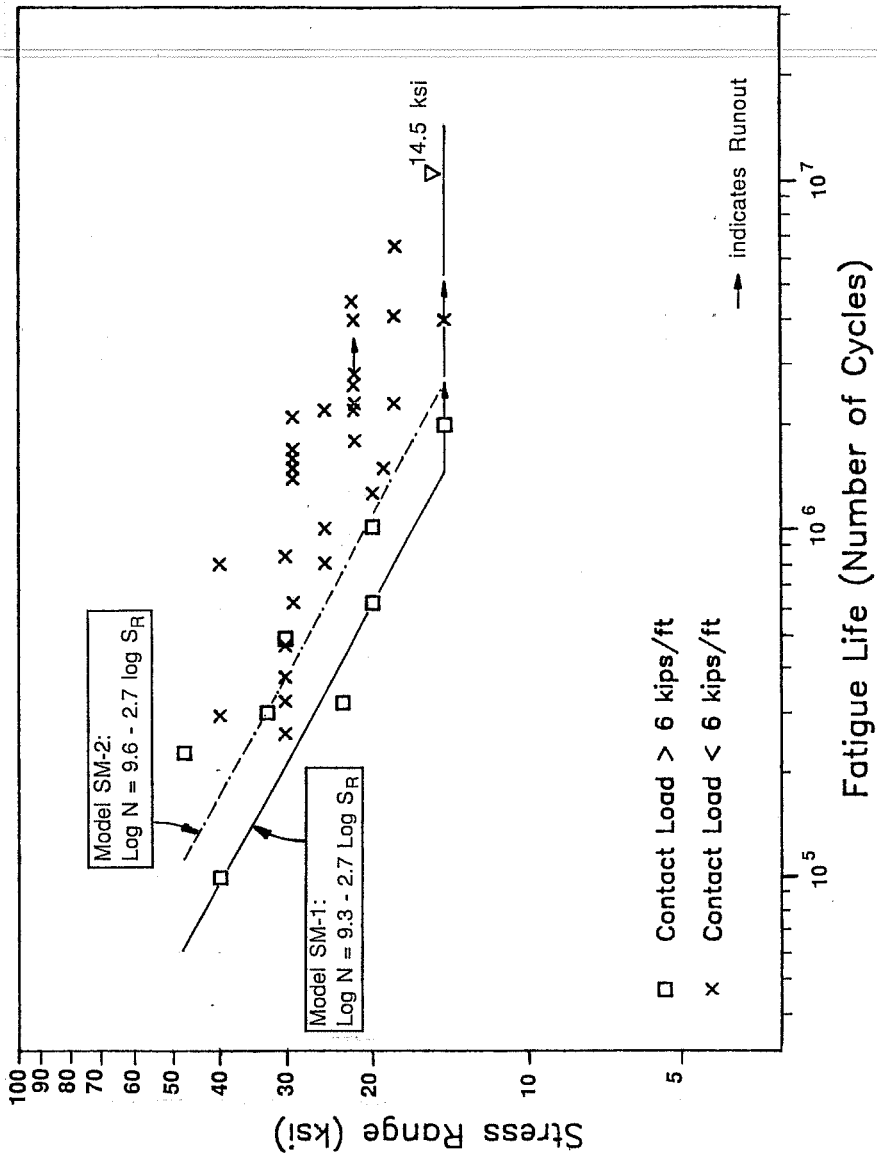
Figure 5.17   Fretting fatigue life Models SM-1 and SM- 2.

132
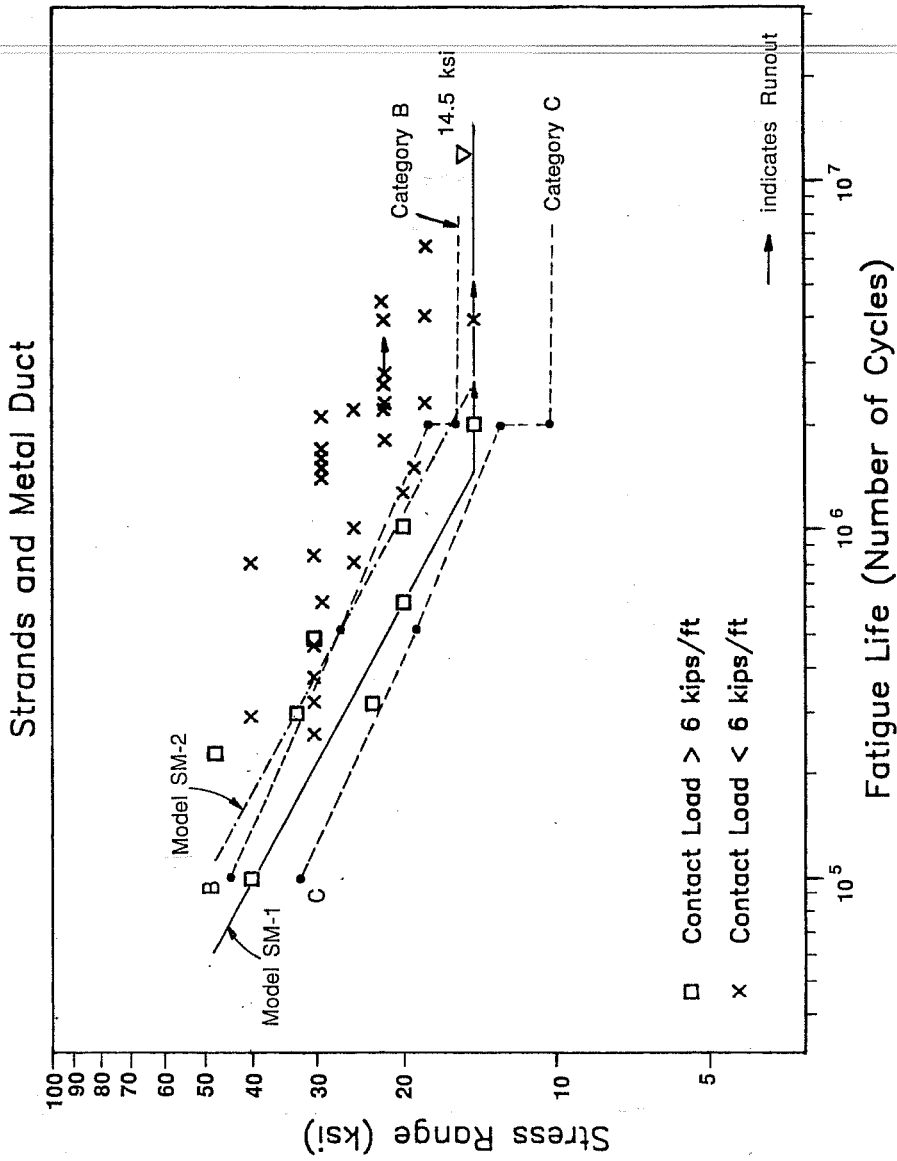
Figure 5.18   Comparison of Models SM-1 and SM-2 with AASHTO
Category B and C Recommendations

Table 5.3 K-Factors for Typical Tendon Arrangements

data point	d_1 / d_2	number of strands	K-factor
1	2.57	3	0.88
2	2.57	3	0.65
3	3.20	3	0.56
4	3.20	4	0.53
5	3.33	4	0.69
6	2.57	4	0.83
7	4.29	5	0.54
8	3.50	5	0.56
9	4.00	6	0.51
10	4.00	7	0.47
11	5.00	7	0.34
12	5.00	10	0.38
13	5.00	12	0.37
14	5.57	16	0.32
15	8.00	16	0.28
16	7.10	20	0.31
17	6.40	20	0.24
18	7.20	25	0.25
19	8.00	30	0.23
20	11.10	54	0.18

d_1 ... Inner Diameter of Duct

d_2 ... Strand or Wire Diameter
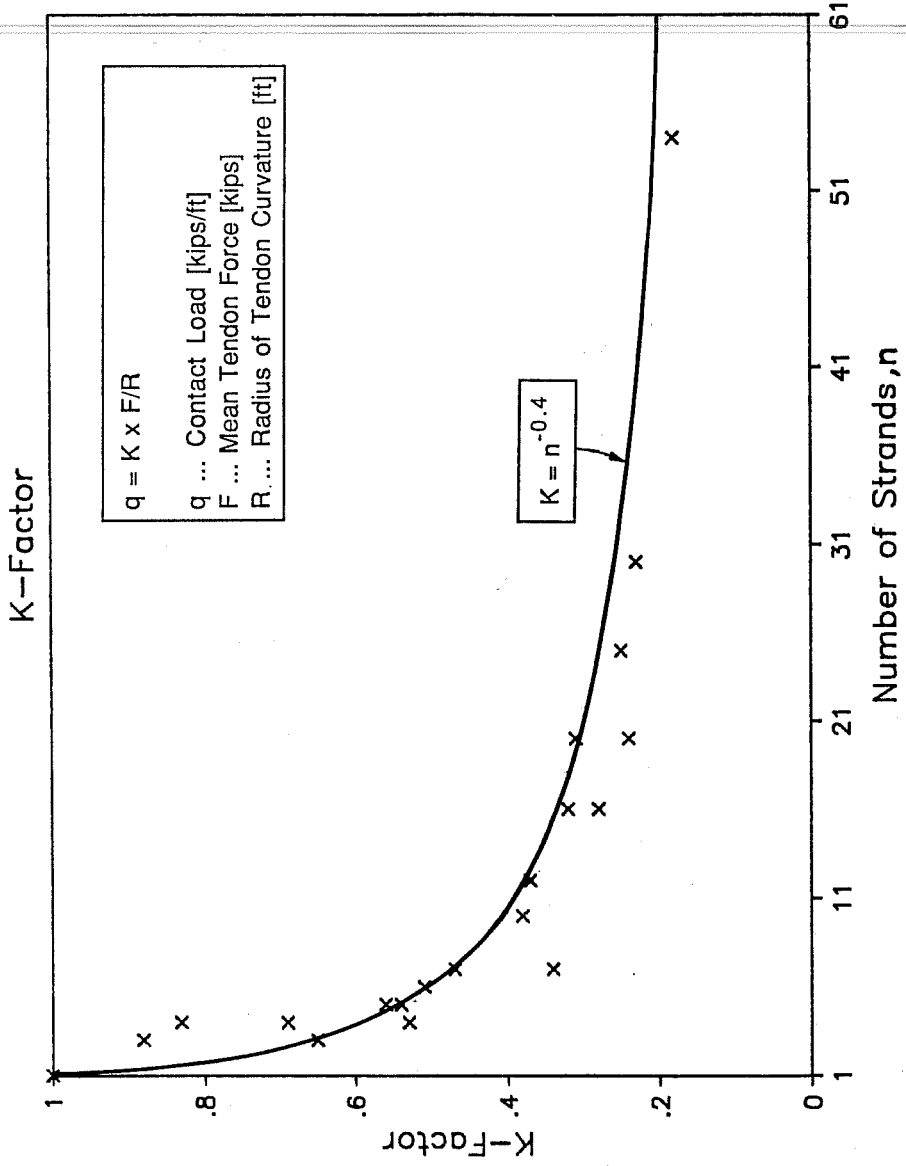
Figure 5.19   Determination of K-Factor

5.19. A curve was fitted through the data points in Figure 5.19 yielding a simple equation for the K - factor in terms of the number of strands in the tendon. Actually, the ratio of duct diameter to strand diameter also affects the K - factor, but this parameter can be eliminated by choosing a somewhat conservative curve fitting. The calculation of the mean tendon force F in Figure 5.19 should be based on a cracked section analysis. The average between the tendon force under full dead and live load and under dead load alone should be taken.

Table 5.4 lists typical minimum radii of curvature for different numbers of strands, strand diameters, and allowable contact loads. These values are based on an assumed mean tendon stress of 190 ksi. Use of sharper curvatures will increase the tendency for fretting. For tendons with more than five strands the radii listed in Table 5.4 are larger than allowable radii by most standards in Europe. However, no test results with contact loads greater than ten kips/ft are available at this time, and more research is definitely needed to establish recommendations for tendons with larger contact loads.

The determination of the K - factor and the contact load is based on the assumption of parallel alignment of the strands within the tendon. It was shown in Section 4.6 of the present study that twisting of some of the strands may result in concentrated contact loads and greatly accelerate fretting fatigue failures at such locations. In Figure 5.16 multiple strand reduced beam specimen Q6-8-30-0.26 with the twisted strands is indicated. Although the nominal contact load was only four kips/ft, it failed at a fatigue life of 280,000 cycles, which would correspond to a contact load twice as large. It would seem less likely for longer tendons that twisting of the strands and zones critical for fretting fatigue would coincide, but the possibility cannot be excluded.

5.3.6 Other Parameters. There are a number of other parameters affecting fretting fatigue but for which no data is currently available.

It has been shown in fretting fatigue tests for applications in mechanical engineering that the slip amplitude of the fretting motion has a very significant, nonlinear influence on the fretting fatigue performance [30,31]. The fatigue life decreases with increasing slip amplitude until the slip reaches a critical value. Beyond this value fretting fatigue becomes less severe rapidly.

This implies that a reduction of the tendon curvature would not necessarily improve the fatigue performance. Although a larger radius of curvature results in smaller contact loads, the friction between strand and duct also decreases, leading to a larger slip amplitude. This increased slip may offset the beneficial effect of the reduced contact load.

The effect of decreasing impact of the slip amplitude beyond a critical value was confirmed by a comparison of the fretting fatigue behavior of grouted and ungrouted post-tensioning tendons [19]. For the ungrouted tendons the slip amplitude was so large

Table 5.4   Typical Minimum Radii
of Tendon Curvature* [ft]

Strand Diameter Contact load Number of Strands	0.5 in. dia.		0.6 in. dia.	
	6 kips/ft	8 kips/ft	6 kips/ft	8 kips/ft
5	12.7	9.5	18.0	13.5
10	19.3	14.5	27.4	20.5
20	29.2	21.9	41.5	31.1
30	37.3	28.0	52.9	39.7
40	44.3	33.2	62.8	47.1
50	50.7	38.0	71.9	53.9

*) based on 190 ksi mean tendon stress

that previously formed cracks were worn away in subsequent movements, and no crack propagation took place. Failure occurred due to normal fatigue initiated away from the contact points between strand and duct.

Another factor may be the number of contact points where fretting occurs [31]. The larger this number, the more likely a fretting fatigue failure becomes. This is analogous to the length effect for strand in air tests, where longer strand samples tend to exhibit a lower fatigue life. The probability of a material flaw, which serves as the stress concentration from which the fatigue crack can propagate, increases with the length of the specimen. This may be an explanation of the consistently higher test results of the fretting simulation tests by Cordes, et al. [9], as shown in Figure 5.1b. Their apparatus simulated fretting only on a very limited portion of the specimen.

The differences between laboratory specimens and applications in actual structures, such as load history and environment, are discussed in Section 5.2.2.

5.4 Comparison with U.S. Fatigue Design Recommendations

Figure 5.20 shows a comparison of the recommended fretting fatigue models SM-1 and SM-2 of this study and of the recommendations by ACI Committees 215 and 358. Also included are the AASHTO Category B and C provisions for redundant load path steel structures. Current recommendations for concrete structures do not recognize the finite life portion of the stress range - fatigue life curve and also appear to be very conservative. Models SM-1 and SM-2 are based on 39 test results from this and previous studies and provide information on allowable stress ranges for a finite number of load cycles. An endurance limit is indicated, but should not be considered a true endurance limit that ensures an unlimited number of load cycles without fatigue distress. However, a stress range of 14.5 ksi or less should ensure a fatigue life of at least two million load cycles.

It is emphasized again that the determination of the tendon stress range should be based on a cracked section analysis. If flexural cracking of a girder can be precluded, the tendon stress range should be significantly lower and tendon fatigue should not be a problem.
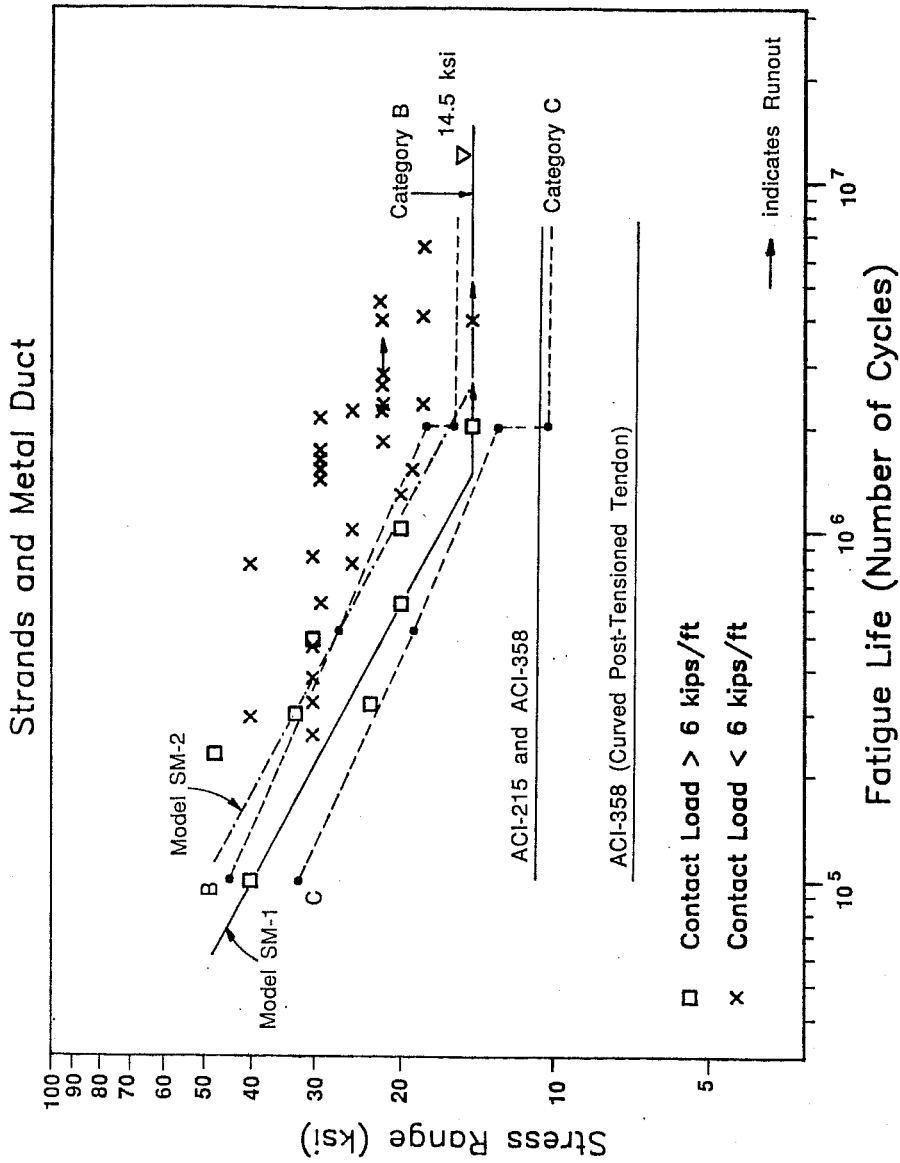
138

Figure 5.20   Comparison with current U.S. fatigue design recommendations.

C H A P T E R   6

SUMMARY, CONCLUSIONS, AND RECOMMENDATIONS

6.1   Summary

Recent studies in Europe indicate that the fatigue life of cracked post-tensioned girders may be substantially reduced as compared to pretensioned girders. A comprehensive study was initiated at The University of Texas at Austin to learn more about the adverse effects of fretting fatigue in post-tensioned concrete. The project comprises three test series: 13-single strand reduced beams, 9-multiple strand reduced beams, and 8-girder tests. Variables examined included the influence of number of strands in a tendon, tendon stress range, tendon curvature, duct material, and strand coating on the fatigue performance of post-tensioning tendons. A short introduction to the problem of fretting fatigue and a summary of previous research is included. Fabrication, test procedure, and test results are discussed in detail. Based on the evaluation and comparison of the results of this and previous studies a fretting fatigue life model for strand type tendons is suggested.

6.2   Conclusions

The following conclusions are based on a relatively small number of results from girder tests and reduced beam tests. Some important limitations should be kept in mind:

- Only tendons with six or fewer strands were tested.

- Test results of tendons with radii of curvature equal to 2.0m (79 in.), 3.5m (138 in.), 6.6m (258 in.) and 34.5m (1360 in.) were evaluated.

- All tests were conducted under laboratory conditions, which means the specimens were protected from environmental influences.

- The load frequency was constant for all tests.

   The following conclusions were drawn:

a)   Fretting fatigue reduces the fatigue life of cracked post-tensioned concrete girders. If cracking of the girder can be prevented, tendon fatigue should not be a problem.

b)   In tendons with metal duct, the predominant cause for wire fractures is fretting between strands and duct. Particularly in tendons with plastic duct, fractures also occurred due to fretting between individual strands of a tendon. After fracture of the first wire of a strand, subsequent fractures occurred due to fretting between individual wires of a strand.

139

c) Fretting between individual strands of a tendon depends largely on the strand arrangement. Fretting is a problem between strand and duct or between interior and peripheral strands of a tendon but does not seem to be a problem between strands of the same layer.

d) Tendon stress range, contact load, and strand coating are important parameters in the fretting fatigue performance of a post-tensioning tendon. The influence of the slip amplitude may be significant, but no pertinent test results are currently available.

e) Both single strand and multiple strand reduced beams reproduce accurately the important conditions in girders with metal duct tendons. However, single strand reduced beams fail to reproduce fretting between individual strands in a duct. Since this is the predominant failure mode for strand type tendons with plastic duct, single strand reduced beams do not adequately predict the fatigue performance of multiple strand tendons with plastic duct.

f) Twisting of strands within the tendon may cause concentrated contact loads and lead to premature wire fractures.

6.3   Recommendations

6.3.1   Measures to Minimize Fretting Fatigue. Several measures can be taken to minimize fretting fatigue in post-tensioning tendons and thus to increase their fatigue life:

a) Limitation of the tendon stress range:

The calculation of the tendon stress range should be based on a cracked section analysis, if there is a possibility that the girder may become cracked. The effects of passive reinforcement may be included in this analysis. Prevention of cracking will reduce the tendon stress range and should eliminate most fatigue problems. The actual tendon stress range in a bridge in service will be greatly influenced by the level of effective prestress. Very conservative estimates of effective prestress should be used which reflect the possibility of substantial prestress losses due to construction and environmental factors.

b) Limitation of contact load:

A reduction of the contact load can be achieved either by increasing the radius of tendon curvature or by reducing the number of strands within a tendon.

c) Use of coated strand:

The limited examination of one specimen with epoxy coated strand indicated that the coating effectively prevented fretting between strands and duct, and

between individual strands, and greatly improved the fatigue performance of post-tensioning tendons.

The use of plastic duct prevents fretting between strands and duct. However, fretting between individual strands may become critical for certain strand arrangements, particularly where strands are placed in more than one layer. In addition, if the strands are twisted in the tendon, fretting is a distinct possibility. Because of these factors, the use of plastic duct for multistrand tendons would not guarantee safety from fretting.

6.3.2 Design Recommendations. Figure 6.1 shows design recommendations for strand type tendons with metal duct. Two models, according to the maximum nominal contact load between strands and duct, are suggested. Model SM-1 applies to tendons with a contact load not more than eight kips/ft, model SM-2 may be used for contact loads less than six kips/ft. AASHTO Category C and B fatigue design models for steel structures with redundant load path may be used if desired for the same respective contact load limits. In view of the experimental evidence of the possibility of wire fractures due to strand to strand fretting and until more data are available, the same fretting fatigue life model as for metal duct tendons is recommended for multistrand tendons with plastic duct.

The horizontal branch of the fatigue models in Figure 6.1 at 14.5 ksi ensures a fatigue life of at least two million load cycles, but may not represent a true endurance limit. Tendon stress range and contact load should be determined from a cracked section analysis. The contact load should be based on an average value of the mean tendon force. The K - factor may be computed by the equation shown in Figure 6.1.

6.3.3 Recommendations for Further Research. More research on fretting fatigue of post-tensioning tendons is desirable to clarify some of the questions not yet answered:

a) More tests with multiple strand tendons and plastic duct are necessary to determine the influence of the duct material. Single strand tendon tests do not adequately predict the fatigue life of multistrand tendons with plastic duct, but both multiple strand reduced beams or girder tests may be used. The tendon should be composed of enough strands to achieve a strand arrangement with interior and peripheral strands.

b) Additional tests would be desirable to verify the influence of epoxy coating of the strands.

c) Systematic research of important parameters for fretting fatigue, such as slip amplitude, contact pressure, and load history is lacking. There is no data available for contact loads greater than 10k/ft.
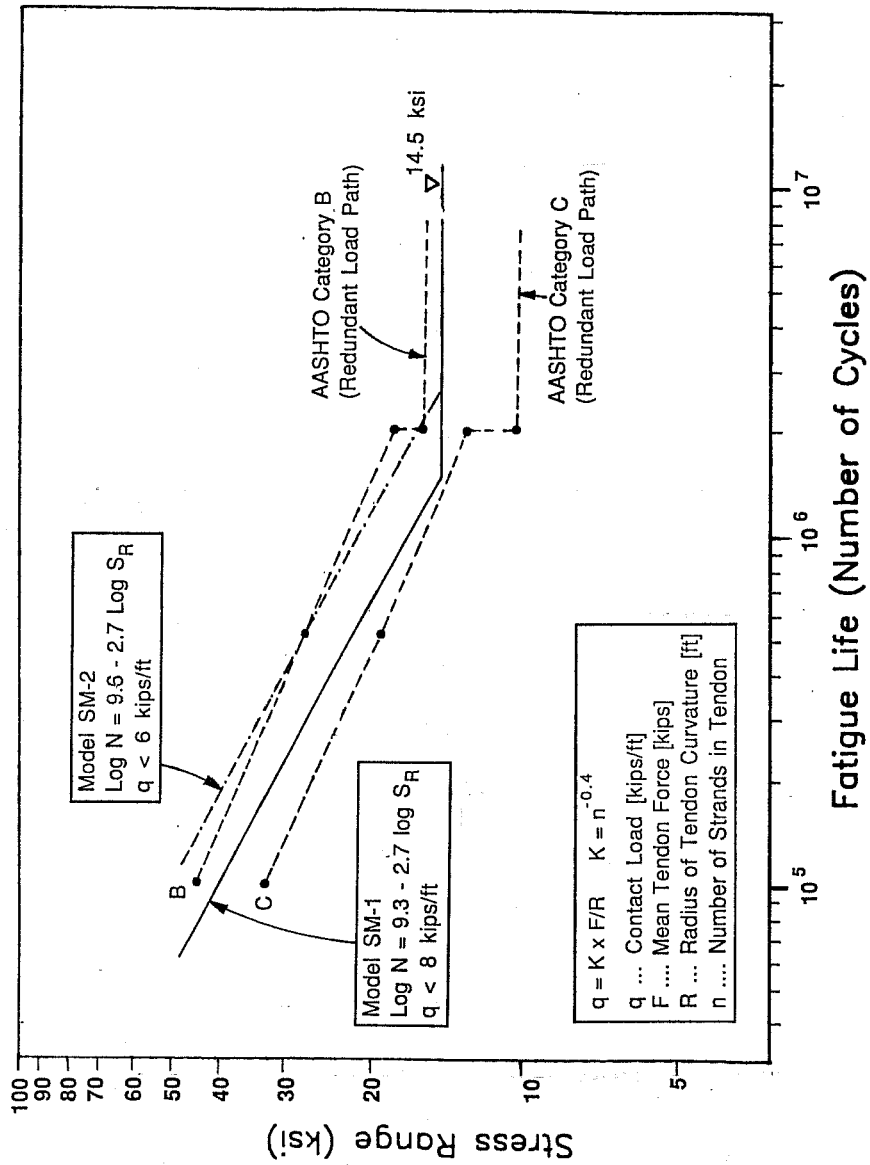
Figure 6.1 Design Recommendations

d)   Additional low stress range tests are necessary to verify the applicability of the endurance limit currently suggested for structures subjected to more than two million load cycles.

REFERENCES

1. AASHTO, Standard Specification for Highway Bridges, American Association of State Highway and Transportation Officials, 13th Edition, 1983.

2. Abeles, P.W., Barton, F.W., and Brown, E.I., II., "Fatigue Behavior of Prestressed Concrete Bridge Beams", First International Symposium on Concrete Bridge Design, SP-23, American Concrete Institute, Detroit, 1969, pp. 579-599.

3. ACI-Committee 318, "Building Code Requirements for Reinforced Concrete", American Concrete Institute, Detroit, 1983.

4. ACI-Committee 215, "Considerations for Design of Concrete Structures Subjected to Fatigue Loading", ACI Manual of Concrete Practice, Part 1, 1987, pp. 215R-16 - 215R-19.

5. ACI-Committee 358, "Analysis and Design of Reinforced Concrete Guideway Structures", ACI Journal, September - October 1986, pp. 862-866.

6. Broek, D., Elementary Engineering Fracture Mechanics, Third Revised Edition, Martinas Nijhoff Publishers, Boston 1982, 469 pp.

7. CEB/FIP, "CEB-FIP Model Code for Concrete Structures", International System of Unified Standard Codes of Practice for Structures, Vol.2, Third Edition, 1978, pp.345-346.

8. Canteli, A.F., Esslinger, V., and Thurlimann, B., "Ermudungsfestigkeit von Bewehrungs- und Spannstahlen (Fatigue Strength of Reinforcing and Prestressing Steel)", Institut fur Baustatik und Konstruktion, ETH Zurich (Swiss Federal Institute of Technology), Report 8002-1, February 1984.

9. Cordes, H., and Lapp-Emden, H., "Untersuchung zur Dauerfestigkeit von Spanngliedern fur die besonderen Bedingungen der teilweisen Vorspannung (Investigation of the Fatigue Strength of Tendons in Partially Prestressed Concrete Structures)", Report 18/84, Institut fur Massivbau, Technical University Aachen, June 1984.

10. Cousin, T.E., Jonston, D.W., and Zia, P., "Bond of Epoxy Coated Prestressing Strand", Research Report FHWAINC/87- 005, Center for Transportation Engineering Studies, North Carolina State University at Raleigh, December 1986.

11. Diab, J.G., "Fatigue Tests of Post-Tensioned Concrete Girders", Unpublished M.S. Thesis, The University of Texas at Austin, December 1988.

12. DIN 4227/Part 2, "Spannbeton-Bauteile mit teilweiser Vorspannung (German Code on Partially Prestressed Concrete Structures)".

13. Ekberg, C.E., Jr., Walther, R.E., and Slutter, R.G., "Fatigue Resistance of Prestressed Concrete Beams in Bending", Journal of the Structural Division ASCE, 83 (ST4), Proc. 1304.

14. Foo, M.H., and Warner, R.T., "Fatigue Tests on Partially Prestressed Concrete Beams", Presented at the NATO- Advanced Research Workshop, Paris, France, June 18-22, 1984.

15. Georgiou, T., "Fretting Fatigue in Post-Tensioned Concrete Girders", Unpublished M.S. Thesis, The University of Texas, December 1988.

16. Lin, T.Y., and Burns, N.H., Design of Prestressed Concrete Structures, Third Edition, John Wiley and Sons, New York, 1981.

17. Magura, D.D., and Hognestad, E., "Tests of Partially Prestressed Concrete Girders", ASCE Proceedings, Vol.92, ST.1, February 1966, p. 327-350.

18. Muller, H.H., "Fatigue Strength of Prestressing Tendons", Betonwerk und Fertigteiltechnik, December 1986, pp. 804- 808.

19. Oertle, J., Thurlimann, B., and Esslinger, V., "Versuche zur Reibermudung einbetonierter Spannkabel (Fretting Fatigue Tests of Post-Tensioning Tendons)", Institut fur Baustatik und Konstruktion, ETH Zurich (Swiss Federal Institute of Technology), Report 8101-2, October 1987.

20. Oertle, J., and Thurlimann, B., "Reibermudung einbetonierter Spannkabel (Fretting Fatigue of Post-Tensioning Tendons)", Festschrift Christian

Menn zum 60. Geburtstag, Institut fur Boustatik and Konstruktion, ETH Zurich (Swiss Federal Institute of Technology), 1986, pp. 33-38.

21. Overman, T.R., Breen, J.E., and Frank, K.H., "Fatigue Behavior of Pretensioned Concrete Girders", Research Report 300-2F, Center for Transportation Research, The University of Texas at Austin, November 1984.

22. Paulson, C., Jr., "A Fatigue Study of Prestressing Strand", M.S. Thesis, The University of Texas at Austin, August 1982.

23. PTI Ad Hoc Committee on Cable Stayed Bridges, "Recommendations for Stay Cable Design and Testing", Post- Tensioning Institute, January 1986.

24. Quade, C.E., "Distribution of Post-Tensioning Forces Prior to Grouting Tendons", M.S. Thesis, The University of Texas at Austin, May 1988.

25. Rabbat, B.G., Karr, P.H., Russel, H.G., and Bruce, N.G.,Jr., "Fatigue Tests of Full Size Prestressed Girders", Research Report II3, Portland Cement Association, June 1978.

26. Rigon, C., and Thurlimann, B., "Fatigue Tests on Post-Tensioned Concrete Beams", Report 8101-1, Institut fur Baustatik und Konstruktion, ETH Zurich (Swiss Federal Institute of Technology), May 1985.

27. Schlaich, J., Schafer, K., Jennewein, M., "Toward a Consistent Design of Structural Concrete", PCI Journal May/June 1987, Vol.32, Nr.3.

28. Tilly, G.P., "Performance of Bridge Cables", First Oleg Kerensky Memorial Conference, London, June 21, 1988.

29. Waterhouse, R.B., Fretting Fatigue, Applied Science Publishers Ltd., London,1981.

30. Waterhouse, R.B., Fretting Corrosion, Pergamon Press Ltd., 1972.

31. Yates, D.L., "A Study of Fretting Fatigue in Post- Tensioned Concrete Beams", M.S. Thesis, The University of Texas at Austin, December 1987.

32. CEB Task Force Group 15, "Fatigue of Concrete Structures", Bulletin d'Information Nr.188, June 1988.

33. Oertle, J., "Reibermudung einbetonierter Spannkabel (Fretting Fatigue of Post-Tensioning Tendons)", Dissertation ETH Nr.8609, ETH Zurich (Swiss Federal Institute of Technology), 1988.

34. Wollmann, G.P., "Fretting Fatigue of Multiple Strand Tendons in Post-Tensioned Concrete Beams," M.S. Thesis, The University of Texas at Austin, December, 1988.

35. Bill, R.C., "Review of Factors that influence fretting wear,", ASTM STP 780, American Society for Testing and Materials, 1982, pp. 165-182.

36. Krueger, F.E., "Fretting Failures," *Metals Handbook*, Vol. 10, American Society for Metals, 8th Edication, pp. 154-160.

37. Waterhouse, R.B., "Occurrence of Fretting in Practice and Its Simulation in the Laboratory," *Materials Evaluation Under Fretting Conditions*, ASTM STP 780 American Society for Testing and Materials, 1982, pp. 3-16.